Revista Mexicana de Astronomía y Astrofísica, **47**, 83–112 (2011)

MID- AND FAR-INFRARED PHOTOMETRY OF GALACTIC PLANETARY NEBULAE WITH THE AKARI ALL-SKY SURVEY

J. P. Phillips and R. A. Márquez-Lugo

Instituto de Astronomía y Meteorología
Universidad de Guadalajara, Mexico

Received 2010 December 14; accepted 2011 January 28

RESUMEN

Presentamos fotometría en el medio y lejano infrarrojo de 857 nebulosas planetarias (NPs) galácticas utilizando datos provenientes del AKARI All-Sky Survey. Se incluyen flujos a 9 y 18 μm obtenidos con la Infrared Camera (IRC), y a 65, 90, 140 y 160 μm producto de la far-Infrared Surveyor (FIS). Se nota que la luminosidad IR de las NPs más jóvenes es comparable a la luminosidad total la estrella central y que posteriormente decrece hasta $\sim 5\times10^2$ $L_\odot$ cuando $D > 0.08$ pc, lo cual es congruente con la evolución de la opacidad del polvo de las NPs y la apreciable absorción en las NPs jóvenes y en las proto NPs. Además notamos que hay poca evidencia de la evolución en los cocientes de los flujos IR/radio sugerida por autores previos. También hacemos notar que la disminución de la temperatura del polvo al aumentar el diámetro nebular es similar a la obtenida en estudios previos, mientras que los niveles de calentamiento por fotones de Lyα son <0.5 de la energía disponible para los granos. Parece haber una evolución del exceso infrarrojo (IRE) con la expansión de las nebulosas, el cual adquiere sus valores máximos cuando las NPs son más compactas.

ABSTRACT

We provide mid- and far-infrared photometry of 857 Galactic planetary nebulae (PNe) using data derived from the AKARI All-Sky Survey. These include fluxes at 9 and 18 μm obtained with the Infrared Camera (IRC), and at 65, 90, 140 and 160 μm using the far-Infrared Surveyor (FIS). It is noted that the IR luminosities of the youngest PNe are comparable to the total luminosities of the central stars, and subsequently decline to $\sim 5\times10^2$ $L_\odot$ where $D > 0.08$ pc. This is consistent with an evolution of PNe dust opacities, and appreciable absorption in young and proto-PNe. We also note that there is little evidence for the evolution in IR/radio flux ratios suggested by previous authors. The fall-off of dust temperatures with increasing nebular diameter is similar to that determined in previous studies, whilst levels of Lyα heating are <0.5 of the total energy budget of the grains. There appears to be an evolution in the infrared excess (IRE) as nebulae expand, with the largest values occurring in the most compact PNe.

Key Words: dust, extinction — infrared: ISM — ISM: jets and outflows — planetary nebulae: general

1. INTRODUCTION

Several large-scale surveys at infrared wavelengths have been undertaken in the last thirty or so years, permitting a clearer understanding of the properties of dust in planetary nebulae (PNe). Thus for instance, Pottasch et al. (1984) investigated the thermal and physical characteristics of grains using photometry taken with the *Infrared Astronomical Satellite* (*IRAS*; Neugebauer et al. 1984). They found that dust temperatures decline with increasing nebular radius R, and that dust/gas mass ratios decrease with expansion of the shells. A further analysis by Lenzuni, Natta, & Panagia (1989) found that grain radii also decreased with radius,

whilst the volume density of particles increased as $\propto R^{4.19}$; tendencies which were attributed to grain-grain collisions, sputtering by stellar winds, or the selective destruction of larger grains. A further analysis by Stasinska & Szczerba (1999), however, found no change in either of the latter two parameters.

A subsequent survey of PNe has been undertaken in the near infrared (NIR) using the 2MASS all-sky survey (Ramos-Larios & Phillips 2005), whilst a more restrictive survey, taken with the *Spitzer Space Telescope* (*Spitzer*; Werner et al. 2004), has enabled mid-infrared (MIR) observations of PNe close to the Galactic plane (see e.g., Cohen et al. 2005; Phillips & Ramos-Larios 2008; Ramos-Larios & Phillips 2008; Zhang & Kwok 2009; Phillips & Márquez-Lugo 2011). These latter results have shown the importance of polycyclic aromatic hydrocarbons (PAHs) in enhancing MIR emission at 5.8 and 8.0 μm, and revealed the presence of extensive emission outside of the ionized regimes, likely arising from photo-dissociation regimes (PDRs).

A more recent AKARI infrared survey has now completed the major phase of its observational program, and the point source catalogue (PSC) was made available in March 2010. This represents an updated version of the IRAS project, containing as it does more photometric channels, higher levels of spatial resolution, and higher sensitivity detectors. We present photometry for 857 Galactic PNe taken with the infrared camera (IRC) and far-infrared surveyor (FIS), and use this to analyse the evolution in grain temperatures and FIR luminosities.

2. OBSERVATIONS

The AKARI space mission (Murakami et al. 2007) was launched in 2006, and contains the IRC (Onaka et al. 2007) for observations in the range 2–26 μm, and the FIS (Kawada et al. 2007) for the 50–200 μm regime. The Ritchey-Chretien type telescope has a 0.685 m primary mirror, cooled to 6 K by liquid helium and mechanical coolers. One of the primary objectives of this mission was an all sky IRC/FIS survey, undertaken between 2006 May and 2007 August. The resulting PSCs [Kataza et al. 2010 (IRC); Yamamura et al. 2010 (FIS)] were published in 2010 March.

The IRC filter profiles extend between 6.76 and 11.6 μm (in the case of MIR-S), with an effective wavelength of 9 μm, and between 13.9 and 25.6 μm (MIR-L) with an effective wavelength of 18 μm. The camera field of view (FOV) was 10×9.6 arcmin^2 for MIR-S, and 10.7×10.2 arcmin^2 for MIR-L, whilst the pixel scales were 2.34×2.34 arcsec^2 (MIR-S) and 2.31×2.39 arcsec^2 (MIR-L). Each of four adjacent pixels were subsequently binned to create so-called "virtual" pixels, with areas 4×4 times greater than those of the original pixels. However, subsequent processing of two independent survey grids resulted in an improvement in spatial resolution, and point spread functions (PSFs) with FWHM ∼5.5 arcsec at 9 μm, and 5.7 arcsec for the 18 μm channel.

The FIS survey, by contrast, permitted observations at effective wavelengths of 65 μm (filter N60, bandwidth $\Delta\lambda = 21.7$ μm), 90 μm (Wide-S, $\Delta\lambda = 37.9$ μm), 140 μm (Wide-L, $\Delta\lambda = 52.4$ μm) and 160 μm ($\Delta\lambda = 34.1$ μm). The 65 and 90 μm results were taken with a monolithic Ge:Ga detector having a pixel size 26.8 arcsec, whilst the longer wave (140 and 160 μm) data were acquired using a stressed Ge:Ga detector, and pixel scale of 44.2 arcsec. The FOVs were in all cases ∼1 arcmin, whilst the FWHM of the PSFs were 37 arcsec (at 65 μm), 39 arcsec (90 μm), 58 arcsec (140 μm) and 61 arcsec (160 μm). Detector sensitivities are important in determining the rates of source detection, and quoted values range between 0.55 Jy at 90 μm to as high as 25 Jy for the 160 μm results. This question is further examined in § 3.4, where we consider its importance in determining nebular emission trends.

Details of the source selection procedure are provided in the following sections, together with a description of the catalogue results, the infrared dimensions of the PNe, and a comparison of the AKARI and IRAS photometry.

2.1. *Planetary Nebula Data Base and Search Radius*

The positions of the PNe investigated in this present study are taken from the listing of coordinates by Kerber et al. (2003). This provides positions for 1086 sources based on the 2$^{\rm nd}$ generation General Star Catalogue. The coordinates for sources which are compact (or have central stars) are quoted as being accurate to 0.35 arcsec, whilst the positions for 226 more extended PNe are accurate to ∼5 arcsec.

By contrast, the AKARI/IRC All-Sky Survey Release Point Source Catalogue - Release Note (Rev. 1) (Kataza et al. 2010) suggests that the mean angular separation of the AKARI and 2MASS sources is of order ≅0.77 arcsec, with 95% of the sources having angular separations of <2 arcsec. Similarly, the positional errors of the longer wave FIS sources (Yamamura et al. 2010) are determined through a comparison with the SIMBAD database, yielding flux independent uncertainties of order ∼6 arcsec.

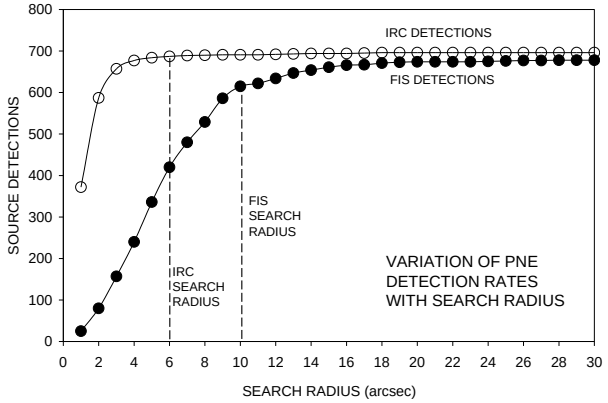

Fig. 1. The variations in the numbers of PNe with size of the search radius θ_S. Note how the numbers of IRC detections achieve a maximum within ∼2 arcsec of the nominal PNe positions, whilst the number of FIS detections increases more slowly, and peaks at radii close to 15–20 arcsec. This difference in detection rates reflects the difference in the positional accuracies of the surveys. Finally, the flattening of detection rates towards larger search radii confirms the low levels of contamination by background sources.

Given that the PNe data base is identical for the FIS and IRC searches, it follows that search radii need to be larger for FIS than for the IRC results.

That this is the case is apparent from Figure 1, where it is seen that the rates of source detection increase with increasing search radius, eventually reaching plateau values of 696 sources for the IRC detections, and 678 sources for the FIS results. It is also apparent that whilst most of the PNe are detected within radii $\theta_S \sim 3$ arcsec for the IRC results, a radius of order $\theta_S \sim 14$ arcsec is required for comparable rates of FIS detection. We have adopted a search radius $\theta_S = 6$ arcsec for the IRC results, and $\theta_S = 10$ arcsec for the FIS photometry.

There are two reasons to suspect that background contamination is extremely modest. It is apparent, for instance, that rates of source detection are flat as θ_S increases from ∼15 arcsec to 30 arcsec, implying that any field source contamination is likely to be $< 2\%$. We also note that the AKARI FIS catalogue includes a parameter NDENS, corresponding to the number of sources within 5 arcmin of the central (PNe) positions. This takes a mean value of ∼2.2 for 415 estimates of the parameter in the most sensitive (90 μm) channel, suggesting again that background contamination is extremely low. A similar conclusion applies for the NDENS parameters at 9 and 18 μm, corresponding to the numbers of sources within 45 arcsec of the search positions. We determine mean values NDENS09 = 0.068 (for 396 estimates of the parameter), and NDENS18 = 0.020 (for 612 estimates of NDENS), implying that very few of our identifications are likely to be spurious.

2.2. *Catalogue Results for Galactic PNe*

Photometric results for 857 PNe detected in the IRC catalogue are presented in Table 1, where all of the fluxes have FQUAL values of 3 (i.e. all of the data are classified as being valid). An analysis by the AKARI team of trends in photometric errors shows that the most probable uncertainties are of the order of ∼2–3%, with 80% of the data having errors of $< 15\%$. It is found that the signal to noise ratio (S/N) for the 9 μm data is of order ∼19 for sources having $F(9\ \mu\mathrm{m}) > 0.5$ Jy, and falls as approximately S/N ∼32 $F_\nu(9\ \mu\mathrm{m}) + 4$ for smaller flux levels. Similarly, it is found that the S/N for 18 μm results is ∼15 where $F(18\ \mu\mathrm{m}) > 0.8$ Jy, and decreases as ∼17 $F_\nu(18\ \mu\mathrm{m}) + 3$ below this limit.

We have, apart from this, specified the numbers of the PNe in the Kerber et al. (2003) list of coordinates (Column 1); the commonly accepted names of the sources (Column 2); and the right ascensions and declinations of the nebulae (Columns 3 and 4). The angular diameter θ is based upon radio and optical results, where we have taken values from Acker et al. (1992), Zhang (1995), Cahn & Kaler (1971), Tylenda et al. (2003), Perek & Kohoutek (1967), and Siodmiak & Tylenda (2001). Where maximal and minimal diameters θ_{MAX} and θ_{MIN} are quoted, then we have employed harmonic mean values $\theta = (\theta_{\mathrm{MAX}}\theta_{\mathrm{MIN}})^{0.5}$. Similarly, the AKARI mean radii at 18 μm (denoted in the catalogue by MEAN_AB18) are provided in Column 8, and labeled MN_18. The 1.4 GHz results (Column 9) are taken from the uniform data base of Condon et al. (1998), whilst the 5 GHz measures (Column 10) derive from the compilations of Acker et al. (1992), Zhang (1995) and Siodmiak & Tylenda (2001). Finally, the distances of PNe remain notoriously uncertain, and the numbers of more reliable distances (i.e. those based on trigonometric, reddening, gravitational and kinematic measures, among others) are still pitifully small. We have therefore quoted distances based on larger-scale statistical measures, whilst recognizing that these are prone to systematic and random errors. Typical uncertainties in distance are probably of the order ≈30%. We have used values quoted by Phillips (2004) and Zhang (1995) in that order of priority, and these are listed in Column 11 of Table 1. These estimates are also combined with the angular diameters in Column 7 to determine the physical diameters in Column 12.

TABLE 1

GALACTIC PNE IDENTIFIED IN THE AKARI IRC CATALOGUE

KN	NAME	R.A. (2000)	DEC (2000)	F (9 μm)	F (18 μm)	θ	MN_18	F(1.4 GHz)	F(5 GHz)	DIST	DIAM
		H:M:S	D:M:S	Jy	Jy	arcsec	arcsec	mJy	mJy	kpc	pc
4	010.2+02.7	17 58 14.415	−18 41 26.15	–	0.844	–	3.53	18.3	–	–	–
5	021.9+02.7	18 21 21.115	−08 31 42.30	0.285	4.516	–	4.12	36.2	–	–	–
6	050.6+19.7	18 08 20.083	+24 10 43.26	2.483	13.329	–	4.8	–	–	–	–
7	099.3−01.9	22 04 12.301	+53 04 01.36	0.46	11.917	–	4.74	–	–	–	–
9	19W32	17 39 02.870	−28 56 35.10	–	6.588	24	4.46	13.5	21.3	–	–
10	341.4−09.0	17 35 02.502	−49 26 26.38	5.541	77.831	–	6.67	–	–	–	–
27	A 30	08 46 53.514	+17 52 45.47	0.548	18.039	4.47	6.04	–	2.3	2.55	0.055
31	A 35	12 53 32.792	−22 52 22.57	0.114	–	772	–	–	255	0.74	2.77
42	A 47	18 35 22.569	−00 13 49.68	–	0.143	17	2.13	7.3	–	–	–
43	A 48	18 42 46.908	−03 13 17.30	–	3.342	40	6.97	159.4	–	–	–
48	A 53	19 06 45.910	+06 23 52.47	–	1.043	31	5.16	33.6	85.7	1.68	0.252
53	A 58	19 18 20.476	+01 46 59.62	2.846	15.29	–	4.95	–	–	–	–
73	A 78	21 35 29.410	+31 41 45.39	0.986	30.5	107	7.23	3.7	4.9	2.22	1.152
83	Al 2-E	17 30 14.398	−27 30 19.41	–	0.873	–	3.44	14.7	–	–	–
85	Al 2-G	17 32 22.670	−28 14 27.32	–	1.013	–	3.39	–	–	–	–
90	Al 2-0	17 51 44.663	−31 36 00.18	–	0.775	5.7	3.18	38	33	–	–
92	Al 2-R	17 53 36.431	−31 25 25.19	–	0.306	–	3.17	–	–	–	–
94	Ap 1-12	18 11 35.088	−28 22 37.02	0.207	3.286	12	4.03	6.6	18.7	5.34	0.311
96	BD+30 3639	19 34 45.235	+30 30 58.94	47.546	148.573	7.6	7.65	235.2	630	–	–
102	Bl 2-1	22 20 16.638	+58 14 16.59	1.554	4.116	1.6	3.99	21.6	54	6.94	0.054
103	Bl 3-10	17 55 20.537	−29 57 36.13	–	0.357	–	3.01	4.7	–	–	–
104	Bl 3-13	17 56 02.759	−29 11 16.21	–	0.809	–	3.31	4.7	10	–	–
105	Bl 3-15	17 52 35.947	−29 06 38.97	–	0.372	–	2.67	–	–	–	–
106	Bl B	17 36 59.836	−29 40 08.93	–	1.641	–	3.65	8.9	–	–	–
108	Bl M	17 53 47.180	−28 27 16.88	–	1.249	4.5	3.61	9.3	17	7.03	0.153
109	Bl O	17 53 49.717	−28 59 11.26	0.149	1.534	–	3.7	3.6	–	–	–
110	Bl Q	17 54 34.866	−28 12 43.04	0.195	1.65	–	3.76	18.2	–	–	–
112	CRBB 1	20 19 28.702	−41 31 27.46	–	0.647	–	3.37	–	–	–	–
113	CRL 618	04 42 53.672	+36 06 53.17	189.266	–	12	–	4	67	2.72	0.158
119	Cn 1-1	15 51 15.936	−48 44 58.67	13.024	27.81	–	5.27	–	10	–	–
120	Cn 1-3	17 26 12.392	−44 11 24.52	0.525	–	–	–	–	–	–	–
122	Cn 1-5	18 29 11.653	−31 29 59.21	–	4.672	7	4.16	51	44	4.43	0.15
123	Cn 2-1	17 54 32.978	−34 22 20.84	–	3.665	2.2	3.84	25.2	49	6.17	0.066
124	Cn 3-1	18 17 34.133	+10 09 03.99	0.239	6.365	4.5	4.33	59.5	75	4	0.087
126	DdDm 1	16 40 18.156	+38 42 19.92	–	0.233	1	2.69	5.7	6	15.85	0.077
150	Fg 1	11 28 36.205	−52 56 04.01	0.416	0.92	16	5.32	–	55	2.02	0.157
151	Fg 2	17 39 19.847	−44 09 37.14	0.227	1.226	–	3.66	–	–	–	–
152	Fg 3	18 00 11.819	−38 49 52.73	1.441	16.842	2	5.1	42	107	–	–
154	G001.1+00.8	17 45 11.085	−27 32 38.00	1.182	4.009	–	4.48	73	–	–	–
155	G001.5−00.7	17 52 08.717	−28 02 16.56	0.394	3.804	–	4.32	17.2	–	–	–
158	G002.5+05.1	17 32 12.788	−24 04 59.56	1.138	9.218	–	4.56	–	–	–	–
163	G009.3+05.7	17 45 14.155	−17 56 46.57	–	13.562	–	4.75	–	–	–	–
164	G010.2+07.5	17 41 00.035	−16 18 12.50	–	3.076	–	3.83	–	–	–	–
165	G011.1−07.9	18 40 19.914	−22 54 29.23	–	2.813	–	3.75	–	–	–	–
168	G013.1−13.2	19 04 43.548	−23 26 08.82	7.78	–	–	–	–	–	–	–
170	G014.2+03.8	18 02 38.257	−14 42 03.22	0.421	7.042	–	4.29	–	–	–	–
172	G014.5−36.1	20 42 45.967	+30 04 06.51	3.74	37.172	–	5.88	–	–	–	–
175	G017.0+11.1	17 42 14.430	−08 43 18.61	–	2.126	–	4.32	23.4	–	–	–
179	G019.2−04.4	18 42 24.770	−14 15 11.81	–	0.495	–	3.76	7.3	–	–	–
180	G020.4+00.6	18 25 58.081	−10 45 28.49	0.447	5.891	–	4.2	48.7	–	–	–
182	G032.0−01.7	18 56 15.684	−01 34 00.31	–	0.485	–	2.89	10.7	–	–	–
184	G033.7−02.0	19 00 16.133	−00 14 32.59	–	0.347	–	2.89	3.5	–	–	–
185	G034.5−11.7	19 36 17.531	−03 53 25.26	0.151	3.996	–	3.98	8.8	–	–	–
186	G038.4+01.8	18 54 54.139	+05 48 11.29	0.211	2.773	–	3.92	20.5	–	–	–
188	G039.1−02.2	19 10 53.284	+04 27 28.50	–	0.439	–	3.26	11	–	–	–
191	G044.1+01.5	19 06 32.146	+10 43 23.93	–	0.815	–	3.24	19.4	–	–	–
193	G047.2+01.7	19 11 35.828	+13 31 11.58	0.78	3.869	–	4.07	–	–	–	–
195	G051.5+00.2	19 25 40.679	+16 33 05.56	–	3.863	–	4.38	77	–	–	–
200	G059.4−00.7	19 45 34.244	+22 58 34.41	–	0.958	–	3.35	26.5	–	–	–
202	G069.2+01.2	20 00 41.998	+32 27 41.23	–	0.516	–	3.6	17	–	–	–
204	G076.6−05.7	20 48 16.627	+34 27 24.36	0.11	6.21	–	4.27	–	–	–	–
207	G095.0−05.5	21 56 32.945	+47 36 13.40	0.369	1.764	–	3.67	–	–	–	–
219	G199.4+14.3	07 20 01.614	+18 17 26.47	0.147	0.689	–	3.09	–	–	–	–
221	G222.8−04.2	06 54 13.406	−10 45 38.27	0.204	1.727	–	4	2.7	–	–	–
226	G255.3−03.6	08 06 28.339	−38 53 23.93	0.091	1.275	–	3.56	2.8	–	–	–
228	G260.1+00.2	08 37 24.599	−40 38 07.46	0.318	2.612	–	4.41	–	–	–	–
229	G270.1−02.9	08 59 02.971	−50 23 39.68	0.262	1.373	–	3.64	–	–	–	–
231	G277.1−01.5	09 37 51.861	−54 27 08.59	0.724	3.141	–	3.94	–	–	–	–
232	G279.1−00.4	09 53 27.058	−54 52 39.60	0.059	0.866	–	3.46	–	–	–	–
234	G282.6−00.4	10 13 19.673	−56 55 32.24	0.313	3.065	–	3.99	–	–	–	–
235	G285.1−02.7	10 19 32.466	−60 13 29.41	3.022	17.044	–	5.16	–	–	–	–
238	G301.1−01.4	12 34 35.968	−64 18 16.99	2.012	17.086	–	5.08	–	–	–	–
241	G308.5−03.5	13 46 25.712	−65 46 24.26	0.176	2.768	–	3.93	–	–	–	–
243	G313.1+02.1	14 16 51.803	−58 53 10.01	0.136	1.979	–	3.72	–	–	–	–
244	G313.3+01.1	14 15 53.284	−60 01 37.31	0.948	9.663	–	4.49	–	–	–	–
245	G314.4+02.2	14 21 19.909	−58 38 22.10	0.543	5.337	–	4.08	–	–	–	–
246	G316.2+00.8	14 38 19.980	−59 11 46.12	1.053	10.213	–	4.51	–	–	–	–
251	G328.4−02.8	16 09 20.143	−55 36 09.84	0.301	2.054	–	3.85	–	–	–	–
253	G331.3−12.1	17 16 21.107	−59 29 23.35	0.089	2.566	–	3.9	–	–	–	–
254	G336.1+04.1	16 15 02.803	−45 11 54.10	0.314	2.13	–	3.98	–	–	–	–
255	G340.3−03.2	17 03 10.027	−47 00 27.68	18.997	158.829	–	7.92	–	–	–	–
259	G342.2−00.3	16 56 33.989	−43 46 13.55	0.793	9.718	–	4.45	–	–	–	–
261	G343.7−09.6	17 45 33.415	−47 43 50.31	2.362	2.236	–	3.78	–	–	–	–

TABLE 1 (CONTINUED)

KN	NAME	R.A. (2000)	DEC (2000)	F (9 μm)	F (18 μm)	θ	MN_18	F(1.4 GHz)	F(5 GHz)	DIST	DIAM
		H:M:S	D:M:S	Jy	Jy	arcsec	arcsec	mJy	mJy	kpc	pc
263	G344.9−01.9	17 12 22.022	−42 30 41.24	0.487	9.329	–	4.58	–	–	–	–
264	G347.9−06.0	17 40 03.329	−42 24 05.58	–	0.202	–	3.04	–	–	–	–
267	G351.5−06.5	17 52 09.386	−39 32 14.52	–	0.229	–	2.45	–	–	–	–
273	G353.4−02.4	17 39 17.147	−35 46 58.88	0.248	–	–	–	–	–	–	–
276	G353.8−01.2	17 35 27.372	−34 47 42.22	–	0.474	–	2.83	8.2	–	–	–
286	G355.4+02.3	17 25 03.470	−31 28 38.50	–	0.533	–	3.2	10.4	–	–	–
287	G355.4−01.4	17 40 00.347	−33 35 32.29	–	0.34	–	3	8.7	–	–	–
294	G356.8−03.0	17 50 10.734	−33 14 17.97	–	0.436	–	3.03	4.2	–	–	–
295	G357.1+01.2	17 33 50.871	−30 42 36.75	0.206	0.967	–	3.38	11.3	–	–	–
300	G358.4+01.6	17 35 22.745	−29 22 17.40	–	0.452	–	2.91	5.5	–	–	–
301	G358.6−02.4	17 52 00.342	−31 17 49.92	–	0.665	–	3.37	12	–	–	–
308	G359.8+08.9	17 11 38.912	−24 07 32.87	0.755	6.889	–	4.13	–	–	–	–
310	G000.5+01.9	17 39 31.219	−27 27 46.77	–	0.53	–	3.11	6.8	–	–	–
316	G001.5+03.6	17 35 22.074	−25 42 46.48	–	0.934	–	3.45	12.2	–	–	–
318	G001.6+01.5	17 43 16.950	−26 44 17.54	–	0.539	–	3.14	9.8	–	–	–
326	G003.6+04.9	17 35 31.198	−23 11 47.62	–	0.213	–	2.57	4.6	–	–	–
333	G070.9+02.2	20 00 52.927	+34 28 22.18	0.153	3.084	–	4.04	–	–	–	–
335	G000.1−01.2	17 50 24.297	−29 25 18.70	–	2.05	–	3.64	–	–	–	–
339	G000.2−01.4	17 51 53.546	−29 30 53.18	3.23	3.541	–	3.75	–	–	–	–
340	G000.4+01.1	17 42 25.108	−27 55 35.95	–	1.157	–	4.13	23.6	–	–	–
341	G000.6−01.0	17 51 11.504	−28 56 26.16	0.493	–	–	–	–	–	–	–
345	G000.0+02.0	17 37 42.929	−27 49 09.55	–	1.557	–	3.61	6.2		–	–
359	H 1-11	17 21 17.693	−22 18 35.32	–	1.044	6	3.59	20.7	13	7.27	0.211
360	H 1-12	17 26 24.239	−35 01 41.26	–	30.05	<25	6.4	372	719	1.4	–
361	H 1-13	17 28 27.537	−35 07 31.63	–	27.492	14	6.16	474	620	1.39	0.094
363	H 1-15	17 28 37.616	−24 51 06.60	–	1.414	4.3	3.88	13.6	13	7.9	0.165
364	H 1-16	17 29 23.358	−26 26 04.39	0.272	–	2	–	34.7	58	–	–
366	H 1-18	17 29 42.759	−29 32 50.21	0.336	2.667	1.5	3.81	17.6	33	7.37	0.054
368	H 1-2	16 48 54.091	−35 47 09.01	2.425	15.806	1	4.94	14.3	62	–	–
369	H 1-20	17 30 43.799	−28 04 06.68	–	1.924	3.3	3.72	26.9	44	5.12	0.082
371	H 1-22	17 32 22.138	−37 57 23.81	–	1.517	<25	3.6	18.4	–	–	–
373	H 1-24	17 33 37.565	−21 46 24.78	–	1.172	5	3.67	5.1	15	7.32	0.177
374	H 1-26	17 36 29.743	−39 21 56.95	0.385	2.345	<25	5.18	67.1	–	–	–
375	H 1-27	17 40 17.926	−22 19 17.64	–	2.859	5.2	3.88	–	18	10.9	0.275
377	H 1-29	17 44 13.819	−34 17 33.05	0.174	–	<10	–	10.6	–	–	–
379	H 1-30	17 45 06.782	−38 08 49.48	–	0.556	<5	2.97	7	81	5.21	–
381	H 1-32	17 46 06.291	−34 03 46.25	0.266	–	1.1	–	3.4	37	9.09	0.048
382	H 1-33	17 47 49.387	−34 08 05.44	–	0.958	<10	3.5	15.8	12	–	–
383	H 1-34	17 48 07.572	−22 46 47.33	0.352	–	2	–	–	13	–	–
384	H 1-35	17 49 13.940	−34 22 52.96	1.709	19.148	2	4.86	18.4	72	6.03	0.058
385	H 1-36	17 49 48.172	−37 01 29.47	–	20.615	0.8	5.25	11.8	50	–	–
386	H 1-37	17 50 44.569	−39 17 25.98	–	0.508	–	3.56	8.5	–	–	–
388	H 1-39	17 53 21.003	−33 55 58.42	–	1.308	1.7	3.62	10.8	13	10.04	0.083
390	H 1-40	17 55 36.049	−30 33 32.08	1.255	10.494	3	4.48	8.1	31	7.84	0.114
391	H 1-41	17 57 19.145	−34 09 49.12	–	0.557	9.6	3.33	16.6	12	6.6	0.307
392	H 1-42	17 57 25.169	−33 35 42.94	–	1.769	5.8	3.77	34.5	40	4.82	0.136
393	H 1-43	17 58 14.430	−33 47 37.51	0.309	3.571	3	4.03	4	6	11.56	0.168
394	H 1-44	17 58 10.641	−31 42 56.08	–	0.484	<5	2.98	8	–	–	–
395	H 1-45	17 58 21.865	−28 14 52.20	5.23	2.443	<10	3.94	–	23.5	8.2	–
396	H 1-46	17 59 02.490	−32 21 43.42	0.303	3.205	1.2	3.94	18.3	43	7.11	0.041
397	H 1-47	18 00 37.596	−29 21 50.22	0.137	2.257	2.5	3.88	8.1	10	10.01	0.121
398	H 1-5	16 57 23.740	−41 37 57.88	1.631	–	–	–	–	–	–	–
399	H 1-50	18 03 53.461	−32 41 42.15	0.189	2.078	1.4	3.69	19.6	31	7.68	0.052
402	H 1-53	18 05 57.404	−26 29 41.50	–	0.651	<25	3.15	7.2	–	–	–
403	H 1-54	18 07 07.239	−29 13 06.35	0.192	3.092	2.5	3.87	12.7	31	8.01	0.097
404	H 1-55	18 07 14.542	−29 41 24.51	0.176	0.518	10	3.06	2.5	5.3	–	–
405	H 1-56	18 07 53.880	−29 44 34.26	–	0.894	3	3.37	8.3	7.8	10.98	0.16
407	H 1-58	18 09 13.835	−26 02 28.78	0.638	5.951	–	4.24	2.7	–	–	–
408	H 1-59	18 11 29.263	−27 46 15.69	–	0.317	6	2.99	3.4	4.2	11.12	0.323
410	H 1-60	18 12 25.155	−27 29 12.96	–	0.411	3.46	2.73	–	11.3	8.59	0.144
411	H 1-61	18 12 33.977	−24 50 00.28	0.427	–	<25	–	4.7	–	–	–
412	H 1-62	18 13 17.951	−32 19 42.74	0.123	1.979	–	3.78	11.9	–	–	–
413	H 1-63	18 16 19.336	−30 07 35.98	0.578	4.882	–	4.02	2.5	9	–	–
414	H 1-64	18 18 23.908	−23 24 57.15	–	0.297	<25	2.71	8.1	–	–	–
415	H 1-65	18 20 08.847	−24 15 05.09	0.195	2.52	2.5	3.75	5.9	10	10.23	0.124
416	H 1-66	18 24 57.539	−25 41 55.76	–	0.419	<10	3.53	10.4	6	9.5	–
417	H 1-67	18 25 04.976	−22 34 52.64	0.1	–	6	–	12.2	11.9	7.51	0.218
418	H 1-7	17 10 27.389	−41 52 49.42	1.893	13.029	–	4.72	–	–	–	–
419	H 1-8	17 14 42.902	−33 24 47.21	0.292	2.295	3.4	3.99	22.2	–	–	–
421	H 2-1	17 04 36.257	−33 59 18.75	0.967	8.184	2.4	4.23	51.5	61	5.84	0.068
422	H 2-10	17 27 32.848	−28 31 06.90	–	1.045	2	3.44	13.4	20	8.21	0.08
423	H 2-11	17 29 25.947	−25 49 06.64	0.248	–	1.5	–	11.5	27.7	–	–
425	H 2-13	17 31 08.084	−30 10 28.00	–	1.052	–	3.38	17.2	–	–	–
426	H 2-14	17 32 20.093	−39 51 25.60	–	0.326	15	3.7	5.2	4.9	–	–
430	H 2-18	17 43 28.751	−21 09 51.29	–	0.428	3.5	3.26	10.1	11	–	–
431	H 2-20	17 45 39.767	−25 40 00.04	–	1.474	3.5	3.66	13.1	16.3	7.5	0.127
432	H 2-22	17 47 33.926	−21 47 23.11	–	0.236	<8	2.3	5.4	–	–	–
433	H 2-23	17 48 57.994	−34 21 53.28	–	0.269	–	2.48	5.3	–	–	–
434	H 2-24	17 48 36.494	−24 16 34.26	–	3.535	4.9	4	4.5	13	7.77	0.185
437	H 2-27	17 51 50.576	−33 47 35.59	0.098	0.541	–	3	7.9	–	–	–
440	H 2-31	17 56 02.350	−28 14 11.36	–	0.877	–	3.37	5.3	–	–	–
442	H 2-33	17 58 12.535	−31 08 05.99	–	0.393	8	3.25	8.1	5	9.71	0.377
446	H 2-39	18 08 05.759	−28 26 10.50	–	0.208	–	2.43	4.9	–	–	–
450	H 2-43	18 12 47.953	−28 19 59.67	0.802	0.702	9	3.28	–	26.4	5.03	0.219
452	H 2-45	18 14 28.844	−24 43 38.35	–	0.317	4.447	2.82	13.2	–	–	–
454	H 2-48	18 46 35.149	−23 26 48.24	0.65	9.835	2	4.26	31.6	66	6.23	0.06

TABLE 1 (CONTINUED)

KN	NAME	R.A. (2000)	DEC (2000)	F (9 μm)	F (18 μm)	θ	MN_18	F(1.4 GHz)	F(5 GHz)	DIST	DIAM
		H:M:S	D:M:S	Jy	Jy	arcsec	arcsec	mJy	mJy	kpc	pc
455	H 2-7	17 23 24.936	−28 59 06.05	–	0.702	4.2	3.47	11.3	9	9.18	0.187
457	H 3-29	04 37 23.484	+25 02 40.94	0.087	0.711	21	4.06	18.3	18	3.4	0.346
462	HaTr 11	19 02 59.373	+03 02 20.77	–	0.566	–	3.74	17	83	–	–
465	HaTr 2	15 30 18.542	−61 01 38.79	–	0.199	–	2.95	–	–	–	–
474	Hb 12	23 26 14.814	+58 10 54.65	11.885	40.599	0.8	6.06	–	45	10.46	0.041
476	Hb 5	17 47 56.187	−29 59 41.91	–	41.232	3.4	6.43	179.5	548	1.32	0.022
477	Hb 6	17 55 07.023	−21 44 39.98	1.144	–	6	–	190.5	243	2.45	0.071
478	Hb 7	18 55 37.950	−32 15 47.07	0.161	2.143	4	3.78	25.4	30	5.9	0.114
479	He 1-1	19 23 46.875	+21 06 38.60	–	0.611	8	3.4	16	14	–	–
480	He 1-2	19 26 37.757	+21 09 27.04	0.125	2.281	4.7	4.01	14.6	15	–	–
481	He 1-3	19 48 26.422	+22 08 37.62	0.12	–	8	–	53.5	–	–	–
483	He 1-5	20 11 56.057	+20 20 04.43	14.057	5.46	36	4.07	4.8	5.2	6.71	1.171
485	He 2-101	13 54 55.721	−58 27 16.46	1.096	1.054	<10	3.55	–	–	–	–
486	He 2-102	13 58 13.866	−58 54 31.78	0.215	1.276	9	4.09	–	33	3.77	0.164
487	He 2-104	14 11 52.077	−51 26 24.18	7.077	7.358	5	4.24	–	15	–	–
489	He 2-107	14 18 43.339	−63 07 09.48	0.155	4.631	10	4.49	–	65	2.97	0.144
490	He 2-108	14 18 08.889	−52 10 39.76	0.179	4.04	11	4.76	–	32	3.49	0.186
494	He 2-112	14 40 30.924	−52 34 56.66	0.271	3.3	14.6	3.93	–	82	2.36	0.167
495	He 2-113	14 59 53.523	−54 18 07.20	62.991	209.197	–	7.79	–	115	–	–
499	He 2-117	15 05 59.193	−55 59 16.53	1.558	20.941	5	5.32	–	267	2.69	0.065
500	He 2-118	15 06 13.731	−42 59 56.46	–	0.87	5	3.5	–	10	–	–
502	He 2-120	15 11 56.388	−55 39 46.67	–	0.567	27	4.07	–	26	2.51	0.329
503	He 2-123	15 22 19.360	−54 08 12.77	0.419	2.327	4.6	3.88	–	110	3.59	0.08
504	He 2-125	15 23 36.326	−53 51 27.95	0.109	1.87	3	3.84	–	20.4	6.96	0.101
505	He 2-128	15 25 07.841	−51 19 42.29	0.201	2.529	5	3.86	–	40	–	–
506	He 2-129	15 25 32.677	−52 50 37.96	0.143	1.474	1.6	3.59	–	35	7.85	0.061
507	He 2-131	15 37 11.210	−71 54 52.89	2.586	50.505	6	6.43	–	325	2.2	0.064
508	He 2-132	15 38 01.182	−58 44 42.07	0.232	1.382	17.8	4.82	–	25	3.02	0.261
509	He 2-133	15 41 58.788	−56 36 25.72	1.254	16.766	<10	5.03	–	210	3.18	–
510	He 2-136	15 52 10.666	−62 30 46.94	0.137	0.588	10	3.14	–	23	–	–
511	He 2-138	15 56 01.694	−66 09 09.23	1.015	21.099	7	5.5	–	76	3.61	0.123
512	He 2-140	15 58 08.063	−55 41 50.13	0.309	6.339	2.6	4.32	–	80	5.03	0.063
513	He 2-141	15 59 08.762	−58 23 53.15	0.151	1.255	13.8	4.26	–	51	2.77	0.185
514	He 2-142	15 59 57.608	−55 55 32.89	4.033	15.811	3.6	4.89	–	65	4.75	0.083
515	He 2-143	16 00 59.125	−55 05 39.74	0.854	8.233	5.2	4.34	–	120	3.32	0.084
516	He 2-145	16 08 58.902	−51 01 57.74	–	0.713	<25	5.98	–	–	–	–
518	He 2-147	16 14 01.045	−56 59 27.78	5.208	2.678	–	3.65	–	–	–	–
519	He 2-149	16 14 24.266	−54 47 38.82	–	0.542	3	2.96	–	10	8.52	0.124
520	He 2-15	08 53 30.701	−40 03 42.08	0.227	1.209	23.8	4.64	94.5	105	1.92	0.222
521	He 2-151	16 15 42.269	−59 54 00.96	0.616	12.148	5	4.62	–	10	–	–
522	He 2-152	16 15 20.031	−49 13 20.76	1.234	7.995	11	4.64	–	196	2.09	0.111
524	He 2-155	16 19 23.101	−42 15 35.98	0.223	0.721	14.6	3.72	–	70	2.47	0.175
525	He 2-157	16 22 14.264	−53 40 54.09	–	1.951	<5	3.89	–	30	6.24	–
526	He 2-158	16 23 30.605	−58 19 22.64	–	0.455	2	3.37	–	2.7	14.71	0.143
527	He 2-159	16 24 21.417	−54 36 02.82	–	0.303	10	2.52	–	25	3.9	0.189
528	He 2-161	16 24 37.786	−53 22 34.14	0.113	0.717	10	3.43	–	32	3.64	0.176
529	He 2-162	16 27 50.914	−54 01 28.36	0.25	0.927	<5	3.78	–	28	–	–
531	He 2-164	16 29 53.255	−53 23 15.37	0.226	1.529	16	4.6	–	97	2.17	0.168
533	He 2-169	16 34 13.328	−49 21 13.20	0.338	1.699	21.8	4.6	–	128	2.7	0.285
534	He 2-170	16 35 21.170	−53 50 11.11	0.16	1.675	5	3.8	–	15	–	–
535	He 2-171	16 34 04.240	−35 05 26.93	4.775	3.186	10	3.75	–	10	–	–
536	He 2-175	16 39 28.112	−36 34 16.41	0.183	–	6.6	–	19.2	26.8	4.58	0.147
538	He 2-182	16 54 35.167	−64 14 28.43	0.365	4.408	10	4.21	–	62	–	–
539	He 2-185	17 01 17.254	−70 06 03.35	–	0.506	10	3.17	–	18	–	–
540	He 2-186	16 59 36.064	−51 42 06.46	0.091	0.752	3	3.44	–	21	6.9	0.1
541	He 2-187	17 01 36.976	−50 22 57.49	–	0.549	6	3.65	–	–	–	–
543	He 2-21	09 13 52.823	−55 28 16.80	–	0.237	<10	2.46	–	16	8.21	–
545	He 2-25	09 18 01.308	−54 39 29.01	1.781	3.827	4.4	3.95	–	827.9	2.07	0.044
546	He 2-250	17 34 54.710	−26 35 56.92	–	0.728	5	3.4	15.3	15	7.01	0.17
547	He 2-26	09 19 27.476	−59 12 00.39	0.171	1.109	<10	3.54	–	40	1.91	–
548	He 2-262	17 40 12.814	−26 44 21.37	–	1.082	<10	3.46	24.1	26	6.64	–
549	He 2-28	09 22 06.825	−54 09 38.60	–	0.123	10	1.95	–	20	4.15	0.201
550	He 2-29	09 24 45.834	−54 36 15.45	–	0.326	14	3.07	–	24	3.41	0.231
551	He 2-306	17 56 33.706	−43 03 18.90	–	0.83	–	3.32	–	–	–	–
553	He 2-34	09 41 13.997	−49 22 47.18	8.941	6.16	<10	4.19	–	–	–	–
554	He 2-35	09 41 37.504	−49 57 58.71	–	1.009	5	3.61	–	20	5.61	0.136
555	He 2-36	09 43 25.538	−57 16 55.44	0.192	1.686	22	4.25	–	90	3.1	0.331
559	He 2-41	10 07 23.611	−63 54 30.06	–	0.393	<10	2.94	–	41	3.39	–
561	He 2-428	19 13 05.239	+15 46 39.80	–	0.331	8	2.99	26.7	7	6.16	0.239
562	He 2-429	19 13 38.422	+14 59 19.21	0.271	2.24	4.2	3.96	58.5	64.9	4.33	0.088
563	He 2-430	19 14 04.197	+17 31 32.92	0.255	–	1.7	–	18.2	40	7.36	0.061
564	He 2-432	19 23 24.821	+21 08 00.50	0.152	1.286	2.3	3.61	21.3	32	6.88	0.077
565	He 2-434	19 33 49.420	−74 32 58.66	–	1.035	10	3.42	–	–	–	–
566	He 2-436	19 32 06.701	−34 12 57.43	0.327	0.457	10	2.86	–	23	–	–
567	He 2-437	19 32 57.657	+26 52 43.35	2.839	5.478	–	4.11	6.6	–	–	–
568	He 2-440	19 38 08.403	+25 15 40.98	0.233	2.995	2.2	3.98	26.4	43	6.45	0.069
569	He 2-442	19 39 43.376	+26 29 33.05	14.02	7.485	<10	4.24	–	6	–	–
570	He 2-447	19 45 22.164	+21 20 04.03	0.951	6.286	1.2	4.21	22.9	60	7.63	0.044
571	He 2-459	20 13 57.898	+29 33 55.94	2.042	17.276	1.3	5.12	13.9	64	7.24	0.046
572	He 2-47	10 23 09.143	−60 32 42.21	1.4	22.347	5	5.53	–	170	–	–
574	He 2-5	07 47 20.022	−51 15 03.42	0.08	1.011	3	3.51	–	29	6.3	0.092
577	He 2-55	10 48 43.168	−56 03 10.21	–	0.324	<25	3.58	–	–	–	–
579	He 2-62	11 17 43.157	−70 49 32.41	0.075	0.692	<10	3.36	–	–	–	–
582	He 2-67	11 28 47.369	−60 06 37.28	0.224	1.375	5	3.64	–	41	–	–
583	He 2-68	11 31 45.427	−65 58 13.67	0.369	2.549	10	3.9	–	34	–	–
584	He 2-7	08 11 31.890	−48 43 16.71	0.102	0.596	44.6	3.27	–	47	2.91	0.629

TABLE 1 (CONTINUED)

KN	NAME	R.A. (2000)	DEC (2000)	F (9 μm)	F (18 μm)	θ	MN_18	F(1.4 GHz)	F(5 GHz)	DIST	DIAM
		H:M:S	D:M:S	Jy	Jy	arcsec	arcsec	mJy	mJy	kpc	pc
586	He 2-71	11 39 11.198	−68 52 09.14	0.298	3.484	5	3.95	–	12	–	–
588	He 2-73	11 48 38.191	−65 08 37.33	0.378	3.875	4	3.99	–	76	4.23	0.082
589	He 2-76	12 08 25.433	−64 12 09.32	–	0.467	–	3.43	–	–	–	–
590	He 2-78	12 09 10.196	−58 42 37.44	–	0.717	–	3.4	–	–	–	–
591	He 2-81	12 23 01.237	−64 01 45.96	–	0.308	<25	2.7	–	–	–	–
593	He 2-83	12 28 43.997	−62 05 35.05	0.357	6.569	–	4.27	–	–	–	–
594	He 2-84	12 28 46.822	−63 44 37.22	–	0.261	–	2.56	–	–	–	–
595	He 2-85	12 30 07.567	−63 53 00.32	0.463	3.29	10.2	4.26	–	111.7	2.53	0.125
596	He 2-86	12 30 30.426	−64 52 05.58	1.102	12.943	3.6	4.81	–	125	3.85	0.067
598	He 2-9	08 28 27.988	−39 23 40.27	0.754	6.989	4.4	4.37	135.6	194.8	3.11	0.066
599	He 2-90	13 09 36.252	−61 19 35.96	32.451	62.806	10	6.59	–	25	–	–
600	He 2-96	13 42 36.150	−61 22 29.18	0.762	7.397	–	4.25	–	–	–	–
601	He 2-97	13 45 22.394	−71 28 56.13	0.419	4.989	5	4.03	–	30	–	–
602	He 2-99	13 52 30.683	−66 23 26.49	0.366	5.097	17	5.04	–	18	3.4	0.28
603	He 3-1333	17 09 00.932	−56 54 48.25	118.338	165.011	–	7.72	–	26	–	–
605	Hf 2-2	18 32 30.935	−28 43 20.47	–	0.3	–	2.31	4.4	–	–	–
606	Hf 39	10 53 59.586	−60 26 44.31	1.092	8.06	–	10.32	–	–	–	–
607	Hf 48	11 03 55.979	−60 36 04.57	–	0.416	–	3.26	–	–	–	–
608	Hu 1-1	00 28 15.614	+55 57 54.71	0.2	0.665	10	3.59	28	26	3.86	0.187
609	Hu 1-2	21 33 08.349	+39 38 09.57	0.211	1.849	6.5	4.21	107	155	2.53	0.08
610	Hu 2-1	18 49 47.562	+20 50 39.46	0.782	5.679	1.8	4.24	42.6	110	4.52	0.039
612	IC 1297	19 17 23.459	−39 36 46.40	0.32	1.45	7	3.93	59.4	68.9	3.75	0.127
614	IC 1747	01 57 35.896	+63 19 19.36	0.499	2.162	13	4.28	85.8	124	2.23	0.141
615	IC 2003	03 56 21.984	+33 52 30.59	0.245	1.539	10	3.93	54.8	30	3.89	0.189
616	IC 2149	05 56 23.908	+46 06 17.32	0.786	9.271	8.4	5.48	177	280	2.03	0.083
617	IC 2165	06 21 42.775	−12 59 13.96	0.485	4.793	9	4.21	180	188	2.47	0.108
618	IC 2448	09 07 06.261	−69 56 30.74	0.417	1.94	10	5.02	–	73	3.41	0.165
619	IC 2501	09 38 47.213	−60 05 30.92	1.939	13.312	2	4.99	–	261	2.09	0.02
620	IC 2553	10 09 20.856	−62 36 48.40	0.817	5.105	9	4.38	–	92	2.85	0.124
621	IC 2621	11 00 20.111	−65 14 57.77	2.614	15.35	5	4.89	–	195	2.94	0.071
622	IC 289	03 10 19.273	+61 19 00.91	–	5.7	36.8	7.95	152	170	1.18	0.211
623	IC 351	03 47 33.143	+35 02 48.50	–	0.637	7	3.51	31.9	27	4.45	0.151
624	IC 3568	12 33 06.834	+82 33 50.29	0.34	3.57	18	5.27	94.1	95	2.47	0.216
626	IC 4191	13 08 47.343	−67 38 37.67	0.961	9.494	14	4.67	–	172	1.95	0.132
627	IC 4406	14 22 26.278	−44 09 04.35	–	1.841	20	5.83	–	110	1.5	0.145
628	IC 4593	16 11 44.545	+12 04 17.06	0.375	9.95	12.8	5.16	90.6	92	2.42	0.15
629	IC 4634	17 01 33.572	−21 49 32.77	0.505	6.146	5.5	4.38	116	100	3.47	0.093
630	IC 4637	17 05 10.506	−40 53 08.44	–	9.044	18.6	5.7	–	132.5	2.29	0.207
631	IC 4642	17 11 45.025	−55 24 01.47	–	2.797	16.6	5.51	–	60	2.52	0.203
633	IC 4673	18 03 18.408	−27 06 22.61	0.692	3.057	16	5.02	53.4	62	3.12	0.242
634	IC 4699	18 18 32.024	−45 59 01.70	–	0.283	5	2.86	–	20	4.91	0.119
635	IC 4732	18 33 54.633	−22 38 40.91	0.203	–	3	–	12.2	49	4.79	0.07
636	IC 4846	19 16 28.220	−09 02 36.57	0.131	2.038	2.9	3.85	38.7	43	5.72	0.08
637	IC 4997	20 20 08.741	+16 43 53.71	1.143	16.078	2	4.97	30.1	127	5.45	0.053
638	IC 5117	21 32 31.027	+44 35 48.53	6.448	26.937	1.5	5.6	34.1	210	5.01	0.036
639	IC 5217	22 23 55.725	+50 58 00.43	0.278	1.772	6.5	3.89	50.4	163	2.71	0.085
643	J 320	05 05 34.313	+10 42 22.73	–	0.545	7.1	3.32	29.6	23	4.63	0.159
644	J 900	06 25 57.275	+17 47 27.19	1.467	4.976	6	4.24	107.8	100	3.29	0.096
653	KFL 15	18 14 19.324	−25 20 51.22	–	0.451	8.5	3.31	11	11.2	–	–
681	K 2-16	16 44 49.050	−28 04 04.56	2.535	–	–	–	–	–	–	–
687	K 3-11	18 41 07.311	−08 55 58.97	0.154	3.265	3	3.99	14.5	17	7.33	0.107
688	K 3-13	18 45 24.582	+02 01 23.85	–	1.335	3.7	3.54	30.6	34	5.5	0.099
689	K 3-14	18 48 32.821	+10 35 50.74	–	0.667	1	3.31	–	4.8	16.89	0.082
690	K 3-15	18 51 41.522	+09 54 53.06	0.478	–	0.3	–	–	4	–	–
692	K 3-17	18 56 18.171	+07 07 26.31	1.967	18.124	8	5.47	319.5	345	2.04	0.079
693	K 3-18	19 00 34.829	−02 11 57.62	–	9.729	3.5	4.82	–	11	13.98	0.235
694	K 3-19	19 01 36.575	−01 19 07.85	0.131	1.262	1.2	3.56	11.8	23	8.93	0.052
695	K 3-2	18 25 00.576	−01 30 52.64	0.082	2.431	2.8	3.77	25.9	31	6.37	0.086
698	K 3-22	19 09 26.658	+12 00 44.05	0.832	0.715	–	3.21	–	–	–	–
699	K 3-24	19 12 05.820	+15 09 04.47	–	0.268	6.2	2.7	8.5	–	–	–
700	K 3-26	19 14 39.178	+00 13 36.29	–	0.286	–	3.03	6.4	0.5	–	–
702	K 3-29	19 15 30.561	+14 03 49.83	0.869	7.708	1	4.29	13.9	65	8.07	0.039
703	K 3-3	18 27 09.338	+01 14 26.88	0.321	1.614	10	4.05	35.9	34	3.43	0.166
704	K 3-30	19 16 27.691	+05 13 19.47	0.11	0.662	3.3	3.23	12.1	23	6.46	0.103
705	K 3-31	19 19 02.666	+19 02 20.85	0.269	2.394	1.5	3.86	16.8	39	7.83	0.057
706	K 3-33	19 22 26.670	+10 41 21.39	–	1.613	1.1	3.83	8.6	17	11.33	0.06
708	K 3-35	19 27 44.036	+21 30 03.83	0.37	6.017	1.7	4.35	14.5	60	6.56	0.054
709	K 3-36	19 32 39.557	+07 27 51.57	–	0.164	–	1.88	3.1	0.2	–	–
710	K 3-37	19 33 46.749	+24 32 27.09	–	0.466	2.5	2.97	14.4	17	7.93	0.096
711	K 3-38	19 35 18.354	+17 13 00.71	0.236	1.362	5	3.81	28.7	31	5.09	0.123
712	K 3-39	19 35 54.469	+24 54 48.20	0.393	4.122	1	4.15	3.6	11	13.35	0.065
713	K 3-4	18 31 00.227	+02 25 27.35	–	0.18	21	2.84	17	21	–	–
714	K 3-40	19 36 21.828	+23 39 47.93	0.216	1.597	4	3.76	17.1	20	6.18	0.12
720	K 3-49	19 54 00.702	+33 22 12.95	0.227	2.631	–	3.87	5.5	7	34.5	–
721	K 3-5	18 31 45.833	+04 05 09.12	0.109	0.276	10	2.86	6.7	3	7.11	0.345
723	K 3-52	20 03 11.435	+30 32 34.15	0.877	7.924	0.7	4.28	16.9	65	9.42	0.032
724	K 3-53	20 03 22.475	+27 00 54.73	1.36	7.328	0.9	4.31	10	69	9.27	0.04
725	K 3-54	20 04 58.639	+25 26 37.36	0.155	0.638	0.8	3.29	4.8	7.5	16.39	0.064
726	K 3-55	20 06 56.210	+32 16 33.60	0.325	2.551	8.2	4.05	86.6	90	2.96	0.118
728	K 3-57	20 12 47.679	+34 20 32.52	0.245	1.861	6.3	3.96	46.8	60	3.72	0.114
731	K 3-60	21 27 26.477	+57 39 06.45	0.962	3.113	1.9	3.92	28	43	6.87	0.063
732	K 3-61	21 30 00.710	+54 27 27.45	0.118	0.606	6	3.25	16.6	14	5.73	0.167
733	K 3-62	21 31 50.203	+52 33 51.64	0.748	6.41	2.5	4.29	59.5	115	4.62	0.056
734	K 3-63	21 39 11.976	+55 46 03.94	–	0.443	7	3.18	8.5	29	–	–
737	K 3-66	04 36 37.243	+33 39 29.87	–	0.91	2.1	3.24	15.4	18	8.42	0.086
738	K 3-67	04 39 47.905	+36 45 42.85	0.119	1.456	2.2	3.74	33.3	42	6.49	0.069

TABLE 1 (CONTINUED)

KN	NAME	R.A. (2000)	DEC (2000)	F (9 μm)	F (18 μm)	θ	MN_18	F(1.4 GHz)	F(5 GHz)	DIST	DIAM
		H:M:S	D:M:S	Jy	Jy	arcsec	arcsec	mJy	mJy	kpc	pc
740	K 3-69	05 41 22.147	+39 15 08.09	0.162	0.838	0.46	3.4	2.9	0.4	13.87	0.031
741	K 3-7	18 34 13.601	−02 27 36.41	0.287	1.77	6.3	3.85	29.5	30	4.52	0.138
746	K 3-76	20 25 04.865	+33 34 50.70	–	0.539	0.2	3.76	5.1	12	–	–
747	K 3-78	20 45 22.710	+50 22 39.92	0.146	0.911	3.8	3.55	14.9	15	6.85	0.126
750	K 3-82	21 30 51.636	+50 00 06.96	–	0.951	24	4.73	35.6	30	2.49	0.29
751	K 3-83	21 35 43.877	+50 54 16.94	–	0.172	5	1.92	4.7	6.5	7.71	0.187
753	K 3-87	22 55 06.987	+56 42 31.14	–	0.181	6	2.45	10.6	4.5	7.91	0.23
755	K 3-90	01 24 58.628	+65 38 36.14	–	0.339	8.5	3.25	12.4	13.9	4.6	0.19
761	K 4-19	19 13 22.624	+03 25 00.30	–	0.708	–	3.33	–	–	–	–
762	K 4-28	19 30 16.668	+14 47 21.84	0.129	2.229	0.6	3.82	5	19	14.27	0.042
764	K 4-41	19 56 34.027	+32 22 12.96	–	0.93	3	3.58	11.5	15	7.59	0.11
765	K 4-47	04 20 45.157	+56 18 11.57	0.264	1.525	7.8	3.7	–	7.7	22.46	0.849
766	K 4-48	06 39 55.879	+11 06 30.69	–	0.707	2.2	3.11	11.8	14	8.86	0.095
770	K 4-57	22 48 34.363	+58 29 08.18	1.46	1.081	–	3.41	–	–	–	–
771	K 4-8	18 54 20.003	−08 47 33.17	–	0.229	–	2.91	3.1	–	–	–
773	KjPn 2	20 15 22.209	+40 34 44.76	0.093	0.661	–	3.36	7.3	–	–	–
781	LoTr 5	12 55 33.745	+25 53 30.60	0.137	–	10.6	–	–	5.6	8.69	0.447
798	MA 13	18 30 30.388	−07 27 38.29	0.182	–	–	–	28.7	–	–	–
800	MA 3	18 17 49.379	−06 48 21.55	–	0.564	–	3.19	6.3	–	–	–
801	MGP 1	16 48 48.548	−35 00 57.39	–	0.601	9	3.26	14.7	10.2	–	–
802	M 1-1	01 37 19.430	+50 28 11.50	–	0.433	4.5	2.92	14	8	7.27	0.159
803	M 1-11	07 11 16.693	−19 51 02.87	6.754	31.786	2.2	5.52	25.9	113	4.9	0.052
804	M 1-12	07 19 21.471	−21 43 55.46	1.03	5.606	1.8	4.21	21.9	41	7.13	0.062
805	M 1-13	07 21 14.952	−18 08 36.91	–	0.502	10	3.31	18.9	15	4.51	0.219
807	M 1-16	07 37 18.955	−09 38 49.67	0.195	1.148	3.6	3.67	31.3	31	5.71	0.1
808	M 1-17	07 40 22.206	−11 32 29.81	0.204	0.982	2.5	3.57	18.3	17	8.23	0.1
810	M 1-19	17 03 46.809	−33 29 43.75	–	1.881	2.8	3.8	23.2	20	–	–
811	M 1-2	01 58 49.675	+52 53 48.57	0.861	1.862	0.5	3.64	–	10	–	–
814	M 1-24	17 38 11.588	−19 37 37.64	0.243	3.627	<10	4.34	43.5	–	–	–
815	M 1-25	17 38 30.307	−22 08 38.88	0.237	–	3.2	–	39.9	57	4.93	0.076
816	M 1-26	17 45 57.653	−30 12 00.58	–	104.933	3.2	7.32	66	400	2.42	0.038
817	M 1-27	17 46 45.450	−33 08 35.06	0.446	–	8	–	64.9	63	3.74	0.145
818	M 1-29	17 50 18.003	−30 34 54.90	–	4.343	8.2	4.21	91.5	97	3.3	0.131
820	M 1-31	17 52 41.440	−22 21 56.83	0.435	5.727	2.3	4.23	28.8	60.5	–	–
821	M 1-32	17 56 19.980	−16 29 03.95	1.481	8.938	9	4.63	70.1	61	3.17	0.138
822	M 1-33	17 58 58.794	−15 32 14.79	0.495	4.194	4	4.03	49	60	4.63	0.09
823	M 1-34	18 01 22.193	−33 17 43.08	–	0.575	11.2	3.68	13.6	14.7	5.95	0.323
824	M 1-35	18 03 39.255	−26 43 33.47	0.514	3.572	<25	4.06	54	54	4.63	–
825	M 1-37	18 05 25.801	−28 22 04.19	0.208	3.508	2.5	4.06	10.9	15	8.44	0.102
826	M 1-38	18 06 05.765	−28 40 29.28	–	3.049	3.5	4.06	14.9	24	6.58	0.112
827	M 1-39	18 07 30.699	−13 28 47.61	0.692	–	4	–	58.2	100	3.92	0.076
828	M 1-4	03 41 43.428	+52 17 00.28	0.284	1.806	6	3.89	77.8	90	3.39	0.099
829	M 1-40	18 08 25.994	−22 16 53.25	1.187	11.344	4.5	4.75	163.3	208	2.83	0.062
831	M 1-42	18 11 05.028	−28 58 59.33	–	0.9	9	3.53	28.3	28.5	4.89	0.213
833	M 1-44	18 16 17.365	−27 04 32.47	0.336	0.841	4	3.37	9.4	9	9.24	0.179
834	M 1-45	18 23 07.984	−19 17 05.26	–	3.09	2.5	4.04	15.1	19	7.43	0.09
835	M 1-46	18 27 56.339	−15 32 54.43	0.327	–	11.5	–	78.1	81	2.58	0.144
838	M 1-5	05 46 50.000	+24 22 02.32	0.86	4.338	2.3	3.98	41.1	71	5.49	0.061
839	M 1-50	18 33 20.886	−18 16 36.86	0.285	2.153	5.6	3.95	35.4	50	4.12	0.112
841	M 1-52	18 33 58.542	−14 52 25.02	–	0.303	43.1	3.17	7.8	319	5.93	1.24
842	M 1-53	18 35 48.267	−17 36 08.71	0.126	1.422	6	4.16	19.6	8	3.93	0.114
843	M 1-54	18 36 08.357	−16 59 57.02	0.215	0.933	13	3.57	35.5	53	3.09	0.195
844	M 1-55	18 36 42.550	−21 48 59.09	1.613	0.475	<25	3.07	–	38	–	–
845	M 1-56	18 37 46.250	−17 05 46.55	0.195	2.641	1.5	3.84	14.6	22	9.48	0.069
846	M 1-57	18 40 20.248	−10 39 47.17	0.413	5.209	8	4.37	53.9	70	3.21	0.125
847	M 1-58	18 42 56.979	−11 06 53.10	0.229	–	6.4	–	37.7	60	3.69	0.114
848	M 1-59	18 43 20.178	−09 04 48.64	0.899	3.844	4.8	4.03	90.1	108	3.54	0.082
849	M 1-6	06 35 45.140	−00 05 37.37	1.139	5.895	3	4.25	54.4	86	4.7	0.068
851	M 1-61	18 45 55.072	−14 27 37.93	–	13.886	1.8	4.81	32.5	97	5.59	0.049
852	M 1-62	18 50 26.030	−22 34 22.54	–	0.23	1.5	2.39	13.5	12.8	–	–
855	M 1-65	18 56 33.639	+10 52 10.05	–	1.665	4	3.79	21	23	5.94	0.115
856	M 1-66	18 58 26.247	−01 03 45.70	0.215	–	2.7	–	45.7	59	5.39	0.071
857	M 1-67	19 11 30.881	+16 51 38.21	0.955	–	120.4	–	217.6	250	0.69	0.403
858	M 1-69	19 13 53.961	+03 37 41.90	0.23	1.813	–	3.85	31.4	–	–	–
859	M 1-7	06 37 20.955	+24 00 35.38	–	0.422	11	3.18	18.5	13	4.5	0.24
860	M 1-71	19 36 26.927	+19 42 23.99	1.507	15.253	3	4.89	83.8	204	–	–
861	M 1-72	19 41 33.975	+17 45 17.71	0.547	6.554	0.7	4.25	5.3	30	12.54	0.043
862	M 1-73	19 41 09.323	+14 56 59.37	0.16	3.83	6	4.27	47.7	43	4.17	0.121
863	M 1-74	19 42 18.874	+15 09 08.16	0.292	3.285	1	3.99	7.9	29	10.15	0.049
864	M 1-75	20 04 44.086	+31 27 24.42	0.187	0.739	14	3.81	36.5	26.2	3.32	0.225
865	M 1-77	21 19 07.360	+46 18 47.24	1.874	6.154	8	5.23	29.4	25	4.29	0.166
866	M 1-78	21 20 44.809	+51 53 27.88	19.514	226.731	6	8.41	363.5	1103.9	1.62	0.047
868	M 1-8	06 53 33.795	+03 08 26.96	–	0.303	18.4	2.92	16.3	23	3.06	0.273
869	M 1-80	22 56 19.806	+57 09 20.68	–	0.336	8	2.96	17.9	25	4.29	0.166
870	M 1-9	07 05 19.204	+02 46 59.16	0.113	0.941	2.3	3.34	22.4	27	7.22	0.081
873	M 2-12	17 24 01.451	−25 59 23.16	–	2.228	4.4	3.85	10.3	12.9	–	–
874	M 2-13	17 28 34.188	−13 26 20.82	–	0.888	1.5	3.35	9.7	13	10.68	0.078
876	M 2-15	17 46 54.449	−16 17 24.80	–	0.87	7.4	3.64	18.7	12.5	5.37	0.193
877	M 2-16	17 52 34.362	−32 45 51.10	–	1.38	2.5	3.56	20.4	24.8	5.86	0.071
878	M 2-17	17 52 04.896	−17 36 05.23	0.107	–	8	–	10.6	10	5.57	0.216
879	M 2-18	17 53 37.844	−32 58 47.93	–	1.349	1.5	3.69	11.1	17	9.4	0.068
880	M 2-19	17 53 45.619	−29 43 46.34	0.182	0.52	7.5	3.27	10.5	14	7.4	0.269
881	M 2-2	04 13 15.045	+56 56 58.08	0.31	1.828	6.5	4.57	52	54	3.66	0.115
882	M 2-20	17 54 25.422	−29 36 08.20	0.127	1.934	16.4	3.83	22.2	3.2	–	–
883	M 2-21	17 58 09.565	−29 44 20.08	0.305	0.789	3	3.42	20.3	23	7.01	0.102
884	M 2-22	17 58 32.634	−33 28 36.60	–	0.49	5.2	2.92	9.1	6.5	9.87	0.249

TABLE 1 (CONTINUED)

KN	NAME	R.A. (2000)	DEC (2000)	F (9 μm)	F (18 μm)	θ	MN_18	F(1.4 GHz)	F(5 GHz)	DIST	DIAM
		H:M:S	D:M:S	Jy	Jy	arcsec	arcsec	mJy	mJy	kpc	pc
885	M 2-23	18 01 42.610	−28 25 43.90	–	6.155	8.8	3.98	4.2	41	8.38	0.358
886	M 2-24	18 02 02.881	−34 27 47.07	–	3.19	6.8	3.94	3.2	3	11.79	0.389
888	M 2-26	18 03 11.844	−26 58 30.23	–	0.398	7	2.76	7.9	5	9.43	0.32
889	M 2-27	18 03 52.588	−31 17 46.54	–	3.369	3.8	4	22.5	50	5.65	0.104
890	M 2-28	18 05 02.695	−30 58 17.39	–	0.508	5.3	3.22	11.3	10	8.39	0.216
891	M 2-29	18 06 40.862	−26 54 55.95	–	1.179	<5	4.08	9.4	8	9.98	–
892	M 2-30	18 12 34.414	−27 58 11.59	0.131	0.924	3.5	3.4	13.9	14	8.1	0.137
893	M 2-31	18 13 16.026	−25 30 04.97	0.223	1.653	4	3.66	39.6	51	4.91	0.095
894	M 2-32	18 14 50.617	−32 36 55.21	–	0.585	<10	3.29	9.5	–	–	–
895	M 2-33	18 15 06.534	−30 15 32.89	–	1.138	5	3.77	11.9	12	8.52	0.207
898	M 2-36	18 17 41.418	−29 08 19.59	0.218	–	6.8	–	22.6	13	6.99	0.23
900	M 2-38	18 19 25.162	−26 35 19.92	–	0.522	8	3.2	7.5	8	8.13	0.315
901	M 2-39	18 22 01.148	−24 10 40.18	0.211	0.802	3.2	3.37	7.2	8	10.21	0.158
902	M 2-4	17 01 06.231	−34 49 38.58	0.194	2.996	2	3.87	24.5	32	7.15	0.069
903	M 2-40	18 21 23.851	−06 01 55.79	–	3.62	5.5	4.19	45.5	33	4.67	0.125
905	M 2-42	18 22 32.020	−24 09 28.40	–	0.455	3.9	3.08	9.6	14	7.83	0.148
906	M 2-43	18 26 40.048	−02 42 57.63	9.659	32.6	1.5	5.68	20.4	237	5	0.036
907	M 2-44	18 37 36.908	−03 05 55.96	0.385	2.105	8	3.89	48.3	54	3.45	0.134
908	M 2-45	18 39 21.837	−04 19 50.90	0.76	6.161	6.4	4.28	107	154	2.64	0.082
909	M 2-46	18 46 34.620	−08 28 01.85	0.111	0.455	4.4	3.12	13.1	12	6.48	0.138
910	M 2-47	19 13 34.559	+04 38 04.45	0.18	2.89	6	4.04	38.3	45	4.12	0.12
911	M 2-48	19 50 28.543	+25 54 30.21	–	0.376	4	2.79	16.9	19	7	0.136
912	M 2-49	21 43 17.624	+50 25 14.57	0.408	1.202	2.5	3.5	28.2	35	6.47	0.078
913	M 2-5	17 02 19.069	−33 10 05.01	0.202	–	5	–	14.1	12	7.69	0.186
914	M 2-50	21 57 41.814	+51 41 39.01	–	0.183	4.6	2.45	8.2	6.5	8.07	0.18
916	M 2-52	22 20 30.745	+57 36 21.62	–	0.133	13.5	2.39	14.9	14	3.97	0.26
917	M 2-53	22 32 17.720	+56 10 26.12	–	0.291	18	2.74	14.6	11	3.64	0.318
918	M 2-54	22 51 38.923	+51 50 42.50	0.22	6.06	–	4.19	5.4	8	14.61	–
920	M 2-6	17 04 18.326	−30 53 28.71	–	0.751	2	3.15	13.6	17	–	–
922	M 2-8	17 05 30.673	−32 32 08.30	0.231	0.921	4	3.5	16.2	18	7.27	0.141
923	M 2-9	17 05 37.952	−10 08 34.58	38.07	73.255	17.5	6.93	37.1	36	3.01	0.255
924	M 3-1	07 02 49.980	−31 35 31.50	–	0.21	11.2	2.71	25.7	24	3.78	0.205
925	M 3-10	17 27 20.152	−28 27 51.15	0.311	2.611	3.1	3.81	35.2	29	6.33	0.095
926	M 3-12	17 36 22.634	−21 31 12.22	–	0.616	7.5	3.01	11.2	12.5	6.98	0.254
927	M 3-13	17 41 36.594	−22 13 02.46	0.862	1.893	<7	3.73	–	–	–	–
928	M 3-14	17 44 20.598	−34 06 40.59	0.344	1.89	4	3.91	22.6	30	6.47	0.125
930	M 3-17	17 56 25.640	−31 04 16.82	–	1.075	<5	3.43	10	12	9	–
931	M 3-19	17 58 19.337	−30 00 39.32	–	0.8	7	3.5	7.9	7.4	8.62	0.293
933	M 3-20	17 59 19.318	−28 13 48.05	0.091	–	4	–	16.2	40	5.3	0.103
934	M 3-21	18 02 32.324	−36 39 12.24	0.265	2.617	<5	3.92	15.6	30	5.57	–
935	M 3-22	18 02 19.238	−30 14 25.38	–	0.451	6.4	3.15	10.1	8.7	8.45	0.262
936	M 3-23	18 07 06.148	−30 34 16.96	0.231	1.245	11.5	3.85	30	28	4.58	0.255
937	M 3-24	18 07 53.914	−25 24 02.71	–	0.887	<25	3.4	17.4	–	–	–
938	M 3-25	18 15 16.967	−10 10 09.47	0.831	–	1.5	–	25	76	6.89	0.05
939	M 3-26	18 16 11.405	−27 14 57.46	–	0.479	7	2.96	8.1	8	8.4	0.285
940	M 3-27	18 27 48.273	+14 29 06.06	0.21	0.996	1	3.55	–	53.2	8.55	0.041
941	M 3-28	18 32 41.288	−10 05 50.03	–	1.446	9	5.11	–	33	4.87	0.212
945	M 3-31	18 44 01.767	−19 54 52.52	–	1.205	<10	3.44	–	9	14.79	–
946	M 3-32	18 44 43.127	−25 21 33.85	0.159	0.705	7.5	3.27	12.2	12	7.06	0.257
947	M 3-33	18 48 12.131	−25 28 52.39	–	0.47	6	3.32	9.8	7.5	8.94	0.26
948	M 3-34	19 27 01.897	−06 35 04.63	0.154	1.764	8	3.91	29.6	29	4.12	0.16
949	M 3-35	20 21 03.769	+32 29 23.86	3.437	16.454	1.5	4.97	29.5	140	5.62	0.041
950	M 3-36	17 12 39.152	−25 43 37.39	–	0.577	3.2	3.22	4.9	3.5	13.92	0.216
953	M 3-39	17 21 11.505	−27 11 38.13	1.177	–	19	–	279.4	280	1.7	0.157
956	M 3-41	17 25 59.784	−29 21 50.15	–	1.007	<25	3.35	11.3	75	4.15	–
958	M 3-43	17 50 24.297	−29 25 18.70	–	2.05	3.8	3.64	–	27.2	6.2	0.114
959	M 3-44	17 51 18.894	−30 23 52.99	0.342	6.899	4.2	4.35	24.3	35	–	–
960	M 3-45	17 52 05.927	−30 05 13.81	–	0.614	3.5	3	20.4	24.3	–	–
965	M 3-5	08 02 28.932	−27 41 55.44	–	0.286	7	2.91	11	10	5.9	0.2
969	M 3-53	18 24 07.890	−11 06 42.08	0.233	1.24	–	3.61	19.5	–	–	–
970	M 3-54	18 33 03.745	−13 44 19.95	–	0.422	5.6	3.01	8.6	8	6.92	0.188
972	M 3-6	08 40 40.205	−32 22 33.22	0.407	5.983	11	4.95	77.4	75	2.74	0.146
973	M 3-7	17 24 34.429	−29 24 19.47	0.096	1.553	5	3.08	32.9	28	5.41	0.131
974	M 3-8	17 24 52.152	−28 05 54.61	0.297	–	3.2	–	18	20	7.45	0.116
975	M 3-9	17 25 43.364	−26 11 55.47	0.364	2.22	16	3.81	37.3	35	3.88	0.301
976	M 4-10	18 34 13.821	−13 12 24.57	–	1.92	1.2	3.81	12.1	33	9.04	0.053
979	M 4-17	20 09 01.927	+43 43 43.54	–	0.447	–	3.36	20	–	–	–
980	M 4-18	04 25 50.831	+60 07 12.72	1.687	6.346	3.75	4.22	18.5	22	6.37	0.116
981	M 4-2	07 28 53.808	−35 45 13.92	–	0.481	6	3.25	24.2	19	5.26	0.153
983	M 4-4	17 28 50.344	−30 07 44.47	0.088	–	–	–	13.9	9.8	–	–
985	M 4-7	17 51 44.663	−31 36 00.18	–	0.775	5.7	3.18	38	33	5.2	0.144
986	M 4-8	18 12 09.587	−10 42 58.30	0.117	2.155	1.4	3.67	10.7	19	10.21	0.069
989	MaC 1-11	18 14 50.890	−22 43 55.43	–	0.399	–	3.01	12.2	–	–	–
990	MaC 1-13	18 28 35.242	−08 43 22.82	–	0.683	–	3.5	30.4	–	–	–
1000	MeWe 1-7	16 47 57.070	−50 42 48.32	–	0.356	–	3.3	–	–	–	–
1003	Me 1-1	19 39 09.813	+15 56 48.13	0.45	0.931	4.7	3.46	36	45.1	4.58	0.104
1004	Me 2-1	15 22 19.274	−23 37 31.34	–	0.93	7	3.55	33.6	30	4.32	0.147
1005	Me 2-2	22 31 43.686	+47 48 03.96	0.606	2.556	1.2	3.85	16	40	8.56	0.05
1006	MyCn 18	13 39 35.116	−67 22 51.45	0.862	10.869	12.6	4.66	–	106	3.23	0.197
1007	My 60	10 31 33.390	−55 20 50.87	0.244	1.646	7.6	4.29	–	60	3.47	0.128
1009	Mz 2	16 14 32.433	−54 57 03.76	–	1.763	23	5.5	–	75	2	0.223
1010	Mz 3	16 17 13.392	−51 59 10.31	55.324	267.948	25.4	8.95	–	649	1.03	0.127
1014	NGC 1535	04 14 15.762	−12 44 22.03	1.037	5.562	18.4	8.8	167.8	160	1.77	0.158
1015	NGC 2022	05 42 06.229	+09 05 10.75	0.371	3.789	19.4	6.04	92.3	91	2.02	0.19
1017	NGC 2346	07 09 22.547	−00 48 22.98	0.505	0.595	54.6	3.64	37.6	86	2.07	0.548
1019	NGC 2392	07 29 10.768	+20 54 42.44	0.476	4.368	44.8	6.48	279.9	251	1.44	0.313

TABLE 1 (CONTINUED)

KN	NAME	R.A. (2000)	DEC (2000)	F (9 μm)	F (18 μm)	θ	MN_18	F(1.4 GHz)	F(5 GHz)	DIST	DIAM
		H:M:S	D:M:S	Jy	Jy	arcsec	arcsec	mJy	mJy	kpc	pc
1021	NGC 2452	07 47 26.248	−27 20 07.16	0.288	1.798	18.8	4.71	56	57	2.31	0.211
1024	NGC 2792	09 12 26.596	−42 25 39.90	0.399	3.618	13	5.13	–	116	1.26	0.079
1026	NGC 2867	09 21 25.337	−58 18 40.69	1.312	7.277	16	4.98	–	252	1.69	0.131
1028	NGC 3132	10 07 01.771	−40 26 11.11	0.883	3.437	45	8.18	–	230	1.5	0.327
1029	NGC 3195	10 09 20.910	−80 51 30.73	–	0.933	40	5.07	–	35	1.96	0.38
1030	NGC 3211	10 17 50.549	−62 40 14.57	0.286	2.113	16	4.52	–	228	1.7	0.132
1031	NGC 3242	10 24 46.138	−18 38 32.26	3.211	19.833	37.2	8.87	757.7	860	0.94	0.17
1034	NGC 3918	11 50 17.730	−57 10 56.90	2.747	27.613	18.8	6.14	–	859	1.17	0.107
1035	NGC 40	00 13 01.023	+72 31 19.07	–	54.443	36.4	9.48	510.3	460	0.98	0.173
1037	NGC 4361	12 24 30.754	−18 47 05.51	–	4.061	81	9.86	159.9	207	0.74	0.291
1039	NGC 5307	13 51 03.273	−51 12 20.62	0.26	2.349	12.6	4.41	–	95	2.42	0.148
1040	NGC 5315	13 53 56.972	−66 30 50.96	3.477	34.483	6	5.93	–	442	2.14	0.062
1042	NGC 5882	15 16 49.941	−45 38 58.60	2.331	17.353	14	5.78	–	334	1.74	0.118
1048	NGC 6210	16 44 29.521	+23 47 59.55	1.429	13.331	16.2	5.64	297.8	311	1.55	0.122
1050	NGC 6309	17 14 04.322	−12 54 37.71	–	6.375	17	5.63	131.5	151	2.35	0.194
1051	NGC 6326	17 20 46.301	−51 45 15.33	0.248	1.149	12	4.03	–	70	2.71	0.158
1053	NGC 6369	17 29 20.443	−23 45 34.22	7.301	43.871	28	8.47	1825	2002	0.75	0.102
1054	NGC 6439	17 48 19.797	−16 28 44.21	0.37	–	5	–	51.5	55	4.64	0.112
1056	NGC 6537	18 05 13.059	−19 50 34.86	4.099	26.593	4.7	5.63	427.5	640	1.77	0.04
1057	NGC 6543	17 58 33.409	+66 37 58.79	5.539	57.323	18.8	7.39	771.5	850	1.12	0.102
1059	NGC 6565	18 11 52.470	−28 10 42.27	–	1.057	9.2	3.88	47	37	4.36	0.194
1060	NGC 6567	18 13 45.136	−19 04 33.67	1.778	4.466	8.8	4.19	163	168	2.4	0.102
1061	NGC 6572	18 12 06.404	+06 51 12.17	9.597	93.442	10	7.06	557.5	1374	1.06	0.051
1062	NGC 6578	18 16 16.517	−20 27 02.67	1.357	–	8.6	–	158.2	170	2.31	0.096
1063	NGC 6620	18 22 54.186	−26 49 17.00	0.146	0.802	5	3.43	17.1	20.5	6.42	0.156
1064	NGC 6629	18 25 42.449	−23 12 10.59	0.799	–	15	–	257.8	275	1.84	0.134
1065	NGC 6644	18 32 34.641	−25 07 44.00	–	5.547	2.8	5.22	64.3	97	4.09	0.056
1067	NGC 6741	19 02 37.088	−00 26 56.97	0.682	4.923	8	4.25	131.9	230	2.32	0.09
1068	NGC 6751	19 05 55.560	−05 59 32.92	1.398	11.455	21	5.54	55.1	63	2.18	0.222
1071	NGC 6778	19 18 24.939	−01 35 47.41	0.463	1.644	15.8	4.39	64.6	55	2.54	0.195
1073	NGC 6790	19 22 56.965	+01 30 46.45	6.636	21.477	1.8	5.22	52.6	290	4.1	0.036
1074	NGC 6803	19 31 16.490	+10 03 21.88	0.603	5.242	5	4.15	68.9	114	3.26	0.079
1076	NGC 6807	19 34 33.543	+05 41 02.58	0.22	2.85	0.8	3.94	8	29	11.18	0.043
1077	NGC 6818	19 43 57.844	−14 09 11.91	0.851	6.01	18.2	5.55	290.2	300	1.47	0.13
1078	NGC 6826	19 44 48.161	+50 31 30.33	2.539	24.006	25.4	8.75	414.4	385	1.2	0.148
1083	NGC 6879	20 10 26.682	+16 55 21.30	0.111	0.831	5	3.59	23.1	18	5.78	0.14
1084	NGC 6881	20 10 52.464	+37 24 41.18	0.972	9.369	2.6	4.5	70.4	120	4.48	0.056
1085	NGC 6884	20 10 23.669	+46 27 39.54	0.743	6.356	5.3	4.46	152.4	200	2.7	0.069
1086	NGC 6886	20 12 42.813	+19 59 22.65	0.543	4.595	5.5	4.24	77.6	108	2.94	0.078
1087	NGC 6891	20 15 08.838	+12 42 15.63	0.345	4.865	10.2	5.14	110.8	105	2.35	0.116
1089	NGC 6905	20 22 22.940	+20 06 16.80	–	2.166	40.4	6.79	66.7	52	1.62	0.317
1091	NGC 7009	21 04 10.877	−11 21 48.25	5.275	31.698	28.2	7.24	682	750	1.09	0.149
1093	NGC 7027	21 07 01.696	+42 14 09.50	173.674	977.249	12.5	9.36	1362.4	5200	0.64	0.039
1098	NGC 7354	22 40 19.940	+61 17 08.10	2.748	15.223	20	6.85	581	579	1.19	0.115
1099	NGC 7662	23 25 53.968	+42 32 05.04	2.377	15.165	20	6.74	611.5	631	1.17	0.113
1100	Na 1	17 12 51.900	−03 16 00.13	0.083	0.569	8	3.37	23	22.5	4.2	0.163
1105	PB 1	07 02 46.764	−13 42 34.65	–	0.639	–	3.92	11.9	18	–	–
1106	PB 10	19 28 14.391	+12 19 36.17	0.322	2.045	8	3.94	50.4	50	3.53	0.137
1107	PB 2	08 20 40.188	−46 22 58.82	0.164	0.562	3	3.18	–	40	5.75	0.084
1108	PB 3	08 54 18.323	−50 32 22.34	0.256	1.635	7	3.84	–	70	3.4	0.115
1109	PB 4	09 15 07.747	−54 52 43.78	0.243	1.444	11.2	4.12	–	71	2.81	0.153
1110	PB 5	09 16 09.613	−45 28 42.79	3.014	11.328	5	4.71	–	107	–	–
1111	PB 6	10 13 15.949	−50 19 59.28	0.33	3.205	11	4.18	–	30	3.55	0.189
1112	PB 8	11 33 17.717	−57 06 14.00	0.16	2.536	5	4.06	–	27	5.15	0.125
1113	PB 9	19 27 44.814	+10 24 20.82	0.103	1.029	7	3.74	33.1	40	3.57	0.121
1114	PC 11	16 37 42.697	−55 42 26.49	1.164	5.76	5	4.03	–	11	–	–
1115	PC 12	16 43 53.781	−18 57 11.89	–	1.994	2.2	3.8	14.8	19	8.6	0.092
1117	PC 14	17 06 14.767	−52 30 00.40	0.136	0.809	7	3.64	–	30	4.32	0.147
1118	PC 17	17 35 41.677	−46 59 48.54	–	1.063	5	3.58	–	14.7	6.12	0.148
1120	PC 20	18 43 03.456	−00 16 37.02	0.212	1.123	–	3.59	27.3	–	–	–
1122	PC 22	19 42 03.514	+13 50 37.33	–	0.458	–	3.73	9.2	–	–	–
1123	PC 23	19 51 52.770	+32 59 17.48	0.053	0.691	2.2	3.27	10	21	8.06	0.086
1124	PC 24	20 19 38.133	+27 00 11.23	0.184	0.953	5	3.52	17.1	18	5.78	0.14
1127	PM 1-188	17 54 21.100	−15 55 51.78	6.838	4.779	–	3.92	–	–	–	–
1128	PM 1-276	19 02 17.857	+10 17 34.49	–	1.065	–	4.78	15.3	–	–	–
1129	PM 1-295	19 19 18.760	+17 11 48.09	–	2.02	–	5.32	13.9	–	–	–
1130	PM 1-310	19 38 52.135	+25 05 32.63	0.4	–	–	–	–	–	–	–
1132	PM 1-89	15 19 08.724	−53 09 50.05	0.584	6.983	–	4.53	–	–	–	–
1136	Pe 1-1	10 38 27.607	−56 47 06.40	0.846	8.744	3	4.48	–	125.3	4.16	0.061
1137	Pe 1-11	18 01 42.767	−33 15 26.30	–	0.779	9	3.51	10.9	8	7.9	0.345
1141	Pe 1-15	18 46 24.485	−07 14 34.57	0.079	0.722	5	3.49	8.3	8	7.4	0.179
1142	Pe 1-16	18 47 32.251	−06 54 03.52	–	0.555	–	3.33	14.2	–	–	–
1144	Pe 1-18	18 48 46.454	−05 56 07.71	0.486	–	1.1	–	6.6	42	8.44	0.045
1145	Pe 1-19	18 49 44.643	−07 01 35.03	–	0.366	3.9	3.15	4.8	6	8.42	0.158
1146	Pe 1-2	10 39 32.690	−57 06 13.70	0.269	2.818	–	4.1	–	–	–	–
1147	Pe 1-20	18 57 17.351	−05 59 51.79	–	0.191	8.4	2.51	5.1	29.4	4.52	0.183
1148	Pe 1-21	18 57 49.642	−05 27 39.73	–	0.396	8.6	2.81	6.3	30	3.95	0.165
1151	Pe 1-7	16 30 25.852	−46 02 51.10	2.801	23.646	5	5.27	–	117	–	–
1152	Pe 1-8	17 06 22.558	−44 13 09.96	–	2.47	–	5.23	–	–	–	–
1158	Pe 2-14	18 29 59.545	−19 40 37.74	–	0.527	–	3.13	3.7	–	–	–
1160	Pe 2-4	09 30 48.402	−53 09 59.33	0.11	0.663	–	3.34	–	–	–	–
1162	Pe 2-7	10 41 19.574	−56 09 16.34	0.043	0.511	–	3.18	–	–	–	–
1163	Pe 2-8	15 23 42.860	−57 09 25.02	6.342	39.225	1.6	5.99	–	100	5.83	0.045
1167	SaSt 1-1	08 31 42.877	−27 45 31.70	–	1.819	–	3.77	–	0.3	–	–
1168	SaSt 2-12	17 03 02.870	−53 55 54.16	0.175	1.161	–	3.59	–	–	–	–
1169	SaSt 2-3	07 48 03.683	−14 07 40.40	–	0.151	–	2	4	1.4	–	–

TABLE 1 (CONTINUED)

KN	NAME	R.A. (2000)	DEC (2000)	F (9 μm)	F (18 μm)	θ	MN_18	F(1.4 GHz)	F(5 GHz)	DIST	DIAM
		H:M:S	D:M:S	Jy	Jy	arcsec	arcsec	mJy	mJy	kpc	pc
1173	Sa 1-5	17 11 27.372	−47 25 01.58	–	0.364	–	2.4	–	–	–	–
1175	Sa 1-8	18 50 44.312	−13 31 02.18	–	1.15	5.6	3.8	13.5	11	6.33	0.172
1178	Sa 2-237	17 44 42.282	−15 45 11.45	0.703	2.588	–	4	5.4	–	–	–
1179	Sa 3-134	18 29 19.823	−15 07 39.97	0.083	0.927	–	3.54	2.7	–	–	–
1185	ShWi 2-5	18 03 53.660	−29 51 21.89	0.468	0.8	–	3.16	–	–	–	–
1191	Sn 1	16 21 04.421	−00 16 10.54	–	0.426	3	2.95	10.4	7	9.42	0.137
1193	Sp 3	18 07 15.793	−51 01 10.41	–	1.411	35.6	5.04	–	61	1.75	0.302
1196	StWr 4-10	16 02 13.042	−41 33 35.94	–	0.373	–	2.85	–	–	–	–
1198	Ste 2-1	10 11 57.662	−52 38 17.09	–	0.257	–	2.91	–	–	–	–
1201	SwSt 1	18 16 12.237	−30 52 08.71	9.268	52.915	1.3	6.25	26.7	216	3.79	0.024
1203	Tc 1	17 45 35.298	−46 05 23.81	1.197	5.695	15	5.81	–	801	1.39	0.101
1207	Te 1580	17 43 39.442	−25 36 42.51	–	0.658	–	3.35	11.3	–	–	–
1208	Te 2022	17 42 42.541	−29 51 34.65	–	46.919	–	9.09	–	–	–	–
1209	Te 2111	17 48 28.465	−24 41 25.07	–	0.627	–	3.32	20.7	–	–	–
1212	Th 2-A	13 22 33.854	−63 21 00.96	0.457	1.866	23	5.33	–	60	2.07	0.231
1214	Th 3-10	17 24 40.846	−30 51 59.47	0.153	1.635	2	3.5	21.6	29.5	7.11	0.069
1216	Th 3-12	17 25 06.093	−29 45 16.87	–	0.825	1.8	3.34	2.6	3.5	–	–
1217	Th 3-13	17 25 19.341	−30 40 41.79	–	4.774	2	3.99	7.4	14.3	–	–
1218	Th 3-14	17 25 44.060	−26 57 47.69	0.122	2.248	1.4	3.8	5.8	4	–	–
1221	Th 3-19	17 28 41.787	−28 27 19.32	–	0.967	2	3.4	9.9	4.2	14.64	0.142
1222	Th 3-23	17 30 21.340	−29 10 12.57	–	0.847	–	3.18	46.2	–	–	–
1224	Th 3-25	17 30 46.716	−27 05 59.12	–	0.841	2	3.4	14.9	18	8.77	0.085
1226	Th 3-27	17 35 58.467	−24 25 29.15	–	1.729	3.2	3.69	14.4	13.5	–	–
1228	Th 3-32	17 35 15.533	−28 07 01.70	–	1.842	–	3.73	10.2	–	–	–
1229	Th 3-33	17 35 48.123	−27 43 20.38	–	2.064	–	4.01	4.2	–	–	–
1230	Th 3-35	17 38 42.168	−28 42 45.33	0.259	2.482	–	3.8	10.7	–	–	–
1232	Th 3-55	17 30 58.838	−31 01 05.73	–	1.201	–	3.65	9.8	6.1	–	–
1234	Th 4-1	17 46 20.804	−20 13 48.08	0.227	–	<10	–	–	–	–	–
1235	Th 4-10	17 57 06.599	−18 06 43.43	–	0.562	–	2.94	4.3	–	–	–
1238	Th 4-3	17 48 37.390	−22 16 48.79	–	1.015	–	3.53	2.7	–	–	–
1239	Th 4-6	17 50 57.220	−18 46 48.13	–	0.332	–	2.81	5.9	6.1	–	–
1240	Th 4-7	17 52 22.569	−21 51 13.43	–	0.276	7	2.89	8.8	18.4	–	–
1241	Th 4-9	17 56 00.589	−19 29 26.60	0.595	1.13	–	3.41	3.1	–	–	–
1244	V-V 3-5	18 36 32.291	−19 19 28.01	0.152	0.693	–	3.67	11.6	10	–	–
1250	VBe 3	15 52 59.209	−56 24 27.19	–	0.196	–	2.44	–	–	–	–
1251	VY 2-1	18 27 59.603	−26 06 48.29	–	2.003	3.7	3.81	32.4	37	–	–
1252	Vd 1-1	16 42 33.429	−38 54 31.83	0.149	–	<10	–	6.8	–	–	–
1253	Vd 1-2	16 46 45.141	−38 36 58.10	0.253	4.186	–	3.98	2.7	–	–	–
1255	Vd 1-4	16 50 25.324	−39 08 18.87	0.253	0.556	–	3.09	4.2	–	–	–
1256	Vd 1-5	16 51 33.575	−40 02 56.01	–	0.139	–	2.62	3.7	–	–	–
1257	Vd 1-6	16 54 27.327	−38 44 11.23	–	0.643	–	3.21	11.2	–	–	–
1259	Ve 26	08 43 28.087	−46 06 39.72	1.509	13.141	–	4.86	–	–	–	–
1260	Vo 1	06 59 26.405	−79 38 47.20	17.523	47.264	–	6.18	–	–	–	–
1261	Vo 2	08 16 10.000	−39 51 50.67	0.145	1.134	–	3.69	60.9	–	–	–
1263	Vo 4	13 53 23.072	−60 33 47.40	–	0.849	–	3.61	–	–	–	–
1264	Vy 1-1	00 18 42.167	+53 52 20.03	0.133	0.761	6	3.66	19.8	28.9	5.34	0.155
1265	Vy 1-2	17 54 22.994	+27 59 57.99	0.105	0.786	4.6	3.3	11.1	–	–	–
1266	Vy 1-4	18 54 01.899	−06 26 19.81	–	1.182	4.5	3.9	19.7	22	6.01	0.131
1267	Vy 2-2	19 24 22.229	+09 53 56.66	7.85	56.233	0.6	6.47	5.9	50	9.82	0.029
1268	Vy 2-3	23 22 57.952	+46 53 58.24	–	0.38	4.6	3.29	6.5	3	9.95	0.222
1272	WeSb 4	18 50 40.302	−01 03 11.16	–	0.566	–	3.71	4.3	–	–	–
1287	WhMe 1	19 14 59.755	+17 22 46.01	7.89	13.232	–	4.79	–	–	–	–
1291	Wray 16-128	13 24 21.922	−57 31 19.29	–	0.898	–	4.08	–	–	–	–
1293	Wray 16-199	16 00 22.002	−48 15 35.29	–	0.974	–	3.49	–	–	–	–
1298	Wray 16-286	17 33 00.666	−36 43 52.54	–	3.591	–	3.87	10.7	–	–	–
1303	Wray 16-93	11 30 48.339	−59 17 04.63	–	0.248	–	2.86	–	–	–	–
1306	Wray 17-18	08 23 53.825	−45 31 10.70	–	0.311	–	2.88	–	–	–	–
1311	Y-C 2-5	08 10 41.628	−20 31 32.16	–	0.176	–	2.55	7.1	4.5	–	–

The longer wave FIS identifications are listed in Table 2, where apart from the Kerber et al. (2003) number, and PNe names and coordinates (Columns 1–4), we include photometry at 65, 90, 140 and 160 μm (Columns 5–8). The data have been assigned four levels of quality FQUAL, where FQUAL = 0 corresponds to "non-detections"; FQUAL = 1 implies that the source was not confirmed; FQUAL = 2 is for sources which are confirmed, but for which fluxes are unreliable; and FQUAL = 3 is for high quality fluxes, where the source is confirmed and the flux is reliable. We list sources for which at least one of the four channels has a FQUAL value of 3, and for these cases, include all of the fluxes corresponding to FQUAL = 1–3. As an example, the detection at 90 μm may have been assigned a FQUAL value of 3, but FQUAL factors for the other three channels (65, 140 and 160 μm) may be as low as 1. However, although this photometric listing is relatively complete, and provides more and less reliable results, we have used only FQUAL = 3 fluxes for the analysis below. The FQUAL values for the 65, 90, 140 and 160 μm channels are consecutively indicated in Column 9, whilst the remaining columns define the radio fluxes, distances and diameters described above.

The noise in these results again derives from absolute uncertainties in the fluxes, and relative errors deriving from a variety of instrumental causes, in-

TABLE 2

GALACTIC PNE IDENTIFIED IN THE AKARI FIS CATALOGUE

KN	NAME	R.A. (2000)	DEC (2000)	F (65 μm)	F (90 μm)	F (140 μm)	F (160 μm)	QUAL	DIAM	F (1.4 GHz)	F(5 GHz)	DIST	DIAM
		H:M:S	D:M:S)	Jy	Jy	Jy	Jy		arcsec	mJy	mJy	kpc	pc
1	000.6+08.8	17 14 09.788	−23 31 53.41	1.04	1.86	1.987	2.565	1311	–	10.7	–	–	–
3	008.1+08.2	17 33 35.332	−17 41 16.23	1.046	1.678	0.757	2.497	1311	–	7.5	–	–	–
6	050.6+19.7	18 08 20.083	+24 10 43.26	2.136	1.05	0.462	–	1311	–	–	–	–	–
7	099.3−01.9	22 04 12.301	+53 04 01.36	10.186	8.225	2.369	1.474	3311	–	–	–	–	–
10	341.4−09.0	17 35 02.502	−49 26 26.38	46.648	22.854	5.621	5.089	3331	–	–	–	–	–
11	A 12	06 02 20.045	+09 39 14.09	2.902	3.487	2.301	2.519	1311	37	38.3	36	2.04	0.37
18	A 2	00 45 34.678	+57 57 34.88	–	0.672	0.008	0.334	1311	30.9	7.6	2.3	4.68	0.7
21	A 23	07 43 17.984	−34 45 15.64	–	0.964	0.067	0.835	1311	54	4.2	6.8	2.74	0.72
23	A 26	08 09 01.644	−32 40 24.91	0.253	1.234	1.051	3.25	1311	40	22.5	2.4	4.11	0.8
27	A 30	08 46 53.514	+17 52 45.47	89.781	56.794	26.965	21.707	3333	4.47	–	2.3	2.55	0.06
35	A 40	16 48 34.515	−21 00 50.67	1.165	1.264	2.47	0.438	1311	34	4.5	2	10.2	1.68
41	A 46	18 31 18.290	+26 56 12.86	0.826	0.95	1.52	0.955	1321	63.4	–	5	2.74	0.84
44	A 49	18 53 28.292	−06 28 46.83	0.499	1.17	2.701	–	1311	45	–	–	–	–
47	A 52	19 04 32.342	+17 57 07.13	0.767	1.299	–	–	1311	–	3.4	–	–	–
48	A 53	19 06 45.910	+06 23 52.47	11.713	10.097	19.476	–	3331	31	33.6	85.7	1.68	0.25
50	A 55	19 10 25.768	−02 20 23.46	0.944	2.171	1.047	0.451	1311	54	10.8	6	2.98	0.78
52	A 57	19 17 05.733	+25 37 33.41	0.179	0.415	0.24	–	1311	36.9	2.2	–	–	–
53	A 58	19 18 20.476	+01 46 59.62	26.646	20.791	6.876	3.949	3331	–	–	–	–	–
54	A 59	19 18 40.003	+19 34 32.95	0.467	1.613	2.13	0.899	1311	86.7	13.7	18	1.69	0.71
56	A 60	19 19 17.819	−12 14 36.78	0.209	0.455	0.214	–	1311	74	–	11	2.07	0.74
59	A 63	19 42 10.372	+17 05 14.52	0.532	1.765	1.095	0.782	1311	40	4.5	–	–	–
63	A 68	20 00 10.607	+21 42 55.43	0.636	1.132	–	0.537	1311	–	–	–	–	–
67	A 71	20 32 24.243	+47 21 02.83	–	0.943	1.042	0.91	1311	158	–	82.8	0.84	0.64
69	A 73	20 56 27.032	+57 26 03.05	0.452	1.309	1.011	0.272	1311	73.2	11	7.4	2.31	0.82
71	A 75	21 26 23.540	+62 53 31.83	0.977	2.389	1.605	2.082	1311	56	19.3	17	2.04	0.55
75	A 8	05 06 38.378	+39 08 10.77	–	0.371	–	–	1311	60	4.3	25.6	1.78	0.52
77	A 82	23 45 47.814	+57 03 59.22	0.249	0.755	2.635	1.16	1311	81	7.6	5.3	2.41	0.95
83	Al 2-E	17 30 14.398	−27 30 19.41	1.227	2.023	–	0.022	1311	–	14.7	–	–	–
91	Al 2-Q	17 53 25.040	−29 17 08.73	0.179	3.261	5.271	1.104	1311	–	2.3	–	–	–
94	Ap 1-12	18 11 35.088	−28 22 37.02	8.231	6.48	1.255	1.526	3311	12	6.6	18.7	5.34	0.31
95	Ap 2-1	18 58 10.459	+01 36 57.15	873.272	609.29	793.279	958.062	3333	40	195	320.4	1.13	0.22
97	BV 5-1	00 20 00.450	+62 59 03.16	1.283	1.029	1.138	2.259	1311	41.6	10.6	17.7	4.05	0.82
99	BV 5-3	01 53 03.432	+56 24 17.11	1.01	0.622	0.576	1.718	1311	–	2.7	–	–	–
102	Bl 2-1	22 20 16.638	+58 14 16.59	2.659	2.965	–	1.066	1311	1.6	21.6	54	6.94	0.05
105	Bl 3-15	17 52 35.947	−29 06 38.97	3.78	3.21	3.346	5.144	1311	–	–	–	–	–
106	Bl B	17 36 59.836	−29 40 08.93	5.691	5.45	6.249	2.798	1311	–	8.9	–	–	–
118	CTS 1	18 06 59.785	−08 55 32.80	4.706	4.048	0.471	1.589	3311	–	24	–	–	–
119	Cn 1-1	15 51 15.936	−48 44 58.67	13.214	10.516	4.745	0.806	3331	–	–	10	–	–
120	Cn 1-3	17 26 12.392	−44 11 24.52	3.458	3.029	–	–	3311	–	–	–	–	–
122	Cn 1-5	18 29 11.653	−31 29 59.21	6.379	6.339	2.788	–	3311	7	51	44	4.43	0.15
123	Cn 2-1	17 54 32.978	−34 22 20.84	2.975	2.954	–	0.611	3311	2.2	25.2	49	6.17	0.07
124	Cn 3-1	18 17 34.133	+10 09 03.99	7.298	5.991	1.936	2.188	3311	4.5	59.5	75	4	0.09
127	Dd 1	20 08 43.080	+42 30 11.19	0.819	1.087	–	–	1311	–	–	6	–	–
133	DuRe 1	12 45 51.211	−64 09 38.08	8.398	6.469	11.267	6.274	1331	–	–	–	–	–
138	ESO 040-11	13 34 14.128	−75 46 31.33	1.049	0.991	1.758	–	1311	–	–	–	–	–
150	Fg 1	11 28 36.205	−52 56 04.01	5.624	10.809	6.454	4.621	3331	16	–	55	2.02	0.16
151	Fg 2	17 39 19.847	−44 09 37.14	3.506	2.488	0.622	0.477	1311	–	–	–	–	–
152	Fg 3	18 00 11.819	−38 49 52.73	14.692	11.152	4.286	3.226	3331	2	42	107	–	–
156	G001.6−05.9	18 13 15.842	−30 25 58.49	–	0.428	0.472	0.942	1311	–	–	–	–	–
158	G002.5+05.1	17 32 12.788	−24 04 59.56	15.981	11.822	3.348	1.594	3311	–	–	–	–	–
163	G009.3+05.7	17 45 14.155	−17 56 46.57	56.19	40.015	15.844	12.064	3333	–	–	–	–	–
164	G010.2+07.5	17 41 00.035	−16 18 12.50	1.362	0.956	–	1.539	1311	–	–	–	–	–
165	G011.1−07.9	18 40 19.914	−22 54 29.23	0.841	1.638	0.297	0.189	1311	–	–	–	–	–
168	G013.1−13.2	19 04 43.548	−23 26 08.82	21.108	13.815	4.63	2.404	3331	–	–	–	–	–
171	G014.4−06.1	18 39 40.056	−19 14 12.04	1.014	1.202	1.2	–	1311	–	–	–	–	–
175	G017.0+11.1	17 42 14.430	−08 43 18.61	5.365	5.666	1.605	0.349	3311	–	23.4	–	–	–
179	G019.2−04.4	18 42 24.770	−14 15 11.81	2.374	2.789	0.666	1.03	1311	–	7.3	–	–	–
181	G022.0−04.3	18 47 03.954	−11 41 11.74	8.676	8.306	2.024	1.337	3311	–	8.4	–	–	–
185	G034.5−11.7	19 36 17.531	−03 53 25.26	3.814	2.615	3.426	0.975	3311	–	8.8	–	–	–
186	G038.4+01.8	18 54 54.139	+05 48 11.29	–	2.998	–	–	1311	–	20.5	–	–	–
188	G039.1−02.2	19 10 53.284	+04 27 28.50	1.248	2.49	–	–	1311	–	11	–	–	–
191	G044.1+01.5	19 06 32.146	+10 43 23.93	1.413	3.034	4.193	–	1311	–	19.4	–	–	–
193	G047.2+01.7	19 11 35.828	+13 31 11.58	5.784	4.889	–	–	3311	–	–	–	–	–
202	G069.2+01.2	20 00 41.998	+32 27 41.23	1.094	1.588	–	–	1311	–	17	–	–	–
204	G076.6−05.7	20 48 16.627	+34 27 24.36	8.115	7.002	2.067	–	3311	–	–	–	–	–
207	G095.0−05.5	21 56 32.945	+47 36 13.40	0.858	0.472	–	–	1311	–	–	–	–	–
211	G124.0+02.9	01 02 24.488	+65 46 32.81	2.184	2.741	4.239	3.567	1311	–	7.4	–	–	–
221	G222.8−04.2	06 54 13.406	−10 45 38.27	1.878	1.168	0.744	0.631	1311	–	2.7	–	–	–
226	G255.3−03.6	08 06 28.339	−38 53 23.93	1.622	1.085	0.289	1.12	1311	–	2.8	–	–	–
228	G260.1+00.2	08 37 24.599	−40 38 07.46	4.072	4.911	2.082	0.131	3311	–	–	–	–	–
229	G270.1−02.9	08 59 02.971	−50 23 39.68	1.001	1.265		–	1311	–	–	–	–	–
231	G277.1−01.5	09 37 51.861	−54 27 08.59	1.247	1.106	–	–	1311	–	–	–	–	–
232	G279.1−00.4	09 53 27.058	−54 52 39.60	1.616	2.185	2.079	0.076	1311	–	–	–	–	–
234	G282.6−00.4	10 13 19.673	−56 55 32.24	3.692	3.317	6.231	1.671	1311	–	–	–	–	–
235	G285.1−02.7	10 19 32.466	−60 13 29.41	77.86	58.749	36.452	16.57	3333	–	–	–	–	–
236	G290.7+00.2	11 10 25.122	−60 15 36.85	10.823	13.328	28.365	19.063	3333	–	–	–	–	–
241	G308.5−03.5	13 46 25.712	−65 46 24.26	1.892	1.935	0.503	0.551	1311	–	–	–	–	–
246	G316.2+00.8	14 38 19.980	−59 11 46.12	17.965	12.604	7.104	2.124	3311	–	–	–	–	–
248	G326.4+01.0	15 19 43.867	−48 59 54.65	0.844	2.367	–	0.838	1311	–	–	–	–	–
251	G328.4−02.8	16 09 20.143	−55 36 09.84	10.647	9.904	5.721	6.032	3311	–	–	–	–	–
253	G331.3−12.1	17 16 21.107	−59 29 23.35	2.504	1.926	0.895	1.7	3311	–	–	–	–	–
264	G347.9−06.0	17 40 03.329	−42 24 05.58	1.674	1.07	–	0.135	1311	–	–	–	–	–
267	G351.5−06.5	17 52 09.386	−39 32 14.52	1.246	2.017	0.941	0.884	1311	–	–	–	–	–

TABLE 2 (CONTINUED)

KN	NAME	R.A. (2000)	DEC (2000)	F (65 μm)	F (90 μm)	F (140 μm)	F (160 μm)	QUAL	DIAM	F (1.4 GHz)	F(5 GHz)	DIST	DIAM
		H:M:S	D:M:S)	Jy	Jy	Jy	Jy		arcsec	mJy	mJy	kpc	pc
270	G352.6−04.9	17 47 52.679	−37 48 03.10	0.685	0.733	–	1.812	1311	–	3.7	–	–	–
275	G353.6−03.6	17 44 35.434	−36 14 01.67	0.631	1.004	1.947	1.427	1311	–	–	–	–	–
294	G356.8−03.0	17 50 10.734	−33 14 17.97	4.956	2.522	0.54	4.026	1311	–	4.2	–	–	–
299	G358.3−07.3	18 11 39.900	−34 00 21.99	–	0.701	–	0.763	1311	–	–	–	–	–
302	G358.7+05.1	17 22 43.615	−27 13 36.67	7.125	4.881	3.383	2.801	3311	–	–	–	–	–
307	G359.4−08.5	18 19 26.331	−33 37 04.86	0.298	0.974	–	0.672	1311	–	4.5	–	–	–
310	G000.5+01.9	17 39 31.219	−27 27 46.77	5.529	3.087	3.93	10.456	1311	–	6.8	–	–	–
323	G003.1+04.1	17 37 20.167	−24 03 27.84	1.6	1.494	0.414	0.727	1311	–	5.1	–	–	–
326	G003.6+04.9	17 35 31.198	−23 11 47.62	0.551	1.164	2.137	–	1311	–	4.6	–	–	–
332	G035.4+03.4	18 43 36.599	+03 46 39.24	5.368	5.503	3.326	0.518	3311	–	5.1	–	–	–
359	H 1-11	17 21 17.693	−22 18 35.32	3.175	2.96	2.676	–	3311	6	20.7	13	7.27	0.21
367	H 1-19	17 30 02.546	−27 59 17.54	5.167	4.576	–	1.333	3311	1.4	11.6	26	8.19	0.06
368	H 1-2	16 48 54.091	−35 47 09.01	6.754	7.334	3.178	5.698	3331	1	14.3	62	–	–
369	H 1-20	17 30 43.799	−28 04 06.68	3.73	3.436	–	–	3311	3.3	26.9	43.9	5.12	0.08
372	H 1-23	17 32 46.897	−30 00 15.07	5.346	2.646	1.913	0.27	1311	2.6	24.5	34.8	6.12	0.08
373	H 1-24	17 33 37.565	−21 46 24.78	2.864	4.191	1.34	0.725	1311	5	5.1	15	7.32	0.18
375	H 1-27	17 40 17.926	−22 19 17.64	4.632	4.237	2.276	1.683	3311	5.2	–	18	10.9	0.27
376	H 1-28	17 42 54.066	−39 36 24.04	0.741	1.613	0.91	0.82	1311	–	5.4	–	–	–
378	H 1-3	16 53 31.347	−42 39 23.45	6.802	6.116	14.597	–	1311	15.8	–	–	1.36	0.1
379	H 1-30	17 45 06.782	−38 08 49.48	0.047	2.454	2.628	1.4	1311	<5	7	81.3	5.21	–
380	H 1-31	17 45 32.104	−34 33 55.32	1.182	1.808	3.421	2.872	1311	0.7	6	16	11.8	0.04
385	H 1-36	17 49 48.172	−37 01 29.47	3.996	3.046	1.295	–	1311	0.8	11.8	50	–	–
390	H 1-40	17 55 36.049	−30 33 32.08	8.689	7.947	3.121	2.002	3311	3	8.1	31	7.84	0.11
391	H 1-41	17 57 19.145	−34 09 49.12	1.409	2.46	–	1.307	1311	9.6	16.6	12	6.6	0.31
392	H 1-42	17 57 25.169	−33 35 42.94	1.873	2.163	1.065	1.6	1311	5.8	34.5	40	4.82	0.14
394	H 1-44	17 58 10.641	−31 42 56.08	3.517	3.355	–	–	3311	<5	8	–	–	–
396	H 1-46	17 59 02.490	−32 21 43.42	2.175	1.824	1.577	–	3311	1.2	18.3	43	7.11	0.04
399	H 1-50	18 03 53.461	−32 41 42.15	2.527	1.911	0.001	–	3311	1.4	19.6	31	7.68	0.05
404	H 1-55	18 07 14.542	−29 41 24.51	2.607	2.827	4.162	1.519	1311	10	2.5	5.3	–	–
405	H 1-56	18 07 53.880	−29 44 34.26	1.409	1.586	1.4	–	1311	3	8.3	7.8	10.98	0.16
408	H 1-59	18 11 29.263	−27 46 15.69	1.006	1.115	0.501	–	1311	6	3.4	4.2	11.12	0.32
412	H 1-62	18 13 17.951	−32 19 42.74	4.164	3.569	–	2.715	3311	–	11.9	–	–	–
413	H 1-63	18 16 19.336	−30 07 35.98	1.399	0.981	–	1.129	1311	–	2.5	9	–	–
416	H 1-66	18 24 57.539	−25 41 55.76	1.68	2.448	2.442	4.279	1313	<10	10.4	6	9.5	–
417	H 1-67	18 25 04.976	−22 34 52.64	1.245	1.916	2.312	–	1311	6	12.2	11.9	7.51	0.22
418	H 1-7	17 10 27.389	−41 52 49.42	–	42.37	33.76	10.955	131	–	–	–	–	–
429	H 2-17	17 40 07.428	−24 25 42.57	3.915	2.947	1.795	–	3311	4	8.2	10	8.88	0.17
437	H 2-27	17 51 50.576	−33 47 35.59	2.026	4.543	5.283	3.193	1311	–	7.9	–	–	–
438	H 2-29	17 53 16.794	−32 40 38.56	0.841	1.959	1.309	0.054	1311	–	2.6	–	–	–
442	H 2-33	17 58 12.535	−31 08 05.99	1.633	2.283	–	–	1311	8	8.1	5	9.71	0.38
443	H 2-35	18 00 18.259	−34 27 39.29	0.161	0.981	2.435	0.421	1311	–	–	–	–	–
444	H 2-36	18 04 07.936	−31 39 13.70	0.939	1.627	1.844	1.4	1311	–	3.4	–	–	–
449	H 2-42	18 12 23.255	−26 32 54.02	1.024	1.992	0.43	3.923	1311	–	3.1	–	–	–
453	H 2-46	18 18 37.444	−31 54 45.42	0.751	0.772	–	2.136	1311	25	–	–	–	–
454	H 2-48	18 46 35.149	−23 26 48.24	3.332	2.115	1.08	–	3311	2	31.6	66	6.23	0.06
456	H 2-8	17 24 45.766	−21 33 35.80	–	0.443	2.309	–	1311	–	4.8	–	–	–
457	H 3-29	04 37 23.484	+25 02 40.94	2.391	1.128	–	3.097	1311	21	18.3	18	3.4	0.35
463	HaTr 13	19 08 02.149	+02 21 24.25	0.226	1.281	0.982	1.832	1311	–	3.6	–	–	–
464	HaTr 14	19 09 13.670	+07 05 44.86	1.974	1.872	–	–	1311	–	–	–	–	–
465	HaTr 2	15 30 18.542	−61 01 38.79	0.808	1.883	1.534	–	1311	–	–	–	–	–
467	HaTr 4	16 45 00.155	−51 12 19.83	0.422	1.93	3.937	3.937	1331	–	–	–	–	–
474	Hb 12	23 26 14.814	+58 10 54.65	28.818	19.707	6.499	3.075	3331	0.8	–	45	10.46	0.04
475	Hb 4	17 41 52.763	−24 42 08.07	13.541	14.269	0.952	1.287	3311	7.3	157.6	170	2.68	0.09
477	Hb 6	17 55 07.023	−21 44 39.98	20.768	14.246	6.261	2.636	1311	6	190.5	243	2.45	0.07
479	He 1-1	19 23 46.875	+21 06 38.60	1.896	2.307	–	–	1311	8	16	14	–	–
480	He 1-2	19 26 37.757	+21 09 27.04	4.268	3.83	3.69	2.034	3311	4.7	14.6	15	–	–
481	He 1-3	19 48 26.422	+22 08 37.62	3.687	3.402	–	–	1311	8	53.5	–	–	–
482	He 1-4	19 59 18.014	+31 54 39.14	2.196	3.218	–	–	3311	–	16.1	–	–	–
484	He 1-6	20 17 21.424	+25 21 46.78	–	0.59	0.228	–	1311	22.4	5	20.3	2.91	0.32
486	He 2-102	13 58 13.866	−58 54 31.78	3.526	5.212	–	0.187	3311	9	–	33	3.77	0.16
487	He 2-104	14 11 52.077	−51 26 24.18	5.304	5.412	2.607	1.568	3311	5	–	15	–	–
488	He 2-105	14 15 24.803	−74 12 46.61	2.007	2.755	0.431	0.625	1311	31	–	14	2.67	0.4
490	He 2-108	14 18 08.889	−52 10 39.76	11.056	11.255	2.98	–	3311	11	–	32	3.49	0.19
491	He 2-109	14 20 48.916	−55 27 59.21	0.507	0.868	1.644	1.676	1311	7.4	–	15.8	6.41	0.23
492	He 2-11	08 37 08.445	−39 25 08.09	14.232	29.419	9.803	8.864	3333	65	343.6	444.6	0.77	0.24
494	He 2-112	14 40 30.924	−52 34 56.66	5.436	5.861	2.376	1.855	3311	14.6	–	82	2.36	0.17
495	He 2-113	14 59 53.523	−54 18 07.20	146.924	75.968	29.685	20.859	3333	–	–	115	–	–
496	He 2-114	15 04 08.800	−60 53 18.78	2.378	3.831	2.893	13.696	1331	36.6	–	11	2.8	0.5
497	He 2-115	15 05 16.775	−55 11 10.39	9.04	7.229	3.019	0.869	3311	3	–	156	3.91	0.06
499	He 2-117	15 05 59.193	−55 59 16.53	30.411	20.756	7.71	–	3331	5	–	267	2.69	0.07
503	He 2-123	15 22 19.360	−54 08 12.77	13.454	14.537	6.106	5.808	3331	4.6	–	110	3.59	0.08
504	He 2-125	15 23 36.326	−53 51 27.95	2.858	3.458	1.854	0.569	1311	3	–	20.4	6.96	0.1
505	He 2-128	15 25 07.841	−51 19 42.29	1.343	1.317	–	2.54	1311	5	–	40	–	–
506	He 2-129	15 25 32.677	−52 50 37.96	1.332	1.958	0.083	1.087	1311	1.6	–	35	7.85	0.06
507	He 2-131	15 37 11.210	−71 54 52.89	52.897	32.153	10.413	6.777	3331	6	–	325	2.2	0.06
508	He 2-132	15 38 01.182	−58 44 42.07	5.143	6.911	3.164	–	3311	17.8	–	25	3.02	0.26
509	He 2-133	15 41 58.788	−56 36 25.72	19.455	12.659	2.857	3.351	3311	<10	–	210	3.18	–
510	He 2-136	15 52 10.666	−62 30 46.94	–	1.052	–	–	1311	10	–	23	–	–
511	He 2-138	15 56 01.694	−66 09 09.23	37.174	27.055	8.317	5.173	3333	7	–	76	3.61	0.12
512	He 2-140	15 58 08.063	−55 41 50.13	11.771	8.42	–	0.219	1311	2.6	–	80	5.03	0.06
513	He 2-141	15 59 08.762	−58 23 53.15	2.406	2.797	0.987	1.007	3311	13.8	–	51	2.77	0.19
514	He 2-142	15 59 57.608	−55 55 32.89	8.916	8.153	1.037	0.116	1311	3.6	–	65	4.75	0.08
519	He 2-149	16 14 24.266	−54 47 38.82	–	1.02	–	–	1311	3	–	10	8.52	0.12
520	He 2-15	08 53 30.701	−40 03 42.08	8.855	13.475	7.766	8.121	3331	23.8	94.5	105	1.92	0.22
521	He 2-151	16 15 42.269	−59 54 00.96	4.698	3.035	–	–	3311	5	–	10	–	–
522	He 2-152	16 15 20.031	−49 13 20.76	59.168	34.701	25.057	26.453	1333	11	–	196	2.09	0.11

TABLE 2 (CONTINUED)

KN	NAME	R.A. (2000)	DEC (2000)	F (65 μm)	F (90 μm)	F (140 μm)	F (160 μm)	QUAL	DIAM	F (1.4 GHz)	F(5 GHz)	DIST	DIAM
		H:M:S	D:M:S)	Jy	Jy	Jy	Jy		arcsec	mJy	mJy	kpc	pc
524	He 2-155	16 19 23.101	−42 15 35.98	3.768	6.096	1.291	–	3311	14.6	–	70	2.47	0.17
525	He 2-157	16 22 14.264	−53 40 54.09	2.612	2.42	–	0.963	1311	<5	–	30	6.24	–
526	He 2-158	16 23 30.605	−58 19 22.64	1.124	0.807	–	0.634	1311	2	–	2.7	14.71	0.14
528	He 2-161	16 24 37.786	−53 22 34.14	6.164	4.563	1.665	–	1311	10	–	32	3.64	0.18
530	He 2-163	16 29 31.333	−59 09 25.08	0.548	0.936	–	–	1311	<25	–	3.4	5.08	–
531	He 2-164	16 29 53.255	−53 23 15.37	4.289	4.731	4.26	5.638	1311	16	–	97	2.17	0.17
532	He 2-165	16 30 00.057	−54 09 28.00	1.498	2.651	2.271	5.82	1311	50	–	15.9	2.2	0.53
534	He 2-170	16 35 21.170	−53 50 11.11	1.035	1.091	–	–	1311	5	–	15	–	–
536	He 2-175	16 39 28.112	−36 34 16.41	8.23	8.479	3.012	1.863	3331	6.6	19.2	26.8	4.58	0.15
537	He 2-18	09 08 40.050	−53 19 13.91	0.712	1.44	0.206	0.118	1311	11	–	–	–	–
538	He 2-182	16 54 35.167	−64 14 28.43	0.723	0.97	0.501	–	1311	10	–	62	–	–
539	He 2-185	17 01 17.254	−70 06 03.35	0.31	0.532	0.323	–	1311	10	–	18	–	–
540	He 2-186	16 59 36.064	−51 42 06.46	1.573	1.378	0.342	–	1311	3	–	21	6.9	0.1
541	He 2-187	17 01 36.976	−50 22 57.49	0.606	2.288	1.562	1.152	1311	6	–	–	–	–
545	He 2-25	09 18 01.308	−54 39 29.01	1.808	1.355	1.19	0.091	1311	4.4	–	827.9	2.07	0.04
546	He 2-250	17 34 54.710	−26 35 56.92	2.625	3.212	–	0.965	3311	5	15.3	15	7.01	0.17
549	He 2-28	09 22 06.825	−54 09 38.60	1.481	1.19	0.504	0.84	1311	10	–	20	4.15	0.2
551	He 2-306	17 56 33.706	−43 03 18.90	2.165	1.648	0.535	–	1311	–	–	–	–	–
553	He 2-34	09 41 13.997	−49 22 47.18	1.043	0.693	1.428	–	1311	<10	–	–	–	–
554	He 2-35	09 41 37.504	−49 57 58.71	1.402	1.463	–	–	1311	5	–	20	5.61	0.14
555	He 2-36	09 43 25.538	−57 16 55.44	3.776	5.187	1.768	1.416	3311	22	–	90	3.1	0.33
556	He 2-37	09 47 24.987	−48 58 11.96	0.111	1.566	–	–	1311	23	–	22.6	2.8	0.31
557	He 2-39	10 03 49.164	−60 43 48.26	0.69	0.666	–	1.18	1311	–	–	–	–	–
561	He 2-428	19 13 05.239	+15 46 39.80	2.444	3.763	0.304	–	1311	8	26.7	7	6.16	0.24
562	He 2-429	19 13 38.422	+14 59 19.21	5.302	5.489	1.651	–	3311	4.2	58.5	64.9	4.33	0.09
563	He 2-430	19 14 04.197	+17 31 32.92	4.256	4.174	1.445	0.975	3311	1.7	18.2	40	7.36	0.06
564	He 2-432	19 23 24.821	+21 08 00.50	1.213	1.211	0.805	1.393	1311	2.3	21.3	32	6.88	0.08
565	He 2-434	19 33 49.420	−74 32 58.66	2.155	0.77	0.869	–	1311	10	–	–	–	–
567	He 2-437	19 32 57.657	+26 52 43.35	8.747	9.473	6.01	3.948	3331	–	6.6	–	–	–
568	He 2-440	19 38 08.403	+25 15 40.98	2.7	2.87	0.518	0.509	3311	2.2	26.4	43	6.45	0.07
570	He 2-447	19 45 22.164	+21 20 04.03	4.171	4.547	6.443	4.375	1131	1.2	22.9	60	7.63	0.04
571	He 2-459	20 13 57.898	+29 33 55.94	35.529	24.038	8.141	5.802	3331	1.3	13.9	64	7.24	0.05
572	He 2-47	10 23 09.143	−60 32 42.21	23.166	16.144	9.242	4.43	3331	5	–	170	–	–
575	He 2-50	10 34 19.002	−53 41 03.75	1.386	1.491	1.105	–	1311	<25	–	11.3	4.54	–
576	He 2-51	10 35 45.821	−64 19 11.74	1.019	1.942	2.329	2.343	1311	9	–	57	3.23	0.14
577	He 2-55	10 48 43.168	−56 03 10.21	0.961	1.151	0.498	0.539	1311	<25	–	–	–	–
581	He 2-64	11 27 24.259	−57 17 58.99	0.779	0.495	2.263	0.248	1311	–	–	–	–	–
582	He 2-67	11 28 47.369	−60 06 37.28	3.437	4.045	1.748	1.044	3311	5	–	41	–	–
583	He 2-68	11 31 45.427	−65 58 13.67	1.823	1.576	0.778	0.445	1311	10	–	34	–	–
584	He 2-7	08 11 31.890	−48 43 16.71	1.741	2.074	0.648	–	1311	44.6	–	47	2.91	0.63
586	He 2-71	11 39 11.198	−68 52 09.14	0.973	0.816	1.06	1.173	1311	5	–	12	–	–
588	He 2-73	11 48 38.191	−65 08 37.33	4.998	4.438	2.214	–	3311	4	–	76	4.23	0.08
589	He 2-76	12 08 25.433	−64 12 09.32	–	3.741	1.738	4.622	1311	–	–	–	–	–
590	He 2-78	12 09 10.196	−58 42 37.44	0.664	0.842	1.869	1.298	1311	–	–	–	–	–
591	He 2-81	12 23 01.237	−64 01 45.96	5.655	4.455	–	–	1311	<25	–	–	–	–
593	He 2-83	12 28 43.997	−62 05 35.05	13.117	8.492	1.805	2.953	3311	–	–	–	–	–
594	He 2-84	12 28 46.822	−63 44 37.22	–	3.755	6.61	9.376	1311	–	–	–	–	–
596	He 2-86	12 30 30.426	−64 52 05.58	18.48	14.073	3.369	–	3311	3.6	–	125	3.85	0.07
598	He 2-9	08 28 27.988	−39 23 40.27	5.928	4.829	0.147	1.568	3311	4.4	135.6	194.8	3.11	0.07
599	He 2-90	13 09 36.252	−61 19 35.96	12.683	9.68	7.373	11.11	1311	10	–	25	–	–
600	He 2-96	13 42 36.150	−61 22 29.18	18.266	13.075	5.562	3.139	3311	–	–	–	–	–
601	He 2-97	13 45 22.394	−71 28 56.13	1.942	1.843	–	–	1311	5	–	30	–	–
602	He 2-99	13 52 30.683	−66 23 26.49	8.545	7.715	3.001	2.34	3311	17	–	18	3.4	0.28
603	He 3-1333	17 09 00.932	−56 54 48.25	174.846	94.412	34.594	29.428	1333	–	–	26	–	–
606	Hf 39	10 53 59.586	−60 26 44.31	28.91	22.101	13.034	10.185	3331	–	–	–	–	–
607	Hf 48	11 03 55.979	−60 36 04.57	2.802	2.693	–	7.749	1311	–	–	–	–	–
608	Hu 1-1	00 28 15.614	+55 57 54.71	2.45	2.793	3.616	3.719	1311	10	28	26	3.86	0.19
609	Hu 1-2	21 33 08.349	+39 38 09.57	2.478	2.558	2.059	1.414	3311	6.5	107	155	2.53	0.08
610	Hu 2-1	18 49 47.562	+20 50 39.46	4.192	3.208	2.134	–	3311	1.8	42.6	110	4.52	0.04
611	IC 1295	18 54 37.206	−08 49 39.08	0.714	2.886	2.997	0.009	1311	100	45.9	44	1.18	0.57
612	IC 1297	19 17 23.459	−39 36 46.40	3.558	4.067	0.836	–	3311	7	59.4	68.9	3.75	0.13
613	IC 1454	22 42 24.997	+80 26 31.96	0.582	0.57	–	–	1311	34	3.3	1.3	5.29	0.87
614	IC 1747	01 57 35.896	+63 19 19.36	5.61	5.495	0.416	4.799	3311	13	85.8	124	2.23	0.14
615	IC 2003	03 56 21.984	+33 52 30.59	2.384	2.129	–	–	1311	10	54.8	30	3.89	0.19
616	IC 2149	05 56 23.908	+46 06 17.32	8.351	7.08	3.29	1.772	3331	8.4	177	280	2.03	0.08
617	IC 2165	06 21 42.775	−12 59 13.96	4.002	3.607	–	–	1311	9	180	188	2.47	0.11
618	IC 2448	09 07 06.261	−69 56 30.74	3.367	3.231	0.917	0.015	3311	10	–	73	3.41	0.17
619	IC 2501	09 38 47.213	−60 05 30.92	10.743	9.401	2.776	0.924	3331	2	–	261	2.09	0.02
620	IC 2553	10 09 20.856	−62 36 48.40	10.367	9.642	3.572	2.955	3311	9	–	92	2.85	0.12
621	IC 2621	11 00 20.111	−65 14 57.77	16.66	13.745	6.657	2.474	3331	5	–	195	2.94	0.07
622	IC 289	03 10 19.273	+61 19 00.91	7.28	8.816	1.371	0.208	3311	36.8	152	170	1.18	0.21
623	IC 351	03 47 33.143	+35 02 48.50	0.94	1.23	1.56	1.662	1311	7	31.9	27	4.45	0.15
624	IC 3568	12 33 06.834	+82 33 50.29	4.75	4.54	2.027	–	3311	18	94.1	95	2.47	0.22
626	IC 4191	13 08 47.343	−67 38 37.67	14.074	12.272	3.336	0.74	3331	14	–	172	1.95	0.13
627	IC 4406	14 22 26.278	−44 09 04.35	18.454	21.94	16.635	15.527	3333	20	–	110	1.5	0.15
628	IC 4593	16 11 44.545	+12 04 17.06	13.84	11.52	3.349	1.929	3311	12.8	90.6	92	2.42	0.15
629	IC 4634	17 01 33.572	−21 49 32.77	8.034	6.439	2.37	–	3311	5.5	116	100	3.47	0.09
630	IC 4637	17 05 10.506	−40 53 08.44	9.044	4.84	31.528	6.032	1331	18.6	–	132.5	2.29	0.21
631	IC 4642	17 11 45.025	−55 24 01.47	5.784	5.526	2.109	1.953	3311	16.6	–	60	2.52	0.2
633	IC 4673	18 03 18.408	−27 06 22.61	9.902	9.916	6.94	6.241	1311	16	53.4	62	3.12	0.24
634	IC 4699	18 18 32.024	−45 59 01.70	0.68	1.065	–	–	1311	5	–	20	4.91	0.12
636	IC 4846	19 16 28.220	−09 02 36.57	2.221	1.882	0.336	0.547	1311	2.9	38.7	43	5.72	0.08
637	IC 4997	20 20 08.741	+16 43 53.71	6.372	4.577	1.158	2.358	3311	2	30.1	127	5.45	0.05
638	IC 5117	21 32 31.027	+44 35 48.53	13.535	11.489	3.659	0.543	3111	1.5	34.1	210	5.01	0.04
639	IC 5217	22 23 55.725	+50 58 00.43	3.748	3.111	1.901	0.711	3311	6.5	50.4	163	2.71	0.09
640	IC 972	14 04 25.863	−17 13 40.84	0.633	0.604	0.214	0.676	1311	47	3.9	6.8	2.87	0.65

TABLE 2 (CONTINUED)

KN	NAME	R.A. (2000)	DEC (2000)	F (65 μm)	F (90 μm)	F (140 μm)	F (160 μm)	QUAL	DIAM	F (1.4 GHz)	F(5 GHz)	DIST	DIAM
		H:M:S	D:M:S)	Jy	Jy	Jy	Jy		arcsec	mJy	mJy	kpc	pc
644	J 900	06 25 57.275	+17 47 27.19	5.565	4.194	2.942	1.558	3311	6	107.8	100	3.29	0.1
651	KFL 13	18 12 44.988	−25 44 23.85	0.222	1.359	–	1.112	1311	–	4	3.5	–	–
652	KFL 14	18 13 01.106	−29 25 15.59	0.088	0.977	0.676	–	1311	–	–	1.5	–	–
660	KFL 9	18 07 19.381	−31 42 56.95	–	0.838	–	–	1311	–	2.8	3.1	–	–
666	K 1-14	17 42 36.757	+21 27 02.06	0.454	0.708	0.813	0.763	1311	47	–	–	–	–
669	K 1-17	19 03 37.362	+19 21 22.60	0.61	1.071	0.621	2.994	1311	45	4.6	–	–	–
672	K 1-21	08 04 14.193	−34 16 07.32	0.272	0.796	–	–	1311	29	6.5	5	3.88	0.55
681	K 2-16	16 44 49.050	−28 04 04.56	22.836	17.837	4.856	1.122	3331	–	–	–	–	–
684	K 2-5	17 54 26.179	−12 48 35.95	0.181	0.551	2.464	2.452	1311	24.6	4	3	–	–
686	K 3-1	18 23 21.721	+03 36 27.78	0.22	0.637	0.399	4.204	1311	5	5.4	5	8.31	0.2
687	K 3-11	18 41 07.311	−08 55 58.97	8.769	4.539	1.898	14.47	3111	3	14.5	17	7.33	0.11
693	K 3-18	19 00 34.829	−02 11 57.62	4.782	4.264	–	–	3311	3.5	–	11	13.98	0.23
695	K 3-2	18 25 00.576	−01 30 52.64	2.934	1.956	–	–	3311	2.8	25.9	31	6.37	0.09
696	K 3-20	19 02 10.154	−01 48 45.31	1.358	1.085	0.791	–	1311	–	6.3	–	–	–
697	K 3-21	19 02 40.327	+14 28 50.36	0.15	0.373	–	0.189	1311	–	–	–	–	–
699	K 3-24	19 12 05.820	+15 09 04.47	1.402	1.896	1.19	1.693	1311	6.2	8.5	–	–	–
700	K 3-26	19 14 39.178	+00 13 36.29	1.422	1.442	–	–	1311	–	6.4	0.5	–	–
702	K 3-29	19 15 30.561	+14 03 49.83	5.471	5.005	–	–	1311	1	13.9	65	8.07	0.04
703	K 3-3	18 27 09.338	+01 14 26.88	5.058	7.101	1.615	2.432	3311	10	35.9	34	3.43	0.17
704	K 3-30	19 16 27.691	+05 13 19.47	0.539	1.423	4.218	1.382	1311	3.3	12.1	23	6.46	0.1
705	K 3-31	19 19 02.666	+19 02 20.85	1.665	1.718	–	–	1311	1.5	16.8	39	7.83	0.06
708	K 3-35	19 27 44.036	+21 30 03.83	37.657	19.471	4.673	0.634	3311	1.7	14.5	60	6.56	0.05
709	K 3-36	19 32 39.557	+07 27 51.57	0.342	1.393	1.147	2.954	1311	–	3.1	0.2	–	–
710	K 3-37	19 33 46.749	+24 32 27.09	0.797	0.821	0.198	1.414	1311	2.5	14.4	17	7.93	0.1
711	K 3-38	19 35 18.354	+17 13 00.71	3.674	4.207	4.376	5.177	3311	5	28.7	31	5.09	0.12
712	K 3-39	19 35 54.469	+24 54 48.20	3.351	2.565	0.402	1.241	3311	1	3.6	11	13.35	0.06
713	K 3-4	18 31 00.227	+02 25 27.35	3.694	2.055	4.661	0.696	1311	21	17	21	–	–
714	K 3-40	19 36 21.828	+23 39 47.93	3.452	3.892	–	–	3311	4	17.1	20	6.18	0.12
717	K 3-43	19 40 25.908	+18 49 14.20	0.482	0.69	0.122	–	1311	3	4.8	0.4	–	–
720	K 3-49	19 54 00.702	+33 22 12.95	1.097	1.077	–	–	1311	–	5.5	7	34.5	–
721	K 3-5	18 31 45.833	+04 05 09.12	1.543	1.481	2.463	2.296	1311	10	6.7	3	7.11	0.34
723	K 3-52	20 03 11.435	+30 32 34.15	35.941	24.008	10.002	8.825	3331	0.7	16.9	65	9.42	0.03
724	K 3-53	20 03 22.475	+27 00 54.73	5.133	4.756	0.601	–	3311	0.9	10	69	9.27	0.04
726	K 3-55	20 06 56.210	+32 16 33.60	5.551	7.453	7.527	6.486	1311	8.2	86.6	90	2.96	0.12
728	K 3-57	20 12 47.679	+34 20 32.52	2.474	3.289	1.827	–	1311	6.3	46.8	60	3.72	0.11
729	K 3-58	20 21 58.324	+29 59 22.15	2.219	3.014	2.792	1.481	1311	4.8	5.4	–	–	–
730	K 3-6	18 33 17.490	+00 11 47.19	5.499	4.908	4.12	2.52	3311	0.7	10.4	55	10.2	0.03
732	K 3-61	21 30 00.710	+54 27 27.45	1.973	1.628	–	0.663	1311	6	16.6	14	5.73	0.17
733	K 3-62	21 31 50.203	+52 33 51.64	4.669	3.505	–	–	3311	2.5	59.5	115	4.62	0.06
734	K 3-63	21 39 11.976	+55 46 03.94	0.395	1.098	1.335	–	1311	7	8.5	29	–	–
735	K 3-64	04 13 27.255	+51 51 00.92	–	0.392	0.082	0.596	1311	–	–	–	–	–
737	K 3-66	04 36 37.243	+33 39 29.87	1.272	0.594	0.104	0.766	1311	2.1	15.4	18	8.42	0.09
738	K 3-67	04 39 47.905	+36 45 42.85	1.832	1.82	–	–	1311	2.2	33.3	42	6.49	0.07
740	K 3-69	05 41 22.147	+39 15 08.09	1.857	2.087	2.649	–	3311	0.5	2.9	0.4	13.87	0.03
741	K 3-7	18 34 13.601	−02 27 36.41	4.976	4.56	–	–	1311	6.3	29.5	30	4.52	0.14
742	K 3-70	05 58 45.350	+25 18 43.86	1.236	1.558	2.457	–	1311	1.6	4.4	6	–	–
746	K 3-76	20 25 04.865	+33 34 50.70	2.488	2.112	–	3.736	1311	0.2	5.1	12	–	–
747	K 3-78	20 45 22.710	+50 22 39.92	1.991	2.624	0.09	1.142	1311	3.8	14.9	15	6.85	0.13
750	K 3-82	21 30 51.636	+50 00 06.96	2.461	3.525	2.515	1.426	3311	24	35.6	30	2.49	0.29
751	K 3-83	21 35 43.877	+50 54 16.94	1.27	1.835	–	–	1311	5	4.7	6.5	7.71	0.19
752	K 3-84	21 38 49.006	+46 00 27.81	0.705	0.608	0.535	–	1311	–	2.7	–	–	–
754	K 3-88	23 12 15.494	+64 39 17.73	0.599	0.948	–	0.494	1311	–	7.1	0.3	–	–
755	K 3-90	01 24 58.628	+65 38 36.14	1.083	0.569	–	–	1311	8.5	12.4	13.9	4.6	0.19
757	K 3-92	02 03 41.171	+64 57 37.88	0.237	0.527	–	0.724	1311	13	–	2	7.11	0.45
759	K 3-94	03 36 08.086	+60 03 46.29	0.364	1.022	1.299	0.377	1311	10	6.9	5.5	5.98	0.29
761	K 4-19	19 13 22.624	+03 25 00.30	2.142	1.463	0.425	–	3311	–	–	–	–	–
764	K 4-41	19 56 34.027	+32 22 12.96	2.439	2.5	0.831	0.145	3311	3	11.5	15	7.59	0.11
765	K 4-47	04 20 45.157	+56 18 11.57	5.138	5.585	3.408	1.143	1331	7.8	–	7.7	22.46	0.85
766	K 4-48	06 39 55.879	+11 06 30.69	3.627	3.673	0.833	–	3311	2.2	11.8	14	8.86	0.09
768	K 4-53	20 42 16.744	+37 40 25.58	3.45	5.024	0.89	0.592	3311	–	34.4	–	–	–
769	K 4-55	20 45 10.021	+44 39 14.58	0.211	1.688	–	–	1311	–	6.2	–	–	–
775	KjPn 6	22 49 02.175	+67 01 38.89	0.518	0.873	1.165	1.764	1311	–	8	–	–	–
779	LoTr 10	14 46 20.239	−61 13 35.37	4.579	2.985	2.254	2.351	1311	–	–	–	–	–
782	LoTr 7	14 15 24.025	−67 31 55.87	0.13	0.861	1.249	1.025	1311	–	–	–	–	–
787	Lo 11	16 03 22.211	−36 00 53.73	0.205	1.758	1.073	–	1311	–	2.7	3.5	–	–
790	Lo 16	17 35 41.798	−40 11 26.20	3.656	10.988	4.495	10.058	3311	–	89.9	–	–	–
797	Lo 9	15 42 13.340	−47 40 46.33	0.121	0.63	–	0.09	1311	–	–	–	–	–
798	MA 13	18 30 30.388	−07 27 38.29	10.933	5.667	–	–	3311	–	28.7	–	–	–
799	MA 2	18 15 13.391	−06 57 12.20	1.006	1.304	0.076	0.792	1311	–	7.4	–	–	–
802	M 1-1	01 37 19.430	+50 28 11.50	0.993	0.51	–	1.437	1311	4.5	14	8	7.27	0.16
803	M 1-11	07 11 16.693	−19 51 02.87	18.8	15.084	3.463	1.214	3311	2.2	25.9	113	4.9	0.05
804	M 1-12	07 19 21.471	−21 43 55.46	3.723	2.383	1.515	–	3311	1.8	21.9	41	7.13	0.06
805	M 1-13	07 21 14.952	−18 08 36.91	2.662	4.368	3.749	–	1311	10	18.9	15	4.51	0.22
806	M 1-14	07 27 56.510	−20 13 22.89	2.101	1.844	1.666	0.876	3311	4.7	59.1	60	4.23	0.1
807	M 1-16	07 37 18.955	−09 38 49.67	8.731	7.022	7.089	6.625	3331	3.6	31.3	31	5.71	0.1
808	M 1-17	07 40 22.206	−11 32 29.81	3.93	3.522	2.095	3.194	3311	2.5	18.3	17	8.23	0.1
811	M 1-2	01 58 49.675	+52 53 48.57	1.513	1.075	0.416	0.094	1311	0.5	–	10	–	–
812	M 1-22	17 35 10.239	−18 34 20.41	2.072	1.918	–	2.497	1311	6	7.4	3.5	11.92	0.35
813	M 1-23	17 37 22.003	−18 46 41.87	2.195	3.146	2.712	–	1311	–	14.1	–	–	–
814	M 1-24	17 38 11.588	−19 37 37.64	7.928	7.466	0.478	0.707	3311	<10	43.5	–	–	–
815	M 1-25	17 38 30.307	−22 08 38.88	6.244	6.016	0.689	–	3311	3.2	39.9	57	4.93	0.08
819	M 1-30	17 52 58.946	−34 38 22.99	5.714	5.292	–	–	3311	3.5	23.4	31	5.9	0.1
822	M 1-33	17 58 58.794	−15 32 14.79	6.185	7.632	–	3.584	3311	4	49	60	4.63	0.09
823	M 1-34	18 01 22.193	−33 17 43.08	2.006	3.779	1.363	7.131	1311	11.2	13.6	14.7	5.95	0.32
826	M 1-38	18 06 05.765	−28 40 29.28	–	3.022	–	–	1311	3.5	14.9	24	6.58	0.11
828	M 1-4	03 41 43.428	+52 17 00.28	2.201	2.263	–	–	3311	6	77.8	90	3.39	0.1

TABLE 2 (CONTINUED)

KN	NAME	R.A. (2000)	DEC (2000)	F (65 μm)	F (90 μm)	F (140 μm)	F (160 μm)	QUAL	DIAM	F (1.4 GHz)	F(5 GHz)	DIST	DIAM
		H:M:S	D:M:S)	Jy	Jy	Jy	Jy		arcsec	mJy	mJy	kpc	pc
829	M 1-40	18 08 25.994	−22 16 53.25	44.078	20.96	–	7.625	3311	4.5	163.3	208	2.83	0.06
831	M 1-42	18 11 05.028	−28 58 59.33	5.007	7.279	8.013	4.503	3331	9	28.3	28.5	4.89	0.21
833	M 1-44	18 16 17.365	−27 04 32.47	5.194	5.412	6.768	2.805	1131	4	9.4	9	9.24	0.18
835	M 1-46	18 27 56.339	−15 32 54.43	19.466	12.055	3.57	4.934	3311	11.5	78.1	81	2.58	0.14
836	M 1-47	18 29 11.154	−21 46 53.43	1.007	1.099	–	–	1311	5.5	11.7	14	5.95	0.16
837	M 1-48	18 29 29.991	−19 05 44.58	1.291	2.036	2.169	1.771	1311	4.8	5	6	7.57	0.18
838	M 1-5	05 46 50.000	+24 22 02.32	2.046	1.733	0.522	–	1311	2.3	41.1	71	5.49	0.06
839	M 1-50	18 33 20.886	−18 16 36.86	2.416	3.361	0.749	0.299	1311	5.6	35.4	50	4.12	0.11
842	M 1-53	18 35 48.267	−17 36 08.71	3.355	4.38	4.325	0.782	3331	6	19.6	8	3.93	0.11
843	M 1-54	18 36 08.357	−16 59 57.02	5.805	6.572	5.373	4.726	3331	13	35.5	53	3.09	0.19
845	M 1-56	18 37 46.250	−17 05 46.55	3.028	3.273	0.56	3.358	3311	1.5	14.6	22	9.48	0.07
847	M 1-58	18 42 56.979	−11 06 53.10	5.187	4.822	–	0.323	3311	6.4	37.7	60	3.69	0.11
849	M 1-6	06 35 45.140	−00 05 37.37	3.831	2.361	3.46	–	3111	3	54.4	86	4.7	0.07
850	M 1-60	18 43 38.107	−13 44 48.64	6.538	6.621	0.146	1.54	3311	2.5	35.1	48	5.81	0.07
851	M 1-61	18 45 55.072	−14 27 37.93	11.311	9.759	–	1.401	3311	1.8	32.5	97	5.59	0.05
853	M 1-63	18 51 30.935	−13 10 36.81	1.535	1.661	1.588	–	1311	4.2	8.4	10.2	7.32	0.15
854	M 1-64	18 50 02.090	+35 14 36.10	0.761	0.51	0.321	2.018	1311	17	4.3	2.4	6	0.49
855	M 1-65	18 56 33.639	+10 52 10.05	2.434	1.681	1.962	0.76	3311	4	21	23	5.94	0.12
856	M 1-66	18 58 26.247	−01 03 45.70	2.414	2.583	–	14.087	1311	2.7	45.7	59	5.39	0.07
857	M 1-67	19 11 30.881	+16 51 38.21	26.235	28.609	16.751	8.822	3333	120.4	217.6	250	0.69	0.4
858	M 1-69	19 13 53.961	+03 37 41.90	3.234	3.032	–	–	3311	–	31.4	–	–	–
859	M 1-7	06 37 20.955	+24 00 35.38	3.427	5.261	4.004	2.22	3331	11	18.5	13	4.5	0.24
860	M 1-71	19 36 26.927	+19 42 23.99	14.339	11.593	3.032	4.86	1311	3	83.8	204	–	–
861	M 1-72	19 41 33.975	+17 45 17.71	3.039	2.61	–	0.131	3311	0.7	5.3	30	12.54	0.04
862	M 1-73	19 41 09.323	+14 56 59.37	6.896	7.01	2.241	–	3311	6	47.7	43	4.17	0.12
863	M 1-74	19 42 18.874	+15 09 08.16	2.335	1.682	–	–	1311	1	7.9	29	10.15	0.05
865	M 1-77	21 19 07.360	+46 18 47.24	8.792	7.776	1.68	0.532	3311	8	29.4	25	4.29	0.17
866	M 1-78	21 20 44.809	+51 53 27.88	843.838	742.643	243.538	250.943	1133	6	363.5	1103.9	1.62	0.05
867	M 1-79	21 37 01.500	+48 56 02.62	1.384	3.435	2.012	1.02	1311	31	21.8	19	2.62	0.39
868	M 1-8	06 53 33.795	+03 08 26.96	2.242	3.569	2.483	0.837	3311	18.4	16.3	23	3.06	0.27
869	M 1-80	22 56 19.806	+57 09 20.68	0.845	0.859	–	–	1311	8	17.9	25	4.29	0.17
870	M 1-9	07 05 19.204	+02 46 59.16	1.085	0.68	–	0.802	1311	2.3	22.4	27	7.22	0.08
871	M 2-10	17 14 07.022	−31 19 42.59	3.438	3.612	–	0.79	3311	2.2	11.6	9.1	10.71	0.11
872	M 2-11	17 20 33.252	−29 00 38.66	0.775	1.457	1.927	1.417	1311	2.2	17.4	22	7.32	0.08
873	M 2-12	17 24 01.451	−25 59 23.16	3.449	2.817	–	1.752	3311	4.4	10.3	12.9	–	–
875	M 2-14	17 41 57.252	−24 11 15.64	7.255	7.444	0.303	–	3311	2.2	22.4	39.1	–	–
876	M 2-15	17 46 54.449	−16 17 24.80	2.663	3.981	0.105	–	3311	7.4	18.7	12.5	5.37	0.19
877	M 2-16	17 52 34.362	−32 45 51.10	1.819	4.33	0.702	–	1311	2.5	20.4	24.8	5.86	0.07
881	M 2-2	04 13 15.045	+56 56 58.08	3.482	3.28	–	0.761	3311	6.5	52	54	3.66	0.12
886	M 2-24	18 02 02.881	−34 27 47.07	3.003	3.345	0.489	0.747	3311	6.8	3.2	3	11.79	0.39
889	M 2-27	18 03 52.588	−31 17 46.54	5.258	5.361	1.533	–	3311	3.8	22.5	50	5.65	0.1
892	M 2-30	18 12 34.414	−27 58 11.59	1.596	2.289	3.75	2.127	1311	3.5	13.9	14	8.1	0.14
893	M 2-31	18 13 16.026	−25 30 04.97	3.561	3.598	–	0.951	3311	4	39.6	51	4.91	0.1
895	M 2-33	18 15 06.534	−30 15 32.89	1.963	1.768	2.255	0.189	1331	5	11.9	12	8.52	0.21
896	M 2-34	18 17 15.947	−23 58 54.51	1.342	2.897	–	–	1311	<25	4.8	–	–	–
897	M 2-35	18 17 37.195	−31 56 46.86	–	0.643	–	0.424	1311	–	–	–	–	–
898	M 2-36	18 17 41.418	−29 08 19.59	3.903	3.904	0.449	1.042	3311	6.8	22.6	13	6.99	0.23
899	M 2-37	18 18 38.352	−28 08 01.00	0.83	1.565	2.636	–	1331	–	–	–	–	–
901	M 2-39	18 22 01.148	−24 10 40.18	2.212	1.762	0.729	–	3311	3.2	7.2	8	10.21	0.16
902	M 2-4	17 01 06.231	−34 49 38.58	3.778	3.978	0.977	–	3311	2	24.5	32	7.15	0.07
903	M 2-40	18 21 23.851	−06 01 55.79	7.267	7.246	3.168	–	1311	5.5	45.5	33	4.67	0.12
904	M 2-41	18 22 34.379	−30 43 29.66	1.289	1	0.666	2.018	1311	–	3	–	–	–
905	M 2-42	18 22 32.020	−24 09 28.40	1.337	1.655	1.41	–	1311	3.9	9.6	14	7.83	0.15
906	M 2-43	18 26 40.048	−02 42 57.63	13.475	9.881	4.454	0.769	3331	1.5	20.4	237	5	0.04
907	M 2-44	18 37 36.908	−03 05 55.96	5.521	5.483	–	2.237	1311	8	48.3	54	3.45	0.13
909	M 2-46	18 46 34.620	−08 28 01.85	2.976	4.938	2.008	2.894	3311	4.4	13.1	12	6.48	0.14
910	M 2-47	19 13 34.559	+04 38 04.45	3.707	4.756	0.071	0.869	3311	6	38.3	45	4.12	0.12
913	M 2-5	17 02 19.069	−33 10 05.01	5.407	5.084	2.977	–	3311	5	14.1	12	7.69	0.19
914	M 2-50	21 57 41.814	+51 41 39.01	0.367	0.487	–	0.47	1311	4.6	8.2	6.5	8.07	0.18
915	M 2-51	22 16 03.890	+57 28 33.75	2.498	5.809	7.035	6.729	3331	39.2	27.2	40.6	1.88	0.36
917	M 2-53	22 32 17.720	+56 10 26.12	1.772	2.662	1.949	1.464	1311	18	14.6	11	3.64	0.32
918	M 2-54	22 51 38.923	+51 50 42.50	4.945	3.546	0.724	0.357	3311	–	5.4	8	14.61	–
919	M 2-55	23 31 52.708	+70 22 10.11	1.845	3.756	3.575	1.759	1331	41	25.4	19	2.31	0.46
921	M 2-7	17 05 13.729	−30 32 18.46	1.162	1.162	1.019	–	1311	<25	6	7	8.55	–
924	M 3-1	07 02 49.980	−31 35 31.50	0.68	1.457	0.27	1.05	1311	11.2	25.7	24	3.78	0.21
925	M 3-10	17 27 20.152	−28 27 51.15	2.65	2.658	–	2.107	1311	3.1	35.2	29	6.33	0.1
926	M 3-12	17 36 22.634	−21 31 12.22	2.522	2.64	0.961	0.396	3311	7.5	11.2	12.5	6.98	0.25
927	M 3-13	17 41 36.594	−22 13 02.46	1.684	1.432	–	–	1311	<7	–	–	–	–
933	M 3-20	17 59 19.318	−28 13 48.05	1.786	1.353	–	–	1311	4	16.2	40	5.3	0.1
934	M 3-21	18 02 32.324	−36 39 12.24	2.846	2.546	1.57	0.155	3311	<5	15.6	30	5.57	–
935	M 3-22	18 02 19.238	−30 14 25.38	1.334	1.319	0.941	0.998	1311	6.4	10.1	8.7	8.45	0.26
937	M 3-24	18 07 53.914	−25 24 02.71	5.998	3.891	0.071	–	3311	<25	17.4	–	–	–
938	M 3-25	18 15 16.967	−10 10 09.47	10.367	9.618	3.429	10.727	3311	1.5	25	76	6.89	0.05
940	M 3-27	18 27 48.273	+14 29 06.06	1.087	0.606	2.032	–	1311	1	–	53.2	8.55	0.04
942	M 3-29	18 39 25.772	−30 40 36.71	0.337	0.899	0.928	0.985	1311	8.2	7.6	18.7	5.86	0.23
943	M 3-3	07 26 34.228	−05 21 52.16	0.185	0.596	0.466	–	1311	12.2	–	5.6	5.46	0.32
944	M 3-30	18 41 14.938	−15 33 43.58	2.824	3.184	–	–	3311	17.2	8.5	7	3.97	0.33
946	M 3-32	18 44 43.127	−25 21 33.85	2.932	2.875	3.04	0.488	3311	7.5	12.2	12	7.06	0.26
947	M 3-33	18 48 12.131	−25 28 52.39	2.216	1.695	–	–	1311	6	9.8	7.5	8.94	0.26
948	M 3-34	19 27 01.897	−06 35 04.63	2.664	2.402	0.475	0.162	1311	8	29.6	29	4.12	0.16
949	M 3-35	20 21 03.769	+32 29 23.86	4.837	3.65	–	–	3311	1.5	29.5	140	5.62	0.04
950	M 3-36	17 12 39.152	−25 43 37.39	1.387	1.603	1.946	2.054	1311	3.2	4.9	3.5	13.92	0.22
952	M 3-38	17 21 04.459	−29 02 59.21	6.63	5.961	0.778	0.384	3311	1.8	7.6	21	8.29	0.07
953	M 3-39	17 21 11.505	−27 11 38.13	22.638	24.194	7.809	1.158	3331	19	279.4	280	1.7	0.16
954	M 3-4	07 55 11.398	−23 38 12.46	1.061	1.155	0.983	0.47	1311	13.5	6.3	2.4	6.58	0.43
955	M 3-40	17 22 28.272	−27 08 42.40	5.041	4.717	3.036	2.794	3331	2.6	15.6	17	8.22	0.1

TABLE 2 (CONTINUED)

KN	NAME	R.A. (2000)	DEC (2000)	F (65 μm)	F (90 μm)	F (140 μm)	F (160 μm)	QUAL	DIAM	F (1.4 GHz)	F(5 GHz)	DIST	DIAM
		H:M:S	D:M:S)	Jy	Jy	Jy	Jy		arcsec	mJy	mJy	kpc	pc
963	M 3-48	17 59 56.823	−31 54 27.46	0.104	0.419	–	–	1311	–	–	–	–	–
965	M 3-5	08 02 28.932	−27 41 55.44	2.259	2.633	1.385	–	1311	7	11	10	5.9	0.2
967	M 3-51	18 04 56.233	−32 54 01.23	0.509	0.945	–	1.502	1311	–	3.2	–	–	–
969	M 3-53	18 24 07.890	−11 06 42.08	3.979	5.123	7.331	–	1311	–	19.5	–	–	–
975	M 3-9	17 25 43.364	−26 11 55.47	7.307	9.022	3.599	–	3331	16	37.3	35	3.88	0.3
977	M 4-11	18 54 17.671	−10 05 14.49	1.644	3.396	2.079	0.429	1311	21.2	9.4	–	–	–
978	M 4-14	19 21 00.718	+07 36 52.37	3.094	3.937	5.787	2.183	3311	7.4	11.8	8	6.28	0.23
980	M 4-18	04 25 50.831	+60 07 12.72	3.41	1.863	0.355	1.565	3311	3.8	18.5	22	6.37	0.12
981	M 4-2	07 28 53.808	−35 45 13.92	0.899	0.632	2.254	–	1311	6	24.2	19	5.26	0.15
982	M 4-3	17 10 41.751	−27 08 43.75	1.276	1.264	2.359	3.21	1311	1.6	12.2	28	8.13	0.06
987	M 4-9	18 14 18.360	−04 59 21.30	4.308	8.57	5.261	2.096	3311	44.2	43.8	42	1.72	0.37
990	MaC 1-13	18 28 35.242	−08 43 22.82	8.671	8.271	7.573	3.768	1311	–	30.4	–	–	–
992	MaC 1-2	13 54 27.067	−64 59 36.14	1.084	1.416	–	0.051	1311	–	–	–	–	–
1000	MeWe 1-7	16 47 57.070	−50 42 48.32	3.531	2.735	4.566	1.965	1311	–	–	–	–	–
1001	MeWe 1-8	16 48 40.194	−51 09 20.26	–	1.503	0.576	2.963	1311	–	–	–	–	–
1004	Me 2-1	15 22 19.274	−23 37 31.34	0.842	1.197	–	0.115	1311	7	33.6	30	4.32	0.15
1005	Me 2-2	22 31 43.686	+47 48 03.96	0.965	0.625	0.607	1.937	1311	1.2	16	40	8.56	0.05
1006	MyCn 18	13 39 35.116	−67 22 51.45	17.17	17.185	6.808	6.315	3331	12.6	–	106	3.23	0.2
1007	My 60	10 31 33.390	−55 20 50.87	2.58	3.539	0.41	–	1311	7.6	–	60	3.47	0.13
1009	Mz 2	16 14 32.433	−54 57 03.76	6.386	7.386	2.8	0.136	3111	23	–	75	2	0.22
1012	NGC 1501	04 06 59.190	+60 55 14.34	5.662	12.013	2.975	1.373	3331	51.8	207.7	210	1.03	0.26
1013	NGC 1514	04 09 16.990	+30 46 33.43	0.779	7.38	3.384	4.231	1331	100.4	182.7	288	1.01	0.49
1014	NGC 1535	04 14 15.762	−12 44 22.03	8.439	11.349	2.444	1.103	1311	18.4	167.8	160	1.77	0.16
1015	NGC 2022	05 42 06.229	+09 05 10.75	4.676	5.515	2.809	–	3311	19.4	92.3	91	2.02	0.19
1017	NGC 2346	07 09 22.547	−00 48 22.98	5.761	9.003	10.585	7.978	3331	54.6	37.6	86	2.07	0.55
1018	NGC 2371/2	07 25 34.720	+29 29 25.63	5.715	6.803	4.715	1.4	3331	43.6	48.1	–	2.07	0.44
1019	NGC 2392	07 29 10.768	+20 54 42.44	14.76	18.032	8.169	3.25	3331	44.8	279.9	251	1.44	0.31
1021	NGC 2452	07 47 26.248	−27 20 07.16	3.586	5.514	4.19	–	3311	18.8	56	57	2.31	0.21
1023	NGC 2610	08 33 23.320	−16 08 57.67	1.063	1.386	0.912	0.768	1311	43	29.8	30	1.86	0.39
1024	NGC 2792	09 12 26.596	−42 25 39.90	5.685	6.392	1.133	0.652	3311	13	–	116	1.26	0.08
1025	NGC 2818	09 16 01.656	−36 37 38.76	1.665	2.485	2.807	2.324	1311	40	46.6	33	1.79	0.35
1026	NGC 2867	09 21 25.337	−58 18 40.69	11.091	10.774	2.804	2.917	3311	16	–	252	1.69	0.13
1027	NGC 2899	09 27 03.123	−56 06 21.22	2.701	5.13	5.775	4.372	1331	90	–	86	1.06	0.46
1028	NGC 3132	10 07 01.771	−40 26 11.11	26.899	38.62	23.599	18.285	3131	45	–	230	1.5	0.33
1029	NGC 3195	10 09 20.910	−80 51 30.73	3.459	6.441	3.46	1.028	3331	40	–	35	1.96	0.38
1030	NGC 3211	10 17 50.549	−62 40 14.57	4.017	4.506	2.28	0.502	3311	16	–	228	1.7	0.13
1031	NGC 3242	10 24 46.138	−18 38 32.26	33.512	38.693	7.971	6.4	3333	37.2	757.7	860	0.94	0.17
1033	NGC 3699	11 27 57.745	−59 57 27.71	3.54	7.862	5.69	3.722	3311	44.8	–	67	1.54	0.33
1034	NGC 3918	11 50 17.730	−57 10 56.90	34.408	28.325	7.27	3.945	3331	18.8	–	859	1.17	0.11
1035	NGC 40	00 13 01.023	+72 31 19.07	48.192	36.405	11.212	9.101	3333	36.4	510.3	460	0.98	0.17
1036	NGC 4071	12 04 14.815	−67 18 35.57	1.429	3.284	4.025	1.239	1331	63	–	26	1.73	0.53
1038	NGC 5189	13 33 32.974	−65 58 26.67	15.323	23.021	9.626	7.972	3331	140	–	455	0.55	0.37
1039	NGC 5307	13 51 03.273	−51 12 20.62	3.896	4.726	0.144	1.748	3311	12.6	–	95	2.42	0.15
1040	NGC 5315	13 53 56.972	−66 30 50.96	67.003	47.078	16.764	8.931	3331	6	–	442	2.14	0.06
1041	NGC 5873	15 12 51.052	−38 07 33.65	1.246	0.795	–	–	1311	7	45.5	48	4.23	0.14
1042	NGC 5882	15 16 49.941	−45 38 58.60	38.54	29.7	9.091	5.312	3331	14	–	334	1.74	0.12
1045	NGC 6058	16 04 26.597	+40 40 56.05	1.308	1.251	1.208	0.906	1311	26.4	7	10	3.34	0.43
1046	NGC 6072	16 12 58.079	−36 13 46.06	14.896	25.114	14.516	12.712	3311	70	138.5	164	0.98	0.33
1047	NGC 6153	16 31 30.825	−40 15 14.22	88.194	69.461	19.749	10.285	3331	24.6	–	477	1.17	0.14
1048	NGC 6210	16 44 29.521	+23 47 59.55	28.626	21.385	7.113	6.288	3331	16.2	297.8	311	1.55	0.12
1049	NGC 6302	17 13 44.211	−37 06 15.94	670.18	304.595	188.327	201.675	3333	45	1906.8	3034	0.52	0.11
1050	NGC 6309	17 14 04.322	−12 54 37.71	15.699	16.964	5.961	2.593	3331	17	131.5	151	2.35	0.19
1052	NGC 6337	17 22 15.658	−38 29 03.47	19.391	14.945	–	–	1311	47	45.9	103	1.33	0.3
1053	NGC 6369	17 29 20.443	−23 45 34.22	69.688	61.394	18.329	11.351	3333	28	1825	2002	0.75	0.1
1055	NGC 650-51	01 42 19.948	+51 34 31.15	2.536	7.243	4.019	2.1	1311	138.4	138.9	125	1.56	1.05
1057	NGC 6543	17 58 33.409	+66 37 58.79	117.286	71.842	21.65	13.89	3333	18.8	771.5	850	1.12	0.1
1058	NGC 6563	18 12 02.753	−33 52 07.14	8.647	13.865	10.414	3.326	3331	43	61	69	2.36	0.49
1060	NGC 6567	18 13 45.136	−19 04 33.67	2.308	3.04	1.306	–	1311	8.8	163	168	2.4	0.1
1061	NGC 6572	18 12 06.404	+06 51 12.17	78.382	45.439	13.059	9.839	3333	10	557.5	1374	1.06	0.05
1063	NGC 6620	18 22 54.186	−26 49 17.00	2.124	2.806	1.033	–	1311	5	17.1	20.5	6.42	0.16
1064	NGC 6629	18 25 42.449	−23 12 10.59	25.167	19.057	5.565	3.093	3331	15	257.8	275	1.84	0.13
1065	NGC 6644	18 32 34.641	−25 07 44.00	2.548	2.359	1.031	1.555	1311	2.8	64.3	97	4.09	0.06
1066	NGC 6720	18 53 35.079	+33 01 45.03	31.015	40.615	20.511	20.619	3333	69.2	420.8	360	1.13	0.38
1067	NGC 6741	19 02 37.088	−00 26 56.97	10.43	11.81	–	0.433	1311	8	131.9	230	2.32	0.09
1068	NGC 6751	19 05 55.560	−05 59 32.92	15.44	16.206	6.072	4.448	3331	21	55.1	63	2.18	0.22
1069	NGC 6765	19 11 06.465	+30 32 42.52	0.685	1.27	1.117	–	1311	38	10.1	17.7	2.41	0.44
1070	NGC 6772	19 14 36.373	−02 42 25.04	4.95	10.678	4.095	3.955	3331	90	77.4	73	1.11	0.48
1071	NGC 6778	19 18 24.939	−01 35 47.41	8.968	12.541	6.421	2.524	3311	15.8	64.6	55	2.54	0.19
1073	NGC 6790	19 22 56.965	+01 30 46.45	7.792	6.359	2.105	2.493	3331	1.8	52.6	290	4.1	0.04
1074	NGC 6803	19 31 16.490	+10 03 21.88	7.54	7.287	3.109	0.15	3311	5	68.9	114	3.26	0.08
1075	NGC 6804	19 31 35.175	+09 13 32.01	11.111	11.345	4.413	1.41	3331	31.4	112.7	135	1.32	0.2
1076	NGC 6807	19 34 33.543	+05 41 02.58	0.645	0.718	0.65	1.521	1311	0.8	8	29	11.18	0.04
1077	NGC 6818	19 43 57.844	−14 09 11.91	12.621	14.24	5.929	3.97	1311	18.2	290.2	300	1.47	0.13
1078	NGC 6826	19 44 48.161	+50 31 30.33	27.865	26.039	7.148	3.726	3331	25.4	414.4	385	1.2	0.15
1081	NGC 6852	20 00 39.213	+01 43 40.05	0.96	0.953	0.564	0.786	1311	28	10.4	20	2.66	0.36
1083	NGC 6879	20 10 26.682	+16 55 21.30	1.513	1.296	2.735	–	1311	5	23.1	18	5.78	0.14
1085	NGC 6884	20 10 23.669	+46 27 39.54	11.033	10.902	2.693	1.791	3311	5.3	152.4	200	2.7	0.07
1086	NGC 6886	20 12 42.813	+19 59 22.65	8.122	7.47	3.494	1.503	3331	5.5	77.6	108	2.94	0.08
1087	NGC 6891	20 15 08.838	+12 42 15.63	7.305	8.289	3.144	2.253	3311	10.2	110.8	105	2.35	0.12
1088	NGC 6894	20 16 23.965	+30 33 53.17	2.634	8.688	3.956	–	3311	44	66.1	61	1.44	0.31
1089	NGC 6905	20 22 22.940	+20 06 16.80	5.483	5.801	3.971	1.94	3331	40.4	66.7	52	1.62	0.32
1090	NGC 7008	21 00 32.503	+54 32 36.18	25.227	25.494	10.836	9.013	3333	90	263.3	217	1.31	0.57
1091	NGC 7009	21 04 10.877	−11 21 48.25	70.225	66.268	14.071	11.285	3333	28.2	682	750	1.09	0.15
1092	NGC 7026	21 06 18.209	+47 51 05.35	30.06	29.863	9.726	5.815	3331	15	260.5	260	1.91	0.14
1094	NGC 7048	21 14 15.224	+46 17 17.52	3.555	6.284	4.067	5.812	3311	65	45.6	37	1.5	0.47
1096	NGC 7139	21 46 08.586	+63 47 29.45	0.45	1.675	1.275	0.807	1311	76	29.8	28.9	1.56	0.57

TABLE 2 (CONTINUED)

KN	NAME	R.A. (2000)	DEC (2000)	F (65 μm)	F (90 μm)	F (140 μm)	F (160 μm)	QUAL	DIAM	F (1.4 GHz)	F(5 GHz)	DIST	DIAM
		H:M:S	D:M:S)	Jy	Jy	Jy	Jy		arcsec	mJy	mJy	kpc	pc
1098	NGC 7354	22 40 19.940	+61 17 08.10	33.268	30.543	9.496	4.222	3331	20	581	579	1.19	0.12
1099	NGC 7662	23 25 53.968	+42 32 05.04	22.148	21.669	6.041	4.011	3331	20	611.5	631	1.17	0.11
1100	Na 1	17 12 51.900	−03 16 00.13	1.755	2.016	0.027	–	1311	8	23	22.5	4.2	0.16
1104	PBOZ 34	18 05 25.509	−25 13 37.23	1.296	5.988	1.724	–	1311	–	20.8	52	–	–
1105	PB 1	07 02 46.764	−13 42 34.65	1.675	1.619	1.828	–	1311	–	11.9	18	–	–
1106	PB 10	19 28 14.391	+12 19 36.17	5.336	6.444	4.651	–	3311	8	50.4	50	3.53	0.14
1107	PB 2	08 20 40.188	−46 22 58.82	0.882	0.718	–	–	1311	3	–	40	5.75	0.08
1108	PB 3	08 54 18.323	−50 32 22.34	4.526	4.492	2.307	2.818	3311	7	–	70	3.4	0.12
1109	PB 4	09 15 07.747	−54 52 43.78	4.735	6.393	2.352	0.322	3311	11.2	–	71	2.81	0.15
1110	PB 5	09 16 09.613	−45 28 42.79	9.504	7.797	2.42	3.249	3331	5	–	107	–	–
1111	PB 6	10 13 15.949	−50 19 59.28	3.869	3.036	1.924	–	3311	11	–	30	3.55	0.19
1112	PB 8	11 33 17.717	−57 06 14.00	5.599	5.831	1.735	–	3311	5	–	27	5.15	0.12
1113	PB 9	19 27 44.814	+10 24 20.82	1.854	2.683	2.603	–	1311	7	33.1	40	3.57	0.12
1114	PC 11	16 37 42.697	−55 42 26.49	0.536	1.411	0.574	–	1311	5	–	11	–	–
1116	PC 13	16 50 17.108	−30 19 55.50	0.441	1.149	–	–	1311	–	6.6	–	–	–
1117	PC 14	17 06 14.767	−52 30 00.40	1.694	2.376	2.814	0.399	1331	7	–	30	4.32	0.15
1118	PC 17	17 35 41.677	−46 59 48.54	2.489	1.923	0.244	0.629	1311	5	–	14.7	6.12	0.15
1119	PC 19	18 24 44.524	+02 29 28.10	1.632	0.877	0.617	0.512	1311	2.8	22.4	25.3	6.75	0.09
1120	PC 20	18 43 03.456	−00 16 37.02	8.889	7.243	–	2.627	1311	–	27.3	–	–	–
1121	PC 21	18 45 35.215	−20 34 58.32	1.961	2.703	2.015	1.245	3311	13.4	11.2	–	–	–
1122	PC 22	19 42 03.514	+13 50 37.33	1.509	1.767	–	–	1311	–	9.2	–	–	–
1124	PC 24	20 19 38.133	+27 00 11.23	2.484	2.735	1.285	–	1311	5	17.1	18	5.78	0.14
1127	PM 1-188	17 54 21.100	−15 55 51.78	4.799	4.75	0.318	–	3311	–	–	–	–	–
1128	PM 1-276	19 02 17.857	+10 17 34.49	3.793	5.214	2.516	2.136	3311	–	15.3	–	–	–
1129	PM 1-295	19 19 18.760	+17 11 48.09	7.702	7.546	7.139	0.96	1311	–	13.9	–	–	–
1130	PM 1-310	19 38 52.135	+25 05 32.63	6.213	4.603	1.867	7.758	1311	–	–	–	–	–
1132	PM 1-89	15 19 08.724	−53 09 50.05	10.027	9.316	2.292	–	3311	–	–	–	–	–
1136	Pe 1-1	10 38 27.607	−56 47 06.40	8.965	8.009	7.825	3.319	3331	3	–	125.3	4.16	0.06
1137	Pe 1-11	18 01 42.767	−33 15 26.30	2.643	2.175	0.823	1.553	1311	9	10.9	8	7.9	0.34
1138	Pe 1-12	18 17 42.379	−28 17 13.80	–	0.476	0.66	0.797	1311	12	–	3.4	10.2	0.59
1139	Pe 1-13	18 34 51.659	−22 43 16.97	0.076	0.731	–	1.028	1311	7	4.4	3	8.29	0.28
1141	Pe 1-15	18 46 24.485	−07 14 34.57	2.534	2.029	–	–	3311	5	8.3	8	7.4	0.18
1142	Pe 1-16	18 47 32.251	−06 54 03.52	2.434	2.455	7.163	1.089	3311	–	14.2	–	–	–
1147	Pe 1-20	18 57 17.351	−05 59 51.79	0.354	0.931	0.129	0.342	1311	8.4	5.1	29.4	4.52	0.18
1148	Pe 1-21	18 57 49.642	−05 27 39.73	1.16	1.48	0.549	3.774	1311	8.6	6.3	30	3.95	0.16
1149	Pe 1-3	10 44 31.116	−61 39 38.47	1.051	2.368	3.299	3.222	1311	8	–	24	–	–
1150	Pe 1-6	16 23 54.309	−46 42 15.28	–	4.576	–	–	311	7.2	–	40	3.94	0.14
1151	Pe 1-7	16 30 25.852	−46 02 51.10	42.654	25.28	11.357	2.405	3311	5	–	117	–	–
1152	Pe 1-8	17 06 22.558	−44 13 09.96	6.277	8.943	6.223	0.763	1311	–	–	–	–	–
1160	Pe 2-4	09 30 48.402	−53 09 59.33	2.264	2.602	1.272	0.906	1311	–	–	–	–	–
1162	Pe 2-7	10 41 19.574	−56 09 16.34	1.045	1.399	2.067	0.005	1311	–	–	–	–	–
1167	SaSt 1-1	08 31 42.877	−27 45 31.70	1.739	1.157	1.544	1.723	1311	–	–	0.3	–	–
1170	SaSt 3-166	18 29 11.268	−17 27 12.90	1.586	2.059	0.665	4.097	1311	–	3.2	–	–	–
1171	SaWe 2	17 27 00.197	−27 40 35.11	0.562	2.44	1.572	–	1311	–	14.2	3	–	–
1175	Sa 1-8	18 50 44.312	−13 31 02.18	2.218	2.007	–	0.59	3111	5.6	13.5	11	6.33	0.17
1176	Sa 2-21	08 08 44.278	−19 14 03.13	0.069	0.763	1.683	0.197	1311	40	8.5	2.4	4.11	0.8
1177	Sa 2-230	17 42 02.007	−15 56 07.46	1.949	1.323	–	–	1311	–	4.9	3.8	–	–
1178	Sa 2-237	17 44 42.282	−15 45 11.45	9.836	9.483	–	5.196	1113	–	5.4	–	–	–
1182	Sa 4-1	17 13 50.356	+49 16 11.26	0.427	0.457	0.832	0.571	1311	–	–	–	–	–
1187	Sh 1-89	21 14 07.628	+47 46 22.17	1.096	2.718	0.395	2.673	1311	120	13.5	42.5	1.88	1.09
1191	Sn 1	16 21 04.421	−00 16 10.54	0.277	0.596	1.471	0.928	1311	3	10.4	7	9.42	0.14
1192	Sp 1	15 51 40.934	−51 31 28.39	4.179	8.354	4.189	4.004	1311	72	–	75	1.21	0.42
1193	Sp 3	18 07 15.793	−51 01 10.41	8.052	12.906	6.587	7.967	3333	35.6	–	61	1.75	0.3
1196	StWr 4-10	16 02 13.042	−41 33 35.94	0.041	0.394	–	0.523	1311	–	–	–	–	–
1197	St 3-1	07 06 50.888	−03 05 09.50	0.753	0.932	0.385	–	1311	–	7.5	–	–	–
1198	Ste 2-1	10 11 57.662	−52 38 17.09	–	0.499	–	–	1311	–	–	–	–	–
1201	SwSt 1	18 16 12.237	−30 52 08.71	17.294	13.034	–	0.315	3311	1.3	26.7	216	3.79	0.02
1203	Tc 1	17 45 35.298	−46 05 23.81	10.648	6.85	0.575	0.533	3311	15	–	801	1.39	0.1
1210	Te 2337	17 48 45.272	−26 43 28.80	10.8	8.5	19.643	–	3311	–	15.2	–	–	–
1212	Th 2-A	13 22 33.854	−63 21 00.96	4.078	5.185	–	3.694	1311	23	–	60	2.07	0.23
1216	Th 3-12	17 25 06.093	−29 45 16.87	3.613	4.512	–	–	3311	1.8	2.6	3.5	–	–
1217	Th 3-13	17 25 19.341	−30 40 41.79	8.348	2.537	–	–	3111	2	7.4	14.3	–	–
1218	Th 3-14	17 25 44.060	−26 57 47.69	2.922	2.598	1.308	–	3311	1.4	5.8	4	–	–
1224	Th 3-25	17 30 46.716	−27 05 59.12	0.043	1.042	0.528	2.846	1311	2	14.9	18	8.77	0.09
1225	Th 3-26	17 31 09.297	−28 14 50.42	2.632	2.337	–	–	1311	6.6	10.4	10	7.86	0.25
1226	Th 3-27	17 35 58.467	−24 25 29.15	4.357	5.395	2.905	–	3311	3.2	14.4	13.5	–	–
1228	Th 3-32	17 35 15.533	−28 07 01.70	3.982	3.019	–	1.552	1311	–	10.2	–	–	–
1235	Th 4-10	17 57 06.599	−18 06 43.43	1.819	2.087	–	–	1311	–	4.3	–	–	–
1236	Th 4-11	18 00 08.820	−17 40 43.33	1.832	2.515	2.449	–	1311	<5	–	0.2	–	–
1238	Th 4-3	17 48 37.390	−22 16 48.79	1.11	1.217	0.433	–	1311	–	2.7	–	–	–
1244	V-V 3-5	18 36 32.291	−19 19 28.01	1.906	3.073	0.72	2.982	3311	–	11.6	10	–	–
1246	VBRC 1	08 30 54.197	−38 18 06.98	1.648	3.486	1.496	3.464	1311	–	37.9	–	–	–
1248	VBRC 6	14 41 35.992	−56 15 13.74	0.778	1.629	2.02	1.714	1311	–	–	–	–	–
1251	VY 2-1	18 27 59.603	−26 06 48.29	4.039	4.763	2.109	–	3311	3.7	32.4	37	–	–
1259	Ve 26	08 43 28.087	−46 06 39.72	16.331	10.899	6.139	0.586	3331	–	–	–	–	–
1260	Vo 1	06 59 26.405	−79 38 47.20	33.47	21.452	5.513	4.417	3331	–	–	–	–	–
1261	Vo 2	08 16 10.000	−39 51 50.67	1.385	1.676	–	0.006	1311	–	60.9	–	–	–
1262	Vo 3	08 42 16.561	−40 44 10.57	38.376	49.309	57.133	57.844	3333	–	–	–	–	–
1264	Vy 1-1	00 18 42.167	+53 52 20.03	1.077	1.394	–	0.028	1311	6	19.8	28.9	5.34	0.16
1265	Vy 1-2	17 54 22.994	+27 59 57.99	1.704	1.184	0.697	–	1311	4.6	11.1	–	–	–
1266	Vy 1-4	18 54 01.899	−06 26 19.81	1.821	2.476	–	1.253	1311	4.5	19.7	22	6.01	0.13
1267	Vy 2-2	19 24 22.229	+09 53 56.66	31.892	23.912	4.713	4.645	3111	0.6	5.9	50	9.82	0.03
1268	Vy 2-3	23 22 57.952	+46 53 58.24	0.655	0.785	1.564	–	1311	4.6	6.5	3	9.95	0.22
1271	WeSb 3	18 06 00.766	+00 22 38.57	0.261	0.936	2.347	–	1311	–	13.1	–	–	–
1274	We 1-1	00 38 54.178	+66 23 48.63	0.362	1.02	1.167	0.138	1311	19	5.2	1.5	6.57	0.61
1281	We 1-7	18 44 06.233	−12 12 57.15	–	1.68	3.263	1.739	1311	–	5.3	–	–	–

TABLE 2 (CONTINUED)

KN	NAME	R.A. (2000)	DEC (2000)	F (65 μm)	F (90 μm)	F (140 μm)	F (160 μm)	QUAL	DIAM	F (1.4 GHz)	F(5 GHz)	DIST	DIAM
		H:M:S	D:M:S)	Jy	Jy	Jy	Jy		arcsec	mJy	mJy	kpc	pc
1282	We 1-9	20 09 04.958	+26 26 54.13	0.99	2.131	1.816	2.896	1311	–	9.9	–	–	–
1287	WhMe 1	19 14 59.755	+17 22 46.01	6.393	5.811	1.662	3.378	3311	–	–	–	–	–
1288	Wray 16-120	12 45 54.930	−60 20 17.45	1.296	1.393	0.901	1.815	1311	–	–	–	–	–
1289	Wray 16-121	12 48 30.564	−63 50 01.79	0.016	3.465	3.108	3.314	1311	–	–	–	–	–
1290	Wray 16-122	13 00 41.215	−56 53 40.19	0.147	0.809	–	2.081	1311	–	–	–	–	–
1291	Wray 16-128	13 24 21.922	−57 31 19.29	1.399	1.924	2.794	0.051	1311	–	–	–	–	–
1292	Wray 16-189	15 51 19.819	−48 26 06.93	0.808	1.757	0.916	1.617	1311	–	–	–	–	–
1293	Wray 16-199	16 00 22.002	−48 15 35.29	2.151	2.989	–	–	1311	–	–	–	–	–
1296	Wray 16-266	17 22 36.947	−52 46 34.45	0.491	0.823	0.737	2.13	1311	–	–	–	–	–
1301	Wray 16-411	18 26 41.781	−40 29 52.52	1.512	0.884	0.772	1.506	1311	–	–	–	–	–
1303	Wray 16-93	11 30 48.339	−59 17 04.63	0.487	0.94	0.995	–	1311	–	–	–	–	–
1306	Wray 17-18	08 23 53.825	−45 31 10.70	0.69	1.462	2.112	0	1311	–	–	–	–	–
1308	Wray 17-31	09 31 20.485	−56 17 39.39	0.343	0.881	0.225	–	1311	–	–	–	–	–
1309	Wray 17-40	10 06 59.570	−64 21 49.99	0.157	1.65	0.365	1.062	1311	–	–	–	–	–
1310	Wray 17-59	13 19 29.925	−66 09 07.25	0.381	1.348	–	0.099	1311	–	–	–	–	–
1311	Y-C 2-5	08 10 41.628	−20 31 32.16	0.287	0.541	–	–	1311	–	7.1	4.5	–	–

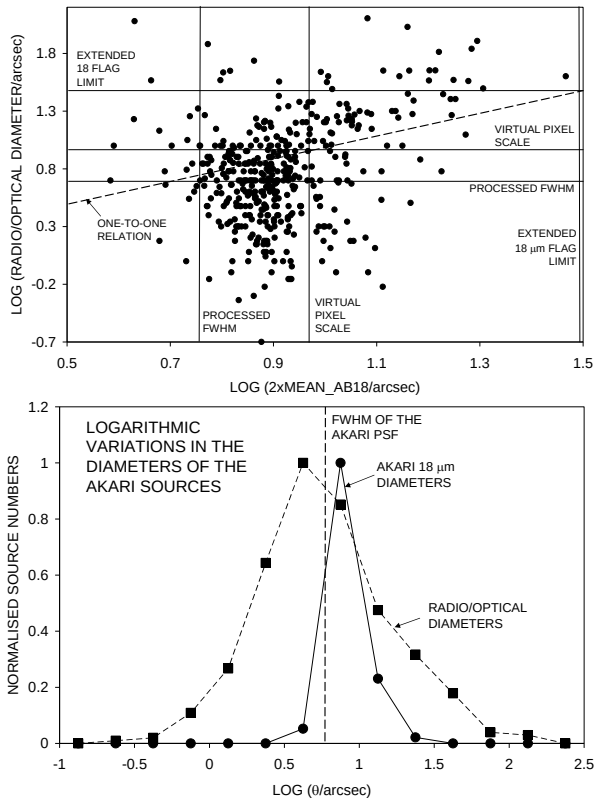

Fig. 2. Comparison between source diameters determined from radio and optical observations, and those determined through AKARI 18 μm observations (upper panel). We also indicate the diameter at which AKARI flags the sources as being extended ("Extended 18 μm Flag Limit"); the size of the virtual pixel scale; and the FWHM of the PSF (identified as the "Processed FWHM"). Although mean AKARI diameters are comparable to those for the optical/radio regime, it is clear that the range in θ is significantly smaller. This is illustrated in the lower panel, where we show distributions for the optical/radio and AKARI results.

cluding glitches, noise, residuals in the responsivity corrections and other anomalies. For the brighter AKARI sources, the absolute uncertainties are of order ∼15%, whilst relative errors are ∼10%, leading to total errors of ∼20% in all of the longer wave bands.

Of the sources listed in Tables 1 and 2, 415 PNe are common to both of the listings. Similarly, a total number of 857 PNe has been measured in this survey, corresponding to 79% of the sources listed in Kerber et al. (2003).

2.3. *Source Sizes in the AKARI Catalog*

We have noted, in § 2, that although virtual pixel sizes for the IRC results are of the order of 9-10 arcsec, the FWHM of the PSFs are ∼5.5–5.7 arcsec. Given that many PNe have dimensions exceeding these limits, it follows that AKARI should permit us to determine the angular dimensions for many of the detected PNe.

The AKARI IRC catalogue includes the flags EXTENDED09 and EXTENDED18, which are triggered when sources have radii >15.6 arcsec. None of the PNe in the present sample are flagged as being extended, even though a reasonable proportion (of order 13%) have radio/optical radii which are greater than these limits. The AKARI catalogue also provides mean radii of the sources at 9 and 18 μm, indicated by the parameters MEAN_AB09 and MEAN_AB18, although here again, the values appear quite different from those in previous studies. This disparity is most clearly to be seen in Figure 2, where we plot the AKARI parameter 2×MEAN_AB18 against the radio/optical diameters from Table 1. It is clear that there is little correlation between the two sets of parameters.

To understand what is happening more clearly, we first concentrate on the distribution of results with respect to the horizontal axis. It is apparent

that most of the sources have values 2×MEAN_AB18 which fall within a narrow range of radii $0.625 < \log(\theta/\mathrm{arcsec}) < 1.125$. The large majority of these are larger than the FWHM of the PSF. Where we now view the distribution of sources with respect to the vertical axis –that is, with respect to values of diameter taken from radio and optical observations– it becomes apparent that half of sources are smaller than the PSF, and that the distribution is very much broader than that of the AKARI results. This latter trend is also apparent in the lower panel of Figure 2, where we show normalized histograms of the AKARI and radio/optical results. Whilst the AKARI dimensions are sharply peaked close to $\theta = 7.5$ arcsec, the radio/optical data extend over a regime which is ∼60 times larger.

It is therefore clear that whilst the mean infrared sizes of the sources are similar to those in other wavelength regimes –the AKARI dimensions are ∼0.86 times as large as those determined through optical and radio observations– the level of agreement for individual sources is much less impressive. It is found that the infrared dimensions are mostly very much larger, or significantly less.

It is no surprise that there is a paucity of AKARI sources with dimensions less than the PSF – sources which are smaller than this limit would be unresolved. What is more surprising is that so many optically compact sources have substantially larger IR diameters, and that these are close to the size of the 18 μm PSF. One explanation for this may be that many smaller radio/optical sources correspond to younger PNe, in which the neutral envelopes are larger than the ionized regimes. Where a large fraction of the IR emission derives from these HI shells, then the dimensions of the sources will be correspondingly enhanced. On the other hand, it is possible that sources which are compact are prone to larger errors in their derived diameters, and that many of the MIR dimensions are significantly too large.

Similarly, it is possible that [OIV] λ25.87 μm and [NeV] λ24.316 μm are dominant in evolved PNe, leading to centralized emission, and smaller mean dimensions. A similar trend has been noted in MIPSGAL 24 μm mapping of PNe (Phillips & Márquez-Lugo 2011; Chu et al. 2009; Ueta 2006; Su et al. 2004, 2007), and this may explain the paucity of sources having larger angular diameters. Here again however, it is possible that weaker, more extended emission falls below the AKARI detection limits, and that this causes a significant reduction in the sizes of the PNe.

It is therefore clear that instrumental errors, and variations in the structures of the PNe are capable of explaining the disparities illustrated in Figure 2. Further analysis is required before these differences can be understood. Given the uncertainties in the veracity of the AKARI results, however, we shall be using radio/optical estimates of diameter in our investigation of evolutionary trends.

2.4. *Comparison of the AKARI and IRAS Photometric results*

We have finally undertaken a comparison between the AKARI photometry and corresponding IRAS results. The flux comparisons are provided in Figure 3, where all of the results have quality factors of 3. For this case, the IRAS PSC was interrogated using a search radius of 18 arcsec, comparable to the positional uncertainty for sources in this catalogue. This resulted in the detection of 573 nebulae with flux quality FQUAL = 3 in at least one of the photometric channels.

The IRAS photometry was undertaken at 12, 25, 60 and 100 μm; wavelengths which are slightly different from those quoted for the present results. It is not therefore possible to undertake a direct one-to-one comparison with the AKARI fluxes, although we are able to compare the closely adjacent channels at 9 and 12 μm, 18 and 25 μm, 65 and 60 μm, and 90 and 100 μm (Figure 3).

It is clear that whilst the fluxes are similar at 90 and 100 μm, the other comparisons show systematic differences in emission. For the most part, the IRAS fluxes are larger than those determined by the AKARI all-sky survey.

One possible explanation for these trends is that there is a calibration problem with the AKARI data, although this seems extremely improbable, and can almost certainly be discounted. The AKARI team has used a broad range of standard stars for the IRC calibration, for instance, including sources in the ecliptic polar regions and Large Magellanic Cloud. They have also used sources employed in calibrating the *Infrared Space Observatory* (*ISO*). There is a non-linear relation between input source fluxes and the AKARI signal; a function which is fitted using a second degree polynomial fit. When this correction is employed, it is clear that residual errors are small; there is certainly little evidence for the biases which are detected in the present work. Similar calibrations are used for the FIS results, where the AKARI team has used stellar, asteroidal, and planetary flux calibrators. Again, non-linear relations are detected between the source fluxes and measured signals, and

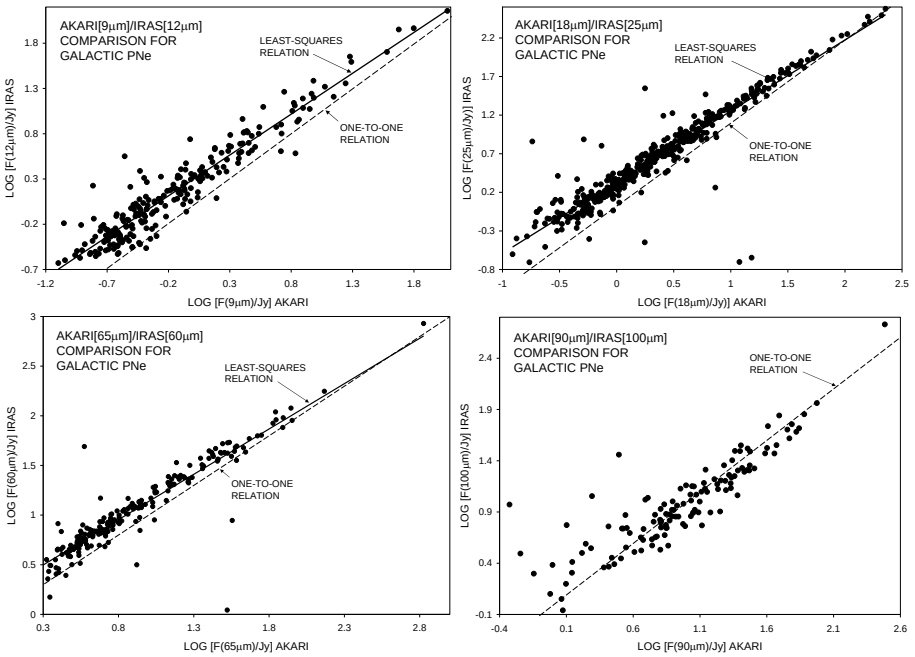

Fig. 3. Comparison of IRAS and AKARI photometric results, whence it is seen that there is a linear relation in all of the panels. However, there is also evidence for a systematic disparity between the trends. This may be partially attributable to differences in the wavelengths of observation, and the spectral gradients of the nebular SEDs.

these trends are subsequently corrected using logarithmic expressions.

We therefore believe that most of the difference can be attributed to the differing mean wavelengths of observation. Thus, where grain temperatures are of the order 110 K, and the grain emissivity function varies as $\epsilon \propto \lambda^{-\gamma}$, $\gamma \cong 1$, then one obtains flux differences similar to those noted in the 18 μm/24 μm panel. A somewhat higher temperature ($\sim$190 K) is required for the 12 μm/9 μm results; a value which is rather larger than is normally attributed to PNe dust continua. It is possible that these latter results are dominated by warmer components of emission, however, such as has been described in the analyses of 2MASS results (e.g., Phillips & Ramos-Larios 2005, 2006, 2007). It is also worth noting that emission at these shorter wavelengths occurs at the Wien limits of the dust continua, where flux levels tend to be lower. As a consequence, emission from lines and bands has a greater impact upon the results (see § 3.1 for a fuller description of these components), and may contribute to the discrepancies noted above.

Although this interpretation of the trends is plausible, and undoubtedly accounts for much of the disparity in the results, we note that flux differences are larger for fainter sources, and almost disappear where sources are brighter. One likely explanation for this trend arises from the fact that sources having larger apparent fluxes also have lower intrinsic radii. We determine that $F_\nu(18\ \mu\mathrm{m}) = 0.20(D/\mathrm{pc})^{-1.17}$, with a correlation coefficient $r \cong 0.51$. Given that sources with smaller diameters also tend to have higher grain temperatures (§ 3.2), this would imply that nebulae having higher fluxes $F_\nu(18\ \mu\mathrm{m})$ also have higher temperature continua. This, where it is the case, would lead to a narrowing of the flux differences.

3. EVOLUTIONARY TRENDS IN THE AKARI PHOTOMETRY

Previous analyses of *IRAS* photometry have suggested that the properties of nebular dust evolve with time. It has been suggested for instance that grain temperatures and dust/gas mass ratios both decrease as nebular radii increase. Similarly, it has been proposed that the masses and sizes of the grains decrease with radius (Pottasch et al. 1984; Lenzuni et al. 1989), although such an evolution has been discounted in the study of Stasinska & Szczerba (1999).

Such broad evolutionary trends are also apparent in the present AKARI spectral energy distributions (SEDs), examples of which are illustrated in Figure 4. In this case, the sources are ordered according to the channel of peak flux, and all of the fluxes have an FQUAL parameter of 3. Sources peaking

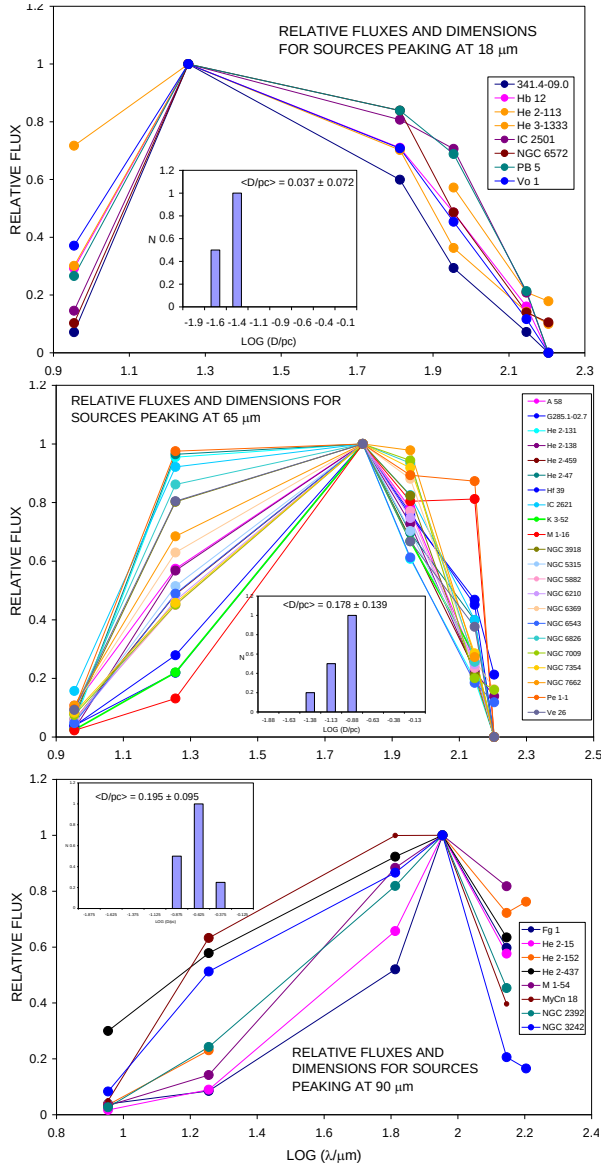

Fig. 4. An illustration of the variety of AKARI SEDs detected in the present analysis, where the sources are sorted with respect to the wavelength of peak emission. The sources in the top-most panel peak at 18 μm, whilst those in the middle and lower panels peak at 65 and 90 μm. There is therefore a cooling of the continua as one passes from the upper to the lower PNe. We have also included histograms and mean values of the nebular diameters D; where estimates for this parameter are taken from optical/radio observations. It is apparent that diameters are smaller for the upper SEDs, and shift to higher values for the lower SEDs. This trend is consistent with previous observations, and our later investigation of grain temperatures $T_{\rm GR}$. The color figure can be viewed online.

at 18 μm are shown in the upper panel, whilst those peaking at 65 and 90 μm are illustrated in the middle and lower graphs. We have also inserted histograms showing the distributions of sources with respect to intrinsic diameter, where the latter refers to the size of the ionized (radio/optical) emission envelope. It is clear that as the continua become cooler (i.e. the wavelength of peak FIR flux increases), so the sizes of the nebulae increase; precisely the trend which has been deduced from previous analyses of IRAS photometry. We shall consider this and further evolutionary trends in the following sections.

3.1. *Line and Band Contributions to the Nebular Fluxes*

FIR spectroscopy of PNe shows that most has continua dominated by emission from nebular grains, with temperatures $T_{\rm GR}$ of order ∼50–150 K. There is little doubt that these contribute the larger part of the emission in the present PNe, and we shall be assuming that this is the case for much of the analysis below. There are however several other bands and lines which are capable of affecting the results, and their contributions may be quite considerable. Thus for instance, the 9 μm IRC filter covers the regime of the PAH emission bands, and these are likely to contribute appreciable fluxes where C/O > 1. Evidence for these bands has been noted from ISO and Spitzer spectroscopy (e.g., Ramos-Larios, Phillips, & Cuesta 2011; Ramos-Larios et al. 2011, in preparation; Cohen & Barlow 2005), and there is evidence that much of the emission arises from PDRs.

The 18 μm filter, by contrast, includes [OIV] λ25.87 μm, [NeV] λ24.316 μm, and the $\lambda\lambda$18.713 and 33.482 μm transitions of [SIII]; the 21 and 30 μm emission features; and broad components associated with crystalline and amorphous silicates. The former (21 and 30 μm) features are found in PNe with C/O > 1, whilst silicates are formed in oxygen rich environments.

Perusal of *ISO*[1] pipeline spectra for 32 PNe reveals that a variety of other transitions affect the longer wave fluxes as well. These include [OIII] λ51.816 μm, [NII] λ57.317 μm, and [OI] λ63.184 μm (in the 65 and 90 μm channels); [OIII] λ88.355 μm (in the 90 μm channel); [NII] λ121.898 μm and [OI] λ145.526 μm (in the 140 μm and 160 μm channels); and [CII] λ157.741 μm (in the 160 μm passband).

Several of these transitions are strong, and may measurably affect the present results. Thus a de-

[1]Based on observations with ISO, an ESA project with instruments funded by ESA Member States (especially the PI countries: France, Germany, the Netherlands and the United Kingdom) and with the participation of ISAS and NASA.

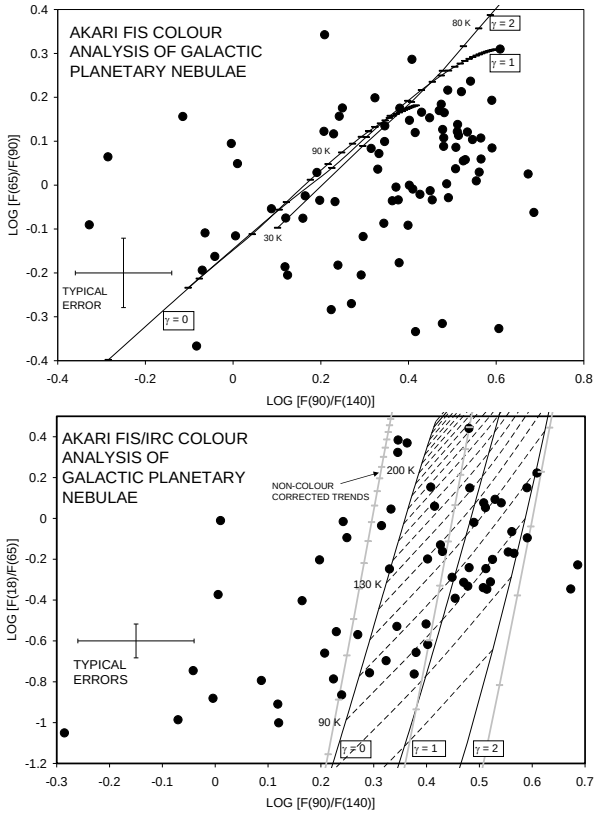

Fig. 5. Positions of PNe in the FIS/IRC colour-colour planes (filled circles), together with diagonal lines corresponding to colour-corrected grain emission loci. The temperatures of the grains are indicated by ticks and dashed lines, and represent increments of 10 K in $T_{\rm GR}$. Similarly, the diagonal loci correspond to emissivity exponents γ = 0, 1, and 2, as indicated in the panels. Finally, we have indicated the mean errors in the colours (error bars to the left-hand side), and the effects of not including colour corrections (the grey diagonal lines in the lower panel). Note that whilst a large fraction of PNe in the lower panel fall within the limits of the dust continuum loci, this is less the case in the upper panel, where most of the nebulae are positioned to the right. Some of these disparities are attributable to errors in the results, and to the contribution of line and band components.

tailed analysis of sources in which the continuum is clearly visible, and the S/N is reasonably high, suggests that [OIV] λ25.87 makes the largest average contribution to the 18 μm band ($\sim$20% of the dust continuum flux), whilst total line enhancement is of the order $\sim$40%. The line contributions to the other channels are less substantial, varying from $\sim$13% (at 65 μm), to $\sim$7% (90 μm), $\sim$0.4% (140 μm) and 4% (160 μm, where [CII] is strongest). Given the nature of the colour-colour mapping to be discussed in § 3.2, it is relevant to note that mean 18 μm/65 μm flux ratios would be increased by $\sim$22% (i.e. points would be shifted by $\sim$0.09 dex), whilst corrections to the other ratios are significantly less.

Finally, of the 32 PNe investigated in this present analysis, nine appear to have strong 30 μm features. These mostly fall between the IRC 18μm filter on the one hand, and the FIS 65 and 90 μm filters on the other. Their contributions to the AKARI photometry are therefore likely to be modest.

Some care must therefore be taken in interpreting the present photometry – a caveat that also applies to previous such analyses. Thus for instance, the analysis of Pottasch et al. (1984) is similar to that we shall be undertaking below, although the authors appear not to have taken account of colour corrections. Stasinska & Szczerba (1999) have attempted a more sophisticated analysis, in which photometry is corrected using SED evolutionary modeling. The authors ignore several important oxygen- and carbon-rich bands, however, whilst their assumptions of invariant abundances, identical nebular structures, a single grain emissivity function, and various other approximations, may lead to misleading results for many of their sample PNe.

3.2. *The AKARI Colour-Colour Planes, and Variation of Grain Temperatures*

The distribution of PNe within the AKARI colour planes is illustrated in Figure 5, where the upper panel shows trends with respect to the 65 μm/90 μm and 90 μm/140 μm flux ratios, and the lower panel represents the corresponding 18 μm/65 μm–90 μm/140 μm ratios. We also indicate the trends to be expected for smooth dust continua having emissivity exponents γ = 0, 1 and 2, and temperatures 30 K $< T_{\rm GR} <$ 270 K. The errors in the fluxes have been discussed in § 2.2, where it is noted that PNe with $F_\nu(18\mu{\rm m}) > 1$ Jy have S/Ns $\sim$15. Similar values apply for the FIS photometric results as well, where combined relative errors of $\sim$10%, and absolute errors of $\sim$15% lead to overall photometric uncertainties of $\sim$20%. We have used these estimates in determining the error bars in Figure 5.

A further correction relates to the broad widths (4.8–52.4 μm) of the AKARI filters, which necessitates a modification to the fluxes depending upon the nature of the SEDs. We have used the colour corrections of Shirahata et al. (2009) and Lorente et al. (2007) to modify the dust continuum trends in Figure 5, leading to shifts in the loci by as much as $\sim$0.1 dex. This leads to an overlapping of loci in

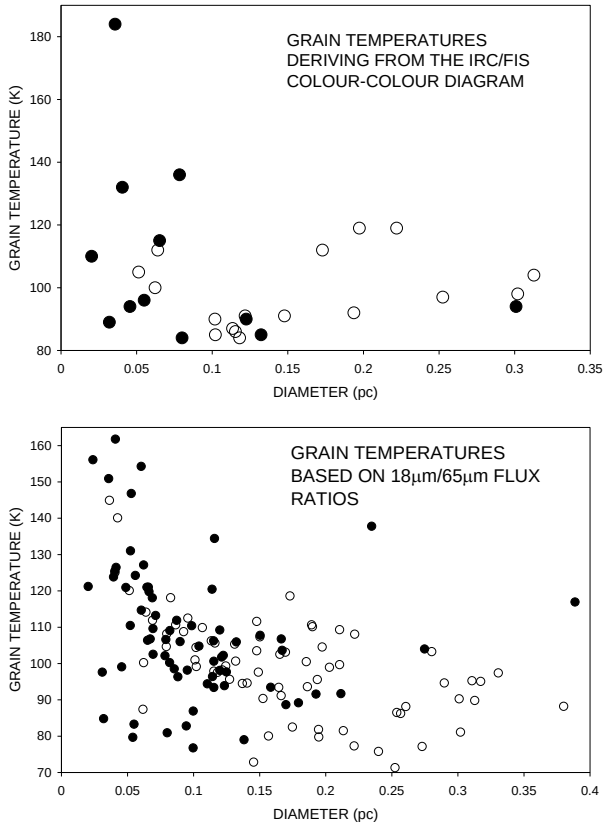

Fig. 6. The variation of grain temperatures as a function of nebular diameter, where we have evaluated $T_{\rm GR}$ using results in the lower panel of Figure 5 (upper panel). Notice how temperatures are larger for diameters < 0.05 pc, and fall within the range $T_{\rm GR} \sim 85-120$ K for larger shell diameters. Sources with angular sizes $\theta < 7$ arcsec are indicated by filled circles, and those having $\theta \geq 7$ arcsec are flagged using open circles. We also show temperatures calculated using 18 and 65 μm fluxes, and assuming an emissivity exponent $\gamma = 1$ (lower panel).

the FIS colour plane (upper panel), and a significant narrowing of the dust regime in the IRC/FIS colour plane (lower panel, where we show examples of the corrected and uncorrected loci).

Where the emission in PNe is dominated by grain continua, then the positions of the sources in Figure 5 will depend upon $T_{\rm GR}$ and γ. However, it is clear that the majority of nebulae in the upper panel fall well away from the dust emission trends. Some of this scatter is likely to be due to errors in the results, although it is interesting to note the bias in the ratios to larger values of 90 μm/140 μm. This is rather larger than would be expected from the *ISO* analysis described in § 3.1. Thus, whilst the shift could be explained in terms of an increase of 20% in the 90 μm flux, this would not be consistent with the smaller mean enhancements expected for ionic transitions in this regime (∼7%; see § 3.1). It would also fail to account for the higher levels of line contamination noted for the 65 μm band, which tend to push PNe to higher positions within this plane.

Similar problems occur for the 18–140 μm trends in the panel below, although in this case, many of the sources lie within the limits of the dust emission loci. We here assume that emission for these sources is dominated by dust continua, and use the positions of the nebulae to determine values for γ and $T_{\rm GR}$. The enhancement in 18 μm/65 μm ratios due to line emission (see § 3.1) may lead to increases in $T_{\rm GR}$ by ∼10–20 K – although see also our comments below concerning the partial detection of 18 μm fluxes.

The corresponding variation of $T_{\rm GR}$ with source diameter is illustrated in Figure 6 (upper panel), where filled circles correspond to sources having $\theta <$ 7 arcsec, and open circles are for nebulae which are larger. It is clear that dust temperatures are significantly higher where the sources have smaller physical dimensions, with $T_{\rm GR}$ approaching ∼180 K where D is less than ∼0.08 pc. By contrast, PNe having larger physical dimensions tend to have smaller values of $T_{\rm GR}$, and fall within a narrower range of values $T_{\rm GR} \sim 85 - 120$ K.

Stasinska & Szczerba (1999) have represented the variation of dust temperatures against Hβ surface brightnesses S(Hβ). The value of $T_{\rm GR}$ is determined using IRAS 25 and 60 μm fluxes, and by assuming that the emissivity exponents γ are uniformly equal to unity. This leads to qualitatively similar trends to those illustrated in the upper panel of Figure 6, although the nature of their procedure permits them to measure many more PNe. The authors find that temperatures are ∼60–100 K where $\log(\mathrm{S(H}\beta)/\mathrm{erg\ cm^{-2}\ s^{-1}\ sr^{-1}}) < -2$, and increase rapidly to higher S(Hβ).

A comparable analysis can be achieved using AKARI photometry at 18 and 65 μm, and where one adopts similar simplifying assumptions. The results are illustrated in Figure 6 (lower panel). It is again clear that there is a marked increase in temperatures for diameters < 0.07 pc; that temperatures are of order ∼70–110 K for larger nebulae; and that there is a significant overlap of values for angularly small and larger PNe. There is little evidence for the linear fall-off of temperatures noted by Pottasch et al. (1984).

Finally, we note that the FIS beams are relatively large, varying from 37 to 61 arcsec. Nevertheless, a small proportion of nebulae have diameters which are larger than these values. Given that the fluxes for

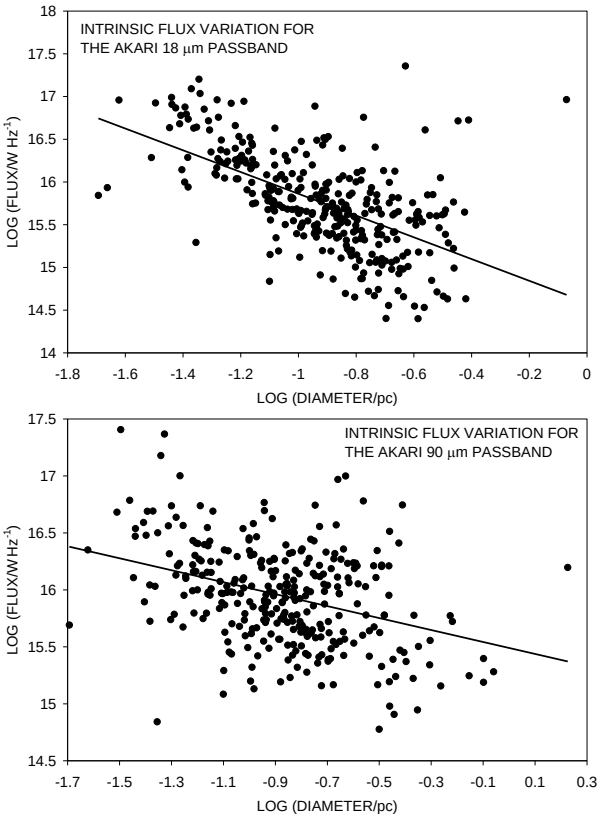

Fig. 7. The variation of the intrinsic 18 and 90 μm fluxes with nebular diameter. In both cases, there is a decrease of flux with increasing diameter, most clearly seen in the 18 μm trends. It is likely that most of this arises from systematic cooling of the IR continua.

these sources may be being only partially detected, we have excluded such nebulae from the present analyses. By contrast, the 18 μm beam sizes are very much smaller, and this may lead to a quite considerable short-fall in certain of the fluxes. This, where it is the case, would counteract the effects of line and band "contamination" noted in § 3.1. We note however that PNe having warmer dust continua tend to be smaller and unresolved (see Figure 6), and their fluxes and temperatures are therefore relatively secure. Similarly, sources having lower values of $T_{\rm GR}$ tend to be angularly large, and their shorter wave fluxes may be significantly too low. However, estimates of $T_{\rm GR}$ for such (lower) grain temperatures are relatively insensitive to uncertainties in the flux, and errors in the trends are likely to be modest. This is consistent with the variations noted in Figure 6, where we see little inconsistency between the estimated temperatures for large and smaller PNe (Figure 6).

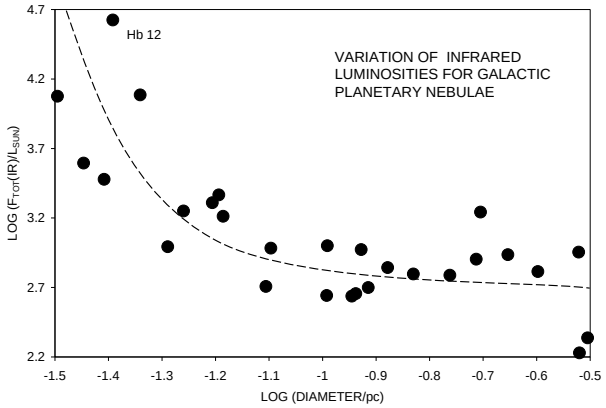

Fig. 8. Variation of total IR luminosity with nebular diameter. It is apparent that luminosities decline with expansion of the PNe, and have maximum values comparable to the luminosities of the central stars. This higher luminosity for the more compact sources suggests appreciable levels of dust opacity. The dashed curve represents an eye-fitting to the results.

3.3. *Variation of Nebular Fluxes and Luminosities with Nebular Evolution*

The emission characteristics of dust in PNe are expected to vary as the nebular envelopes evolve. Thus, expansion of the envelopes would be expected to lead to a reduction in stellar radiative flux densities, and decreases in the levels of direct grain heating. Similarly, the roles of changing stellar temperatures; absorption of Lyα radiation; and the transfer of grains from neutral to ionized regimes, will all be important in determining the energy budgets of the grains and, by extension, the temperature of the dust.

A trivial consequence of such evolution is noted in Figure 7, where we show the variation of intrinsic 18 and 90 μm fluxes as a function of source diameter. It would seem that both of the trends indicate a decrease of flux with D; a variation which may arise through a cooling of the dust continua, such as is noted in Figure 4.

An even more interesting trend is illustrated in Figure 8, where we have estimated total fluxes $F_{\rm TOT}$(IR) for sources within the dust emission regime of Figure 5 (lower panel). For this case, $F_{\rm TOT}$(IR) is determined using the values of γ and $T_{\rm GR}$ obtained from Figure 5; observed 90 μm fluxes; and the distances quoted in Table 1. It is again clear that luminosities decline with increasing nebular dimensions, and have values approaching $\approx 1.5 \times 10^4\ L_\odot$ where $D < 0.05$ pc – perhaps even larger ($\sim 4{\times}10^4\ L_\odot$) for Hb 12. Since this brightness

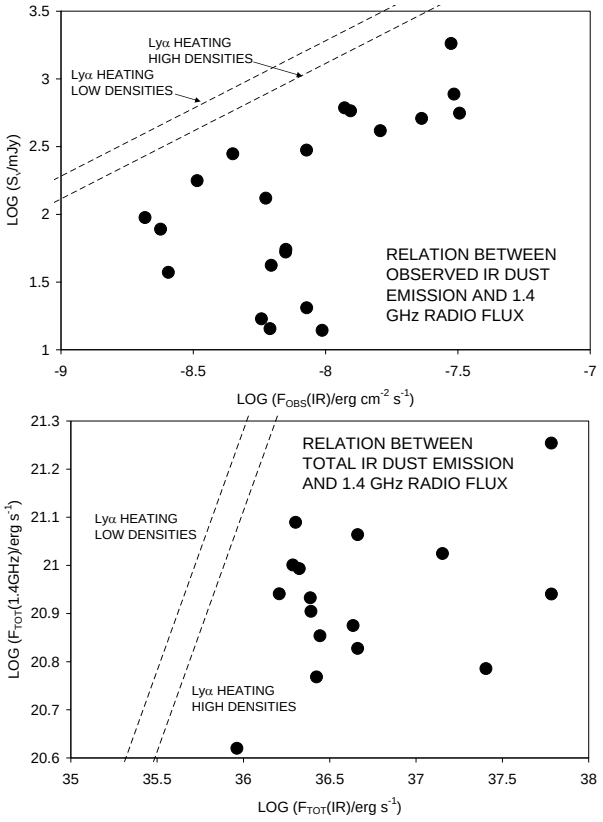

Fig. 9. A comparison between observed 1.4 GHz and integrated FIR fluxes (upper panel), and the intrinsic (distance corrected) counterparts of these fluxes (lower panel). The diagonal lines correspond to the trends where Lyα heating dominates the results, and represent low and high values of the nebular density. It is clear that Lyα heating represents ≤ 0.5 of the energy budget of the IR emitting grains.

is typical of the luminosities of PNe central stars, this suggests that a large fraction of the radiation is being absorbed by dust – a situation which would be consistent with the high levels of reddening observed in proto-planetary nebulae (PPNe).

It is finally interesting to adapt the analysis of Lyα heating of Pottasch et al. (1984) to the present AKARI results. The results of such a procedure are illustrated in Figure 9, where we show the relation between observed integrated IR and 1.4 GHz emission, and between intrinsic (distance corrected) IR and 1.4 GHz results (lower panel). The trends expected for Lyα heating are indicated by the dashed diagonal lines, determined for high and low density nebular regimes. It would appear that the infrared excess (IRE), corresponding to the ratio of the observed flux to Lyα heating, is of order > 2 for all of this present sample PNe. It is therefore clear that further heating of the grains is required over and above that expected by Lyα photons.

One would anticipate that values of the IRE would be largest where PNe are more compact, Lyα fluxes are smaller, and direct heating by the stellar radiation field is greatest. Subsequent nebular expansion would lead to further ionization of the shell; increased fluxes of Lyα photons; and the dilution of the stellar radiation field. Under these circumstances, the IRE would be expected to decline rather precipitously, and achieve minimum values of the order of unity.

To investigate whether some such evolution is actually occurring, we have determined FIR luminosities for a broad range of PNe. This involved using the 18 and 65 μm fluxes to determine $T_{\rm GR}$; assuming a grain emissivity exponent $\gamma = 1$; and employing 1.4 GHz fluxes to evaluate Lyα heating. We assume Lyα photon production rates relevant for lower density PNe, whilst the distances and sizes of the sources are taken from Tables 1 and 2. Under these circumstances, appropriate integration of the emission curves show that the luminosity of the source can be represented through

$$L = 3.11{\times}10^{13}\left[\frac{\mathrm{F}_\nu(90\ \mu m)}{\mathrm{Wm^{-2}Hz}}\right]\left[\frac{d}{\mathrm{kpc}}\right]^2\left[\sum_{i=0}^{4} a_i T_{\rm GR}^i\right]^{-1} L_\odot\,, \quad (1)$$

where d is source distance, the polynomial terms $[a_0, ..., a_4]$ are given by $[7.162 \times 10^{10}, -1.834 \times 10^9, 1.868{\times}10^7, -8.742{\times}10^4, 1.564{\times}10^2]$, and the expression is valid for temperatures $70 < T_{\rm GR}/\mathrm{K} < 160$. Similar expressions may be derived for differing values of γ.

Note that both here, and in the analysis of the results in Figure 5 (see above), we have used 90 μm fluxes to scale the results. This is advantageous for a variety of reasons. Not only are these results taken with the most sensitive of the FIS detectors –leading to larger numbers of PNe detections than in other channels– but this wavelength lies close to the continuum peak for most of the PNe SEDs. We have also assessed that levels of line contamination are likely to be modest (§ 3.1), although there is evidence that contaminants may be larger than is supposed (see § 3.2 and Figure 5). It is unlikely, however, that luminosities are very greatly in error, or that mean biases are greater than ∼0.1 dex.

The results of this analysis are illustrated in Figure 10, where the IRE is represented against nebular diameter. It is plain from this that some evolution does indeed appear to be occurring, with values of IRE approaching ∼50 for diameters < 0.07 pc. Al-

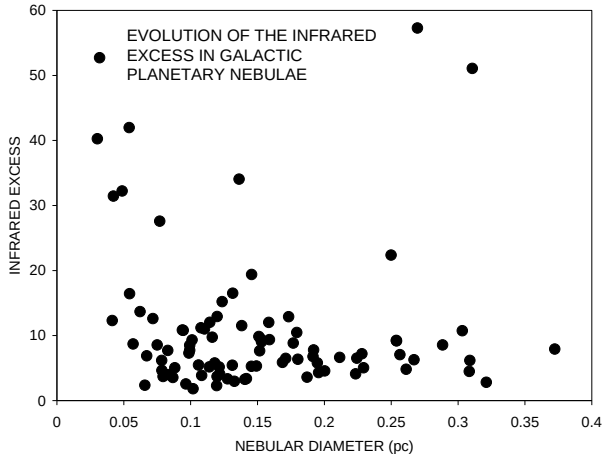

Fig. 10. Variation of the Infrared Excess in Galactic PNe. Notice the evolution in the IRE as nebular dimensions increase.

though the qualitative trend appears consistent with the analysis above, it is interesting to note that the IRE is still relatively large (≈5) even where nebulae are evolved – and that the minimum values are larger than found by Pottasch et al. (1984).

3.4. *Radio Infrared Flux Correlation*

It has been noted that the ratio of infrared to radio fluxes in extragalactic systems is reasonably constant, and invariable with redshift z. Appleton et al. (2004) have noted that the parameter $q_{70} = \log[S_\nu(70\ \mu\text{m})/S_\nu(20\text{cm})]$ is of order ∼2, whilst $q_{24} = \log[S_\nu(24\mu\text{m})/S_\nu(20\text{cm})]$ is ∼1. Cohen & Green (2001) have made a similar analysis for 21 Acker et al. (1992) PNe, using 8.3 μm fluxes taken from the Midcourse Science Experiment (MSX; Price et al. 2001). They derived MIR/radio ratios in the region of 12. However, a later analysis for ten MASH PNe (Parker et al. 2006; Miszalski et al. 2008) yielded a ratio of the order of ∼5 (Cohen et al. 2007). This difference between the less evolved Acker PNe, and more evolved MASH nebulae was attributed to an evolution in the properties of the sources – perhaps a reduction in PAH emission as fluorescent excitation decreased. This mechanism is only applicable, however, where C/O is greater than or close to unity.

A further investigation of this issue has also been undertaken by Zhang & Kwok (2009), using 8 and 24 μm photometry deriving from the GLIMPSE and MIPSGAL surveys. In this case, the authors note a linear relation between MIR and 1.4 GHz fluxes; a trend they interpret as indicating a constancy in the ratios q_{24} and q_8. It is also suggested that the scatter

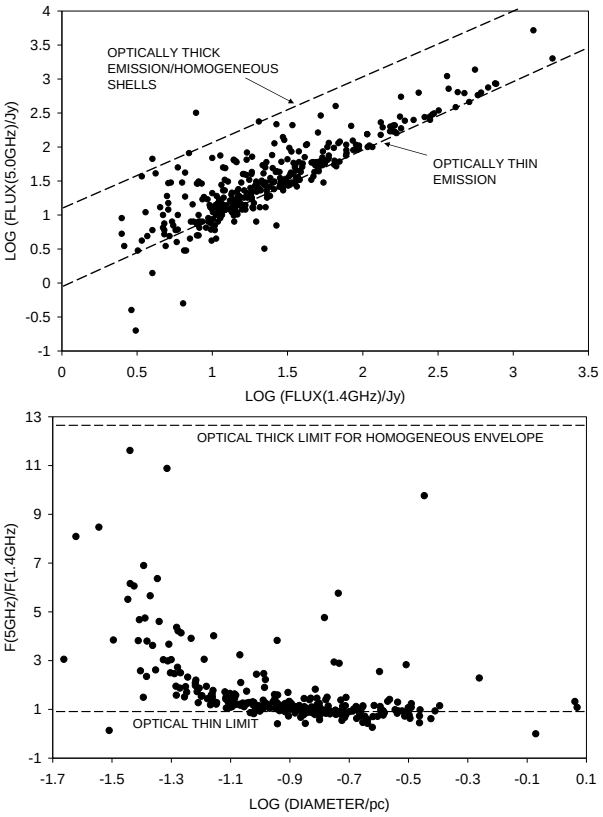

Fig. 11. The 1.4 and 5.0 GHz emission of the AKARI PNe, where we show a comparison between the fluxes (upper panel), and the evolution of the 5.0 GHz/1.4 GHz flux ratios (lower panel). The lower dashed line indicates the limit for optically thin sources, whilst the upper dashed line is for high opacity homogenous PNe. It is clear that most of the nebulae follow the locus for optically thin emission (upper panel), and that only a minority of sources are partially or totally optically thick. The evolution of the ratios (lower panel) indicates higher opacities where $D < 0.07$ pc.

in their figure is attributable to optical thickness at 1.4 GHz – a hypothesis which we will suggest, below, is unlikely to be the case.

We have investigated this question using the present AKARI photometric results, and 1.4 GHz measures deriving from Condon et al. (1998). It should be emphasized that whilst most PNe are likely to be optically thin at 5 GHz, a small proportion may have higher opacities. Thus, we have made a comparison between 5 and 1.4 GHz fluxes in Figure 11 based upon the data summarized in Tables 1 and 2. It is clear that the vast majority of sources follow the trend for optically thin emission (lower dashed line), although ∼20% fall between the optically thick and thin regimes (the former indicated

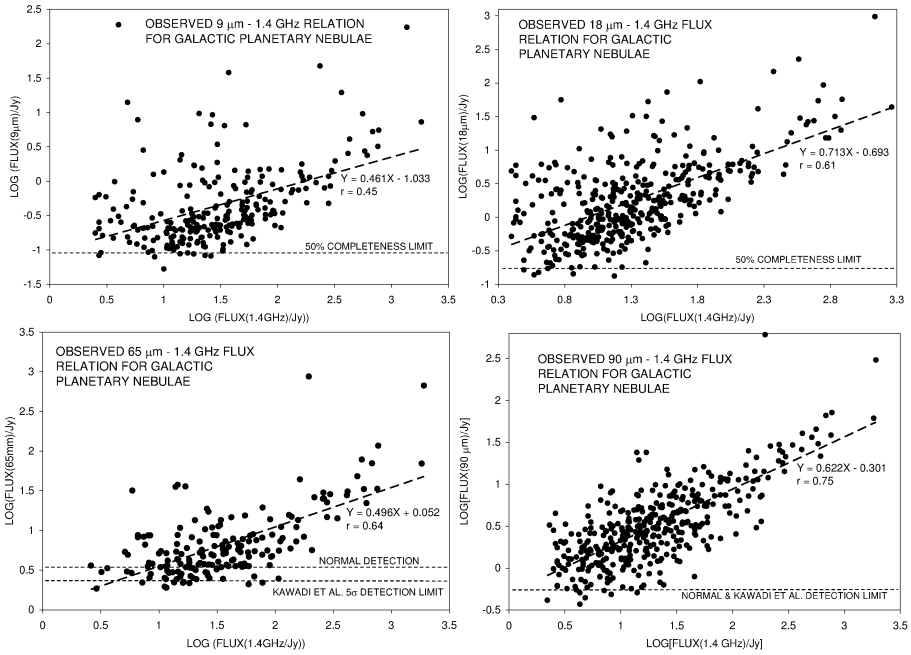

Fig. 12. The variation of infrared fluxes with respect to 1.4 GHz emission, where we illustrate the trends for four of the AKARI photometric channels. All of the results indicate linear trends. Note how the limiting AKARI and radio sensitivities restrict the numbers of observed sources, and appreciably modify the trends. Least-squares fits to the data are indicated using dashed lines, for which we indicate equations and correlation coefficients (r) within each of the panels.

by the upper line). It is therefore clear that whilst certain 5 GHz fluxes derive from partially or fully opaque regimes, the vast majority of 1.4 GHz results are optically thin - and yield fluxes proportional to the total masses of ionised gas.

Phillips (2007) has noted that higher 5 GHz/ 1.4 GHz ratios are confined to more compact sources, where density and emission measures are larger. This is also noted for the PNe investigated here (Figure 11, lower panel), where it is clear that higher 5 GHz opacities arise when diameters are < 0.07 pc; a range similar to that determined for higher values of $T_{\rm GR}$ (§ 3.2).

The variation of infrared emission with 1.4 GHz flux is illustrated in Figure 12, where it is clear that there is a linear relation between the two sets of data. Such trends are strongly affected by a variety of biases, however, and these greatly modify the perceived gradients. In the first place, distance-squared spreading of the fluxes would tend to lead to a one-to-one relation. It is also apparent that source numbers are truncated where $F_\nu(1.4\ {\rm GHz}) \leq 3$ Jy, corresponding to the sensitivity limit of the Condon et al. (1998) survey.

Even greater biases arise from the limiting sensitivities of the differing AKARI channels, however, and we have indicated these using horizontal dashed lines. We have included values corresponding to 50% source detection rates; a so-called "normal mode" detection limit quoted in the FIS Bright Source Catalogue (Yamamura et al. 2010); and the 5σ detection limit quoted by Kawada et al. (2007). Most of these limits are mutually consistent, and accord with the fall-offs in the numbers of PNe. The result, for the 9 and 65 μm results, is for an apparent flattening of the trends. It is apparent however that the 90 and 18 μm samples are significantly more complete, and trends are close to those expected for unbiased samples of PNe. We shall therefore be using these trends to assess variations in q_{18} and q_{90}.

We should finally add that detection limits at 140 and 160 μm are even higher, whilst PNe fluxes tend to be lower. This leads to extraordinarily strong truncations in the numbers of PNe, and we have excluded these results from the present analysis.

Distance corrected measures of the fluxes are illustrated in Figure 13. We note that the linear trends in Figure 12 have now largely disappeared, although the scatter between the nebulae is as large

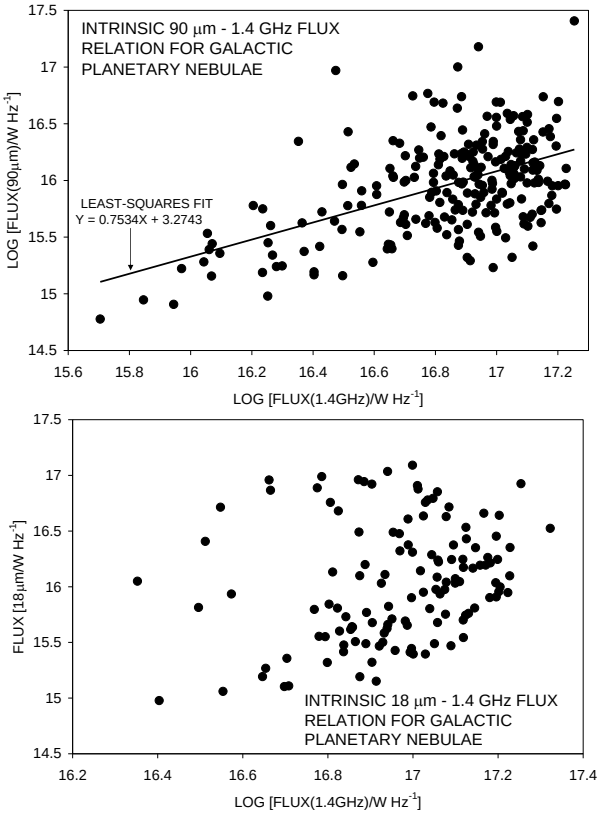

Fig. 13. The variation of intrinsic 18 and 90 μm emission with 1.4 GHz flux. There is still evidence for linearity in the 90 μm trends, although the 18 μm results appear to be random. We have indicated the equation and trend for the least-squares fit in the upper panel.

as before. There is still evidence for linearity between the 90 μm and 1.4 GHz results, although this is consistent with an approximate constancy of IR/radio flux ratios.

It would appear, apart from this, that there is little evidence for evolution or correlation – and certainly nothing like the invariance in q noted for extragalactic systems. The scatter in these planes is huge, and indicates variations of an order of magnitude or more. Most of this scatter likely to be intrinsic to the sources. The combined errors resulting from photometric errors (∼20%) and uncertainties in the distance (∼30%) are likely to be ∼60% for the 90 μm results, for instance – and probably somewhat less than that for the 18 μm trends. This is a factor ∼15 less than is observed in Figure 13.

Whilst it is therefore possible to obtain reasonable values of q for large ensembles of PNe, as has previously been undertaken by the authors cited above, there is little evidence that this parameter is invariant between PNe, or indicates any close relation between the mechanisms responsible for radio and IR emission. Whilst it is undoubtedly the case that UV radiation is stimulating the radio and infrared emission, there is little evidence for the levels of correlation noted in extragalactic systems.

4. CONCLUSIONS

The AKARI all-sky survey has resulted in photometry for 8.77×10^5 sources in the MIR, using the IRC at 9 and 18 μm, and 4.27×10^5 sources in the FIR using the FIS at 65–160 μm. We have interrogated this database to identify the counterparts of Galactic PNe, and undertaken an analysis of the resulting photometry.

Approximately 80% of the Kerber et al. (2003) sources were detected to quality levels FQUAL = 3, of which ∼ half were observed in both the FIR and MIR regimes. A comparison with photometry deriving from the IRAS survey shows that there are systematic differences between the two sets of flux, although much of the variation is attributable to differences in the wavelengths employed. We also note that the mean AKARI dimensions of the sources are similar to those at radio and optical wavelengths, although the distributions of diameters appear to be radically different. This may arise because of centrally concentrated fluxes due to [OIV] and [NeV], and/or high levels of dust emission in extended PDRs. It is also possible that limiting sensitivities and errors are biasing the distribution of AKARI results.

Analysis of the nebulae in the colour-colour planes suggests that many of the SEDs are consistent with dust continuum emission, although emission bands and ionic transitions also contribute to the results. We find evolutionary trends in grain temperatures similar to those measured in previous studies, with values approaching ∼160 K where nebulae are young ($D < 0.08$ pc), and $T_{\rm GR}$ ∼60–120 K where nebulae are more evolved.

Fluxes in the individual channels also show an evolution with nebular diameter, much of which may be attributed to cooling of the grains. However, we also note that total FIR emission declines with increasing nebular diameter, from a peak of $\approx 1.5 \times 10^4\ L_\odot$ where $D < 0.05$ pc, to values ∼600 $L_\odot$ in more evolved PNe. The high luminosities of less evolved sources suggest that dust opacities are appreciable. Although up to ∼0.5 of the grain heating may arise from absorption of Lyα photons, it seems likely that most of the energy budget depends upon absorption of the stellar radiation field. There is ev-

idence for an evolution in the IRE with expansion of the shells, consistent with the variations to be expected in stellar and Lyα heating.

Finally, it has been suggested that PNe may show a consistent IR/radio flux ratio similar to that determined in extragalactic systems, although with some possible evidence of evolution at $\sim$8 μm. Our present results fail to confirm this suggestion. It is plain that whatever the global values of the IR/radio ratio may be, they are highly variable between nebulae, and show little evidence for consistency.

This research is based on observations with AKARI, a JAXA project with the participation of ESA.

REFERENCES

Acker, A., Ochsenbein, F., Stenholm, B., Tylenda, R., Marcout, J., & Schohn, C. 1992, Strasbourg-ESO Catalogue of Galactic Planetary Nebulae (Garching: ESO)
Appleton, P. N., et al. 2004, ApJS, 154, 147
Cahn, J. B., & Kaler, J. B. 1971, ApJS, 22, 319
Chu, Y.-H., et al. 2009, AJ, 138, 691
Cohen, M., & Barlow, M. J. 2005, MNRAS, 362, 1199
Cohen, M., & Green, A. 2001, MNRAS, 325, 531
Cohen, M., et al. 2005, ApJ, 627, 446
Cohen, M., et al. 2007, ApJ, 669, 343
Condon, J. J., Cotton, W. D., Greisen, E. W., Yin, Q. F., Perley, R. A., Taylor, G. B., & Broderick, J. J. 1998, AJ, 115, 1693
Kataza, H., et al. 2010, AKARI/IRC ALL-Sky Survey Point Source Catalogue, Version 1.0 Release, Note Rev. 1, http://irsa.ipac.caltech.edu/data/AKARI/documentation/AKARI-IRC_PSC_V1_RN.pdf
Kawada, M., et al. 2007, PASJ, 59, 389
Kerber, F., Mignani, R. P., Guglielmetti, F., & Wicenec, A. 2003, A&A, 408, 1029
Lenzuni, P., Natta, A., & Panagia, N. 1989, ApJ, 345, 306
Lorente, R., Onaka, T., Ita, Y., Ohyama Y., Tanabe, T., & Pearson, C. 2007, Akari IRC Data User Manual, http://www.sciops.esa.int/SA/ASTROF/docs/IRC_IDUM_1.3.pdf
Miszalski, B., Parker, Q. A., Acker, A., Birkby, J. L., Frew, D. J., & Kovacevic, A. 2008, MNRAS, 384, 525
Murukami, H., et al. 2007, PASJ, 59, 369
Neugebauer, G., et al. 1984, ApJ, 278, L1
Onaka, T., et al. 2007, PASJ, 59, 401
Parker, Q. A., et al. 2006, MNRAS, 373, 79
Perek, L., & Kohoutek, L. 1967, Catalogue of Galactic Planetary Nebulae (Prague: Publishing House of Czechoslovak Academy of Sciences)
Phillips, J. P. 2004, MNRAS, 353, 589
_____. 2007, MNRAS, 378, 231
Phillips, J. P., & Márquez-Lugo, R. A. 2011, MNRAS, 410, 2257
_____. 2005, MNRAS, 364, 849
_____. 2006, MNRAS, 368, 1773
_____. 2007, AJ, 133, 347
_____. 2008, MNRAS, 383, 1029
Pottasch, S. R., et al. 1984, A&A, 138, 10
Price, S. D., Egan, M. P., Carey, S. J., Mizuno, D. R., & Kuchar, D. A. 2001, AJ, 121, 2819
Ramos-Larios, G., & Phillips, J. P. 2005, MNRAS, 357, 732
_____. 2008, MNRAS, 390, 1014
Ramos-Larios, G., Phillips, J. P., & Cuesta, L. C. 2011, MNRAS, 411, 1245
Shirahata, M., et al. 2009, PASJ, 61, 737
Siodmiak, N., & Tylenda, R. 2001, A&A, 373, 1032
Stasinska, G., & Szczerba, R. 1999, A&A, 352, 297
Su, K. Y. L., et al. 2007, ApJ, 657, L41
Su, K. Y. L., et al. 2004, ApJS, 154, 302
Tylenda, R., Siódmiak, N., Górny, S. K., Corradi, R. L. M., & Schwarz, H. E. 2003, A&A, 405, 627
Ueta, T. 2006, ApJ, 650, 228
Werner, M., et al. 2004, ApJS, 154, 1
Yamamura, I., Makiuti, S., Ikeda, N., Fukuda, Y., Oyabu, S., Koga, T., & White, G. J. 2010, AKARI/FIS All-Sky Survey Bright Source Catalogue Version 1.0, http://www.ir.isas.jaxa.jp/AKARI/Observation/PSC/Public
Zhang, C. Y. 1995, ApJS, 98, 659
Zhang, Y., & Kwok, S. 2009, ApJ, 706, 252

J. P. Phillips and R. A. Márquez-Lugo: Instituto de Astronomía y Meteorología, Av. Vallarta No. 2602, Col. Arcos Vallarta, C.P. 44130, Guadalajara, Jalisco, Mexico (jpp, alejmar@astro.iam.udg.mx).